AD-A080 441 OHIO STATE UNIV COLUMBUS ELECTROSCIENCE LAB F/G 20/14
ELECTROMAGNETIC SCATTERING BY A METALLIC DISK.(U)
SEP 79 D P WITHOUARD, D B HODGE N00014-78-C-0049
UNCLASSIFIED ESL-718816-3 NL

1 OF 2
AD
A080441

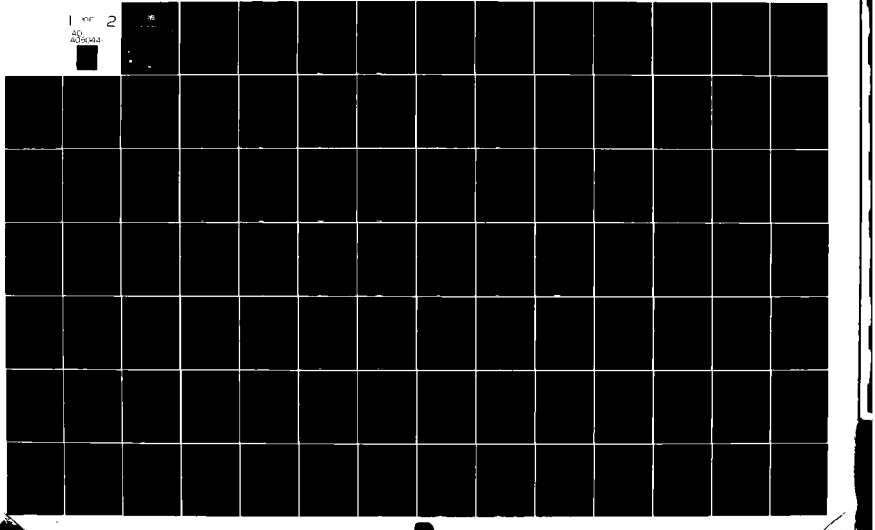

SECURITY CLASSIFICATION OF THIS PAGE *(When Data Entered)*

REPORT DOCUMENTATION PAGE

READ INSTRUCTIONS BEFORE COMPLETING FORM

1. REPORT NUMBER
2. GOVT ACCESSION NO.
3. RECIPIENT'S CATALOG NUMBER

4. TITLE *(and Subtitle)*
ELECTROMAGNETIC SCATTERING BY A METALLIC DISK

5. TYPE OF REPORT & PERIOD COVERED
Technical Report

6. PERFORMING ORG. REPORT NUMBER
ESL-710816-3

7. AUTHOR(s)
Didier P. Mithouard and Daniel B. Hodge

8. CONTRACT OR GRANT NUMBER(s)
Contract N00014-78-C-0049

9. PERFORMING ORGANIZATION NAME AND ADDRESS
The Ohio State University ElectroScience Laboratory, Department of Electrical Engineering
Columbus, Ohio 43212

10. PROGRAM ELEMENT, PROJECT, TASK AREA & WORK UNIT NUMBERS
Project NR 371-021/9-5-78 (427)

11. CONTROLLING OFFICE NAME AND ADDRESS
Dept. of the Navy, Office of Naval Research
800 Quincy Street
Arlington, Virginia 22217

12. REPORT DATE
September 1979

13. NUMBER OF PAGES
124

14. MONITORING AGENCY NAME & ADDRESS *(if different from Controlling Office)*

15. SECURITY CLASS. *(of this report)*
Unclassified

15a. DECLASSIFICATION/DOWNGRADING SCHEDULE

16. DISTRIBUTION STATEMENT *(of this Report)*

This document has been approved for public release and sale; its distribution is unlimited.

17. DISTRIBUTION STATEMENT *(of the abstract entered in Block 20, if different from Report)*

18. SUPPLEMENTARY NOTES

19. KEY WORDS *(Continue on reverse side if necessary and identify by block number)*

Scattering
Radar Cross Section
Disk
Bistatic

20. ABSTRACT *(Continue on reverse side if necessary and identify by block number)*

The scattering of electromagnetic waves by finite obstacles can be rigorously found for only two cases, the sphere and the disk. There exist two exact solutions to the scattering of an electromagnetic plane wave by a circular metallic disk. Flammer's and Meixner's exact approaches are successively considered and compared. In both cases, the fields are expanded in spheroidal vector wave functions, and the

DD FORM 1 JAN 73 1473 EDITION OF 1 NOV 65 IS OBSOLETE

AD A082251

SECURITY CLASSIFICATION OF THIS PAGE *(When Data Entered)*

scattered field is uniquely determined by the boundary conditions on the surface of the disk and the edge condition. The purpose of this work is to find a solution valid everywhere; in particular, it is desired to obtain the surface current and near fields. A numerical test of the bistatic scattered far-field for normal incidence is presented. Problems encountered in Flammer's solution for arbitrary incidence are pointed out. The general form of the scattered field is derived from Meixner's vector potentials. This formulation is appropriate for near-field calculations. Another proof of Meixner's solution using dependence relations of the spheroidal vector wave functions is given.

TABLE OF CONTENTS

CHAPTER I
INTRODUCTION

Among the various problems of electromagnetic scattering by arbitrary bodies, only a few simple shapes have led to exact solutions. The diffraction of an electromagnetic plane wave by a conducting circular disk long remained unsolved. The presence of an edge led to much greater complications than, for example, the sphere which was solved by Mie[1] very early in this century.

First, some limiting cases were derived for the disk problem. Approximate solutions were obtained by Kirchhoff diffraction theory for disks of large electrical circumference kd where k is the wave number and d the diameter of the disk and by Lord Rayleigh[2] for disks of small electrical circumference. After the second world war, extensive work was directed at the disk problem, and two complete general solutions were developed. Meixner and Andrejewski[3] used Hertzian vector potentials to compute the scattered field. They derived the form of the potential from the appropriate boundary conditions, and the uniqueness of the solution was insured by the edge condition developed by Meixner[4]. He showed that the energy density of the total field in the vicinity of an edge must be integrable. This insists that the components of the fields vary at most as $s^{-1/2}$, where s is the distance to the observation point from the edge. Bouwkamp[5] showed that the tangential electric field is zero on the edge, that it approaches this value as $s^{1/2}$, and that the tangential magnetic field remains finite. Tangential, in this context, means parallel to the edge. This solution has been checked by numerous computations made in recent years. Since the development by Hodge[6] of an efficient method of computing the spheroidal eigenvalues, even more efficient computers have allowed extensive comparison between experimental data and computational results with very good agreement.

Shortly after Meixner, Flammer[7] derived another solution using oblate spheroidal vector wave functions to expand the fields. As in the Mie solution for the sphere, the fields of the incoming plane wave were expanded in terms of the vector wave functions. The boundary conditions on the surface of the disk determined the scattering components. In order to insure that the tangential component of the electric field is zero on the edge, two sets of vector wave functions were used and their relative weights in the expansion of the incident plane wave were determined by the edge boundary condition. This led to a unique solution.

The purpose of this work is to compare Meixner's and Flammer's solutions. Apparently, no numerical results have ever been obtained from Flammer's formal solution. Thus, it is necessary to establish that the formal solution is, in fact, valid. If this validity is established, the vector wave function formalism may be more convenient for examination of such characteristics as the surface current distributions and the natural resonances. The reference work used for Meixner's solution is Hodge's version. Hodge[8] used the notation and normalization of the spheroidal functions introduced by Flammer. In order to match Hodge's geometry, Flammer's solution is rederived for the same configuration. The bistatic normal incidence case is more deeply studied, and problems encountered in the derivation of the solution are pointed out. Computations made in the normal incidence case, as studied by Flammer, are compared to the results obtained by Hodge[9]. In addition, Meixner's fields are expressed in terms of spheroidal vector wave functions as well as the vector potentials. Another proof of Meixner's solution with vector wave functions is given.

CHAPTER II
SPECIFICATIONS OF THE PROBLEM

A. Geometry

The scattering object is an infinitely thin, perfectly conducting circular disk of radius a. It lies in the x-y plane of a right-handed Cartesian coordinate system and is centered at the origin.

The following study will be made in the oblate spheroidal coordinate system (η,ξ,ϕ), Figure 2.1, in which the disk is the surface represented by $\xi=0$.

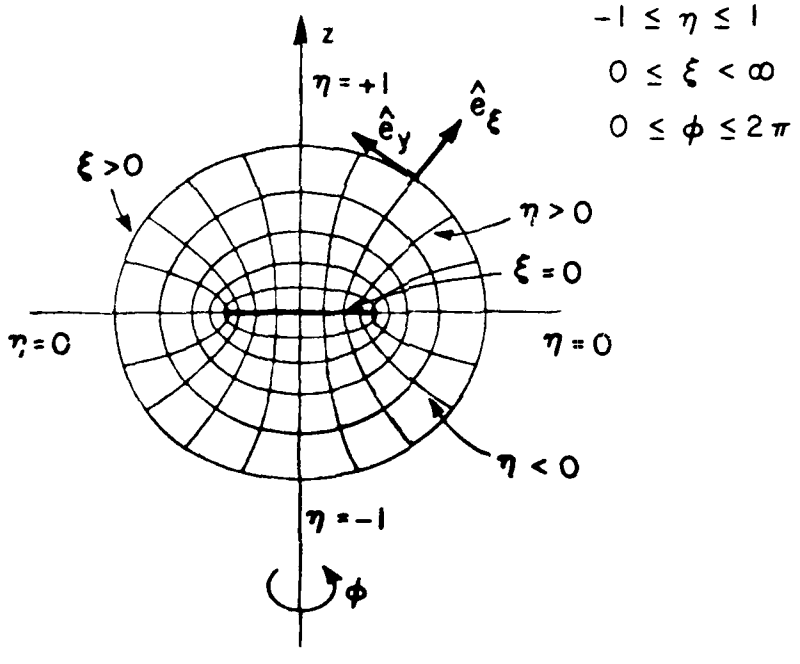

Figure 2.1. The oblate coordinate system.

The transformation from oblate spheroidal to Cartesian coordinates are, as given by Flammer[10],

$$\begin{cases} x = a[(1-\eta^2)(1+\xi^2)]^{1/2} \cos\phi & d=2a \\ y = a[(1-\eta^2)(1+\xi^2)]^{1/2} \sin\phi & \\ z = a\ \eta\xi \end{cases} \qquad (1)$$

In Appendix A, the transformations between the different coordinate systems - Cartesian, cylindrical and spherical - and the oblate spheroidal coordinate system are summarized. Their limiting forms are listed for three cases: at large distances from the disk -ξ large - on the surface of the disk and in the vicinity of the edge.

B. Problem

Because of the rotational symmetry about the z-axis it is possible, without loss of generality, to choose an arbitrary plane of incidence. We will use the notation of Hodge's work[9]. The incident plane wave direction lies in the x-z plane, coming from the x>0 half plane, Figure 2.2. Flammer used the y-z plane as plane of incidence, instead. The whole system is located in free-space.

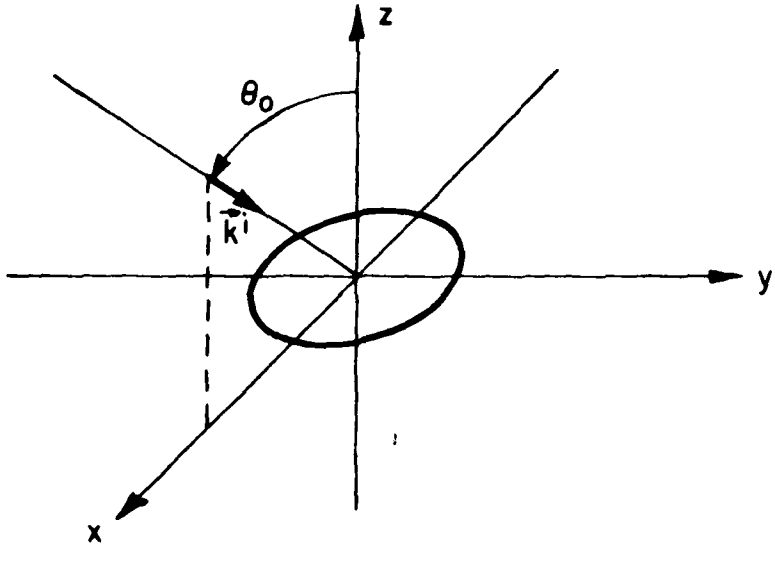

Figure 2.2. Geometry.

We will use the following symbols:

$c=ka$ - electrical circumference

θ_0 - angle of incidence

α - polarization angle

$e^{i\omega t}$ - time dependence

The incident wave vector $\bar{k}^i$ is expressed by:

$$\bar{k}^i = k[-\sin\theta_0\ \hat{e}_x - \cos\theta_0\ \hat{e}_z] \tag{2}$$

The polarization of the incident electric field is measured by the angle α between the plane of incidence and the incident electric field, $\bar{E}^i$, in such a way that α is the conventional azimuthal angle, ϕ, of a coordinate system defined by the unit vectors ($\cos\theta_0\ \hat{e}_x - \sin\theta_0\ \hat{e}_z$, $\hat{e}_y$, $\sin\theta_0\ \hat{e}_x + \cos\theta_0\ \hat{e}_z$) as shown in Figure 2.3. Parallel polarization is obtained for $\alpha=0$ and perpendicular polarization for $\alpha=\pi/2$. The incident electric field is given by

$$\bar{E}^i = E_0(\cos\theta_0\ \cos\alpha\ \hat{e}_x + \sin\alpha\ \hat{e}_y - \sin\theta_0\ \cos\alpha\ \hat{e}_z) \cdot e^{-i\bar{k}^i\cdot\bar{r}}\ e^{i\omega t} \tag{3}$$

where $\bar{r}$ is the usual position vector.

Note that Flammer[7] characterizes the incident wave by the angle ζ between the positive direction of the propagation vector and the positive z axis instead of the angle of incidence θ_0. Those angles are related as follows: $\zeta=\pi-\theta_0$.

In the spheroidal coordinate systems, the boundary conditions satisfied by the electromagnetic field on the surface of the disk and at the edge are on the disk, $\xi=0$:

$$\begin{aligned}(\bar{E}^i+\bar{E}^s)\cdot\hat{e}_\eta &= 0\\ (\bar{E}^i+\bar{E}^s)\cdot\hat{e}_\phi &= 0\\ (\bar{H}^i+\bar{H}^s)\cdot\hat{e}_\xi &= 0\end{aligned} \tag{4}$$

where $\bar{H}^s$, $\bar{E}^s$ is the scattered electromagnetic field.

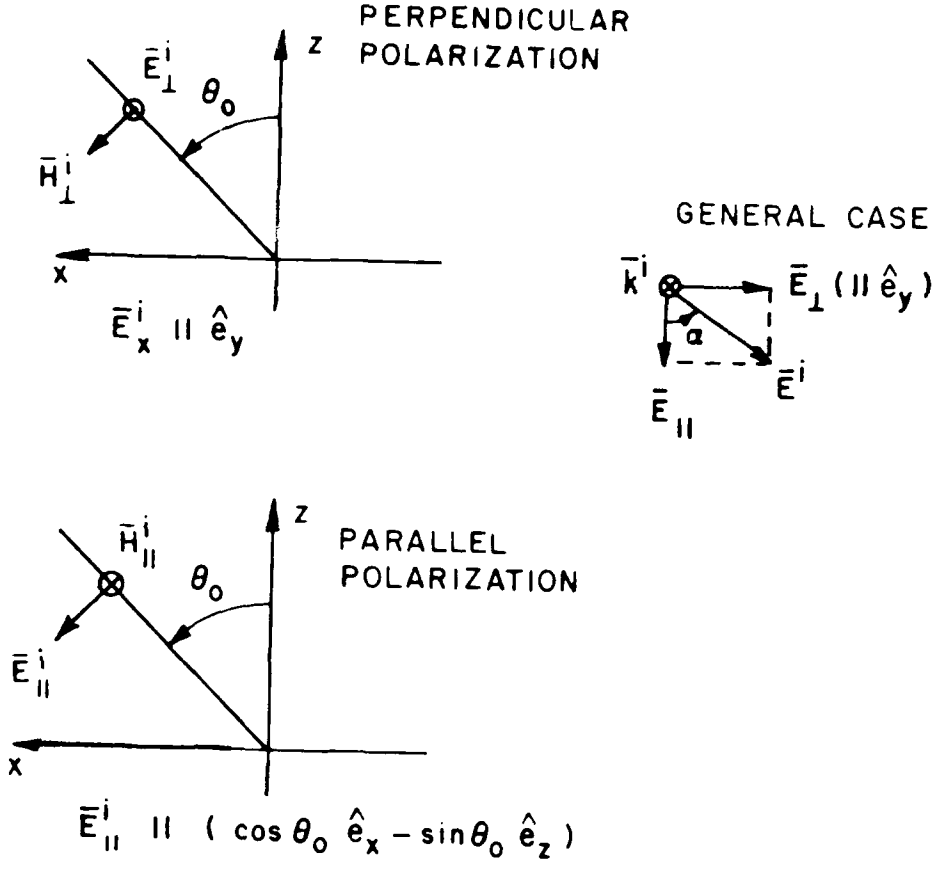

Figure 2.3. Polarization

At the edge, $\zeta=0$ and $\eta=0$, the energy density of the total field must be integrable. The components of the fields may become infinite at most as $s^{-1/2}$, where s is the distance from the edge to the observation point. Bouwhamp[10] showed the following more restrictive conditions on the ϕ-component of the fields:

$$(\vec{E}^i+\vec{E}^s) \cdot \hat{e}_\phi = O(s^{1/2})$$
$$(\vec{H}^i+\vec{H}^s) \cdot \hat{e}_\phi = O(1) \qquad (5)$$

Those orders of variation as function of s are valid only in the vicinity of the edge, $s \ll a$, for the curved edge of a disk.

In this work, we will refer to these behaviors of the components of the total electromagnetic field in the vicinity of the edge as the edge condition. The ϕ-components will also be refered to as tangential to the edge, or parallel to the rim.

We will see that, in Flammer's solution, the condition on $[\vec{E}^i+\vec{E}^r]_\phi$ is equivalent to the whole edge condition. This is due to the particular choice of the vector wave functions used. This will not be true for Meixner's solution, where all the conditions on the components of the field will be needed.

Before we present Flammer's and Meixner's solution we need to introduce the functions that we are going to work with and some of their properties. In Chapter III we will define the spheroidal functions, and in Chapter IV we will derive various plane wave expansions. In the following work, the time dependence $e^{i\omega t}$ will be omitted.

CHAPTER III
THE SPHEROIDAL FUNCTIONS

In this chapter the scalar wave function solution of the scalar wave equation will be introduced and some properties of the spheroidal radial and angular functions will be summarized. The large radial argument, $c\xi$, approximation of the vector wave function solutions of the vector wave equation will be listed.

A. Differential Equation and Scalar Wave Function

In the oblate spheroidal coordinate system, the scalar wave equation can be solved by the method of separation of variables. In Appendix B the different differential operators have been expanded in spheroidal coordinates. The scalar wave equation is:

$$\cdot\ \nabla^2\psi+k^2\psi = 0$$

$$\cdot\ \frac{1}{a^2}\left[-\frac{2\eta}{\xi^2+\eta^2}\frac{\partial\psi}{\partial\eta}+\frac{1-\eta^2}{\xi^2+\eta^2}\frac{\partial^2\psi}{\partial\eta^2}+\frac{2\xi}{\xi^2+\eta^2}\frac{\partial\psi}{\partial\xi}+\frac{1+\xi^2}{\eta^2+\xi^2}\frac{\partial^2\psi}{\partial\xi^2}+\frac{1}{(1+\xi^2)(1-\eta^2)}\frac{\partial^2\psi}{\partial\phi^2}\right]+k^2\psi = 0 \qquad (6)$$

The eigenfunctions associated with the eigenvalue λ_{mn} are:

$$\psi_{\substack{e\\o}mn}^{(i)}(\eta,\xi,\phi) = S_{mn}(-ic,\eta)\,R_{mn}^{(i)}(-ic,i\xi)\begin{Bmatrix}\cos m\phi\\ \sin m\phi\end{Bmatrix} \qquad (7)$$

where $S_{mn}(-ic,\eta)$ is the angular function

$$S_{mn}(-ic,\eta) = \sum_{r=0,1}^{\infty}{}' d_r^{mn}(-ic)\,P_{m+r}^{m}(\eta) \qquad (8)$$

as defined by Flammer[10].

$P^m_{m+r}(\eta)$ is the Legendre associated function as used in spherical coordinates. The expansion coefficients $d_r^{mn}(-ic)$ are computed from a recursion relationship as seen in Flammer's book[10].

The prime over the summation is a notation that will be used throughout the following work to denote that the summation must involve only the even or odd indexes when n-m is even or odd, respectively.

- $R_{mn}^{(i)}(-ic,i\xi)$ is the radial function

From Flammer's book[10],

$$R_{mn}^{(i)}(-ic,i\xi) = \frac{(1+\xi^2)^m}{\xi^m \sum_{r=0,1}^{\infty'} d_r^{mn}(-ic) \frac{(2m+r)!}{r!}} \sum_{r=0,1}^{\infty'} i^{r+m-n} d_r^{mn}(-ic) \frac{(2m+r)!}{r!} z_{n+r}^{(i)}(c\xi) \quad (9)$$

The index (i) denotes the kind of spherical Bessel function, $z_n^{(i)}$, used: i=1 for j_n, i=2 for n_n, i=3 for $h_n^{(1)}$ and i=4 for $h_n^{(2)}$. We will refer to i as the index of the radial function in the rest of this work. The normalization of the radial and angular spheroidal functions are those used by Flammer.

In the following two sections, we will summarize some properties of the angular and radial spheroidal functions.

B. The Angular Function $S_{mn}(-ic,\eta)$

The equation satisfied by the angular functions is:

$$\frac{d}{d\eta}\left[(1-\eta^2)\frac{d}{d\eta}S_{mn}(-ic,\eta)\right] + \left(\lambda_{mn}+c^2\eta^2 - \frac{m^2}{1-\eta^2}\right) S_{mn}(-ic,\eta) = 0 \qquad -1 \le \eta \le 1 \quad (10)$$

The angular functions are orthogonal with weight function 1:

$$\int_{-1}^{1} S_{mn}(-ic,\eta)S_{m\rho}(-ic,\eta)d\eta = \delta_{n\rho}\, N_{mn} \quad (11)$$

where

$$N_{mn} = 2 \sum_{r=0,1}^{\infty}{}' \frac{(r+2m)!}{r!} \frac{(d_r^{mn}(-ic))^2}{2r+2m+1}$$

1. Evaluation at $\eta=0$

From Formula (8), or more easily from the expansion of $S_{mn}(-ic,\eta)$ in powers of $(1-\eta^2)$, - Formula (3-2-7) in Reference [10] -, we can see that

for n-m even $S_{mn}(-ic,\eta)$ is an even function of η

for n-m odd $S_{mn}(-ic,\eta)$ is an odd function of η

From the differential equation and its derivatives, we can evaluate the derivatives of $S_{mn}(-ic,\eta)$ for zero argument:

$$\begin{cases} \dfrac{d^2}{d\eta^2}\ [S_{mn}(-ic,0)] = -\ (\lambda_{mn}-m^2)\ S_{mn}(-ic,0) \\ \dfrac{d^3}{d\eta^3}\ (S_{mn}(-ic,0)) = -\ (\lambda_{mn}-m^2-2)\ S'_{mn}(-ic,0) \\ \dfrac{d^4}{d\eta^4}\ (S_{mn}(-ic,0)) = [(\lambda_{mn}-m^2)(\lambda_{mn}-m^2-6) + 2m^2-2c^2]\ S_{mn}(-ic,0) \end{cases} \tag{12}$$

Thus, the evaluation of $S_{mn}(-ic,\eta)$ and its derivatives around $\eta=0$ can then be described by taking into account the odd and even properties:
η SMALL $\eta<<1$

n-m even

$$\begin{cases} S_{mn}(-ic,\eta) = S_{mn}(-ic,0)\ [1 - \dfrac{\eta^2}{2}\ (\lambda_{mn}-m^2)] + O(\eta^4) \\ S'_{mn}(-ic,\eta) = S_{mn}(-ic,0)\ [-\ \eta(\lambda_{mn}-m^2)] + O(\eta^3) \\ S''_{mn}(-ic,\eta) = S_{mn}(-ic,0)\ [-(\lambda_{mn}-m^2) + \dfrac{\eta^2}{2}\ [(\lambda_{mn}-m^2)(\lambda_{mn}-m^2-6) \\ \qquad\qquad + 2m^2-2c^2]] + O(\eta^4) \end{cases} \tag{13}$$

where the normalization has defined $S_{mn}(-ic,0) = P_n^m(0)$.

n-m odd

$$\begin{cases} S_{mn}(-ic,\eta) = S'_{mn}(-ic,0)[\eta] + 0\ (\eta^3) \\ S'_{mn}(-ic,\eta) = S'_{mn}(-ic,0)\ [1 - \frac{\eta^2}{2}\ (\lambda_{mn}-m^2-2)] + 0(\eta^4) \\ S''_{mn}(-ic,\eta) = S'_{mn}(-ic,0)\ [-\eta(\lambda_{mn}-m^2-2)] + 0(\eta^3) \end{cases} \tag{14}$$

where the normalization has defined $S'_{mn}(-ic,0) = \frac{d}{d\eta}[P_n^m(0)]$

2. Evaluation at $\eta=\pm 1$

The power series expansion is led by $(1-\eta^2)^{m/2}$ due to the $P^m_{m+r}(\eta)$ functions. For m greater than zero,

$$\begin{cases} m \geq 1 \quad S_{mn}(-ic,\pm 1) = 0 \\ m \geq 3 \quad S'_{mn}(-ic,\pm 1) = 0 \end{cases} \tag{15}$$

The evaluation for m=0 and 1 has been given by Flammer[10].

$$\begin{aligned} S_{0n}(-ic,1) &= \sum_{r=0,1}^{\infty}{}' d_r^{0n}(-ic) \\ S'_{0n}(-ic,1) &= \frac{1}{2} \sum_{r=0,1}^{\infty}{}' r(r+1)\ d_r^{0n}(-ic) \\ \lim_{\eta\to 1}(1-\eta^2)^{1/2}\ \frac{d}{d\eta}\ [S_{1n}(ic,\eta)] &= -\frac{1}{2} \sum_{r=0,1}^{\infty}{}' (r+1)(r+2)\ d_r^{1n}(-ic) \\ \lim_{\eta\to 1}\ \frac{S_{1n}(-ic,\eta)}{(1-\eta^2)^{1/2}} &= \sum_{r=0,1}^{\infty}{}' d_r^{1n}(-ic)\ P'_{r+1}(1) \\ &= \frac{1}{2} \sum_{r=0,1}^{\infty} (r+1)(r+2) d_r^{1n}(-ic) \end{aligned} \tag{16}$$

C. The Radial Function $R_{mn}^{(i)}(-ic,i\xi)$

The equation satisfied by the radial functions is:

$$\frac{d}{d\xi}\left[(1+\xi^2)\frac{d}{d\xi}R_{mn}^{(i)}(-ic,i\xi)\right] - \left[\lambda_{mn}-c^2\xi^2 - \frac{m^2}{1+\xi^2}\right]R_{mn}^{(i)}(-ic,i\xi) = 0, \qquad 0 \leq \xi < \infty \tag{17}$$

Unlike their spherical counterparts, Bessel, Neuman and Hankel functions - the oblate spheroidal radial functions and their derivatives are well defined over the whole range of values of ξ. The normalization coefficients of these functions have been defined by Flammer[10] so that they match convenient formulas for large values of the argument $c\xi$,

$$\begin{cases} R_{mn}^{(1)}(-ic,c\xi) \underset{c\xi\to\infty}{\longrightarrow} \frac{1}{c\xi}\cos\left[c\xi - \frac{1}{2}(n+1)\pi\right] \\ R_{mn}^{(4)}(-ic,i\xi) \underset{c\xi\to\infty}{\longrightarrow} \frac{1}{c\xi}\exp\left(-i\left[c\xi - \frac{1}{2}(n+1)\pi\right]\right) \end{cases} \tag{18}$$

With those definitions, we see that the suitable functions for the series expansion of an incoming plane wave will involve $R_{mn}^{(1)}$, and outward traveling waves will involve $R_{mn}^{(4)}$.

1. Wronskian

The Wronskian of the differential equation is, as computed by Flammer[10]:

$$R_{mn}^{(1)}(-ic,i\xi)\frac{dR_{mn}^{(2)}(-ic,i\xi)}{d\xi} - R_{mn}^{(2)}(-ic,i\xi)\frac{dR_{mn}^{(1)}(-ic,i\xi)}{d\xi} = +\frac{1}{c(1+\xi^2)} \tag{19}$$

This can be written in terms of the $R_{mn}^{(1)}$ and $R_{mn}^{(4)}$ functions, using the property $R_{mn}^{(4)}=R_{mn}^{(1)}-iR_{mn}^{(2)}$, and the fact that the Wronskian of two linearly dependent solutions is zero:

$$R_{mn}^{(4)}(-ic,i\xi)\,\frac{d}{d\xi}\,[R_{mn}^{(1)}(-ic,i\xi)] - R_{mn}^{(1)}(-ic,i\xi)\,\frac{d}{d\xi}\,[R_{mn}^{(4)}(-ic,i\xi)] = \frac{i}{c(1+\xi^2)} \qquad (20)$$

2. Evaluation at $\xi=0$

In his book, Flammer lists the values of the radial functions and their derivatives at $\xi=0$. Appendix C of this work contains some corrections to those formulas. After presenting some general properties, we focus on $R_{mn}^{(1)}$ and $R_{mn}^{(4)}$ separately.

From the differential equation and its derivatives we can evaluate the derivatives of $R_{mn}^{(i)}(-ic,i\xi)$ at $\xi=0$:

$$\begin{cases} \dfrac{d^2}{d\xi^2}\,[R_{mn}^{(i)}](-ic,i0) = (\lambda_{mn}-m^2)\,R_{mn}^{(i)}(-ic,i0) \\ \dfrac{d^3}{d\xi^3}\,[R_{mn}^{(i)}](-ic,i0) = (\lambda_{mn}-m^2-2)\,\dfrac{dR_{mn}^{(i)}(-ic,i0)}{d\xi} \\ \dfrac{d^4}{d\xi^4}\,[R_{mn}^{(i)}](-ic,i0) = [(\lambda_{mn}-m^2)(\lambda_{mn}-m^2-6) + 2m^2-2c^2]\,R_{mn}^{(i)}(-ic,i0) \end{cases}$$

where $c=ka$ (21)

a. Properties of $R_{mn}^{(1)}$

Flammer[10] develops a power series expansion of $R_{mn}^{(1)}(-ic,i\xi)$. This function, if extended over the domain $-\infty<\xi<\infty$, would lead to an even or odd function for n-m even or odd, respectively. We can also conclude that, for $k\geq 0$:

$$\frac{d^k}{d\xi^k}\,[R_{mn}^{(1)}](-ic,i0) = 0 \qquad (22)$$

for k even or odd when n-m is odd or even, respectively.

In the vicinity of the disk, the radial functions of the first kind can be expanded as follows:

ξ Small $c\xi \ll 1$

n-m even

$$\begin{cases} R_{mn}^{(1)}(-ic,i\xi) = R_{mn}^{(1)}(-ic,i0)\left[1+(\lambda_{mn}-m^2)\,\frac{\xi^2}{2}\right] + O(\xi^4) \\ R_{mn}^{(1)}{}'(-ic,i\xi) = R_{mn}^{(1)}(-ic,i0)[\xi(\lambda_{mn}-m^2)] + O(\xi^3) \\ R_{mn}^{(1)}{}''(-ic,i\xi) = R_{mn}^{(1)}(-ic,i0)\left[\lambda_{mn}-m^2 + \frac{\xi^2}{2}\,[(\lambda_{mn}-m^2-6) + 2m^2-2c^2)] + O(\xi^4)\right] \end{cases} \tag{23}$$

n-m odd

$$\begin{cases} R_{mn}^{(1)}(-ic,i\xi) = R_{mn}^{(1)}{}'(-ic,i0)[\xi] + O(\xi^3) \\ R_{mn}^{(1)}{}'(-ic,i\xi) = R_{mn}^{(1)}{}'(-ic,i0)\left[1+(\lambda_{mn}-m^2-2)\frac{\xi^2}{2}\right] + O(\xi^4) \\ R_{mn}^{(1)}{}''(-ic,i\xi) = R_{mn}^{(1)}{}'(-ic,i0)\xi(\lambda_{mn}-m^2-2) + O(\xi^3) \end{cases} \tag{24}$$

b. Properties of $R_{mn}^{(4)}$

From Equation (19), the Wronskian of $R_{mn}^{(1)}$ and $R_{mn}^{(4)}$ leads us to the following identities

$$\begin{cases} \text{n-m even} \qquad R_{mn}^{(4)}{}'(-ic,i0) = -\dfrac{i}{c\,R_{mn}^{(1)}(-ic,i0)} \\ \text{n-m odd} \qquad R_{mn}^{(4)}(-ic,i0) = \dfrac{i}{c\,R_{mn}^{(1)}{}'(-ic,i0)} \end{cases} \tag{25}$$

We then get the following expansions in the vicinity of the disk:

For ξ Small, $c\xi << 1$

n-m even

$$\begin{cases} R_{mn}^{(4)}(-ic,i\xi) = R_{mn}^{(4)}(-ic,i0)\left[1 + \frac{\xi^2}{2}(\lambda_{mn}-m^2)\right] \\ \qquad\qquad - \frac{\xi\, i}{c\, R_{mn}^{(1)}(-ic,i0)} + O(\xi^3) \\ R_{mn}^{(4)}{}'(-ic,i\xi) = -\frac{i}{c\, R_{mn}^{(1)}(-ic,i0)}\left[1 + \frac{\xi^2}{2}(\lambda_{mn}-m^2-2)\right] \\ \qquad\qquad + \xi(\lambda_{mn}-m^2)R_{mn}^{(4)}(-ic,i0) + O(\xi^3) \\ R_{mn}^{(4)}{}''(-ic,i\xi) = R_{mn}^{(4)}(-ic,i0) \\ \qquad \left[(\lambda_{mn}-m^2) + \frac{\xi^2}{2}[(\lambda_{mn}-m^2)(\lambda_{mn}-m^2-6) + 2m^2-2c^2)]\right] \\ \qquad -\frac{1}{c\, R_{mn}^{(1)}(-ic,i0)}\xi(\lambda_{mn}-m^2-2) + O(\xi^3) \end{cases} \tag{26}$$

Note that the coefficients of $R_{mn}^{(4)}(-ic,i0)$ in these equations are equal to those of $R_{mn}^{(1)}(-ic,i0)$ in the corresponding equations of Formula (23).

n-m odd

$$\begin{cases} R_{mn}^{(4)}(-ic,i\xi) = \frac{i}{c\, R_{mn}^{(1)}{}'(-ic,i0)}\left[1 + \frac{\xi^2}{2}(\lambda_{mn}-m^2)\right] \\ \qquad\qquad + \xi\, R_{mn}^{(4)}{}'(-ic,io) + O(\xi^3) \\ R_{mn}^{(4)}{}'(-ic,i\xi) = R_{mn}^{(4)}{}'(-ic,i0)\left[1 + \frac{\xi^2}{2}(\lambda_{mn}-m^2-2)\right] \\ \qquad + \frac{i}{c\, R_{mn}^{(1)}{}'(-ic,i0)}\xi(\lambda_{mn}-m^2) + O(\xi^3) \\ R_{mn}^{(4)}{}''(-ic,i\xi) = \frac{i}{c\, R_{mn}^{(1)}{}'(-ic,i0)}\left[\lambda_{mn}-m^2 + \frac{\xi^2}{2}[(\lambda_{mn}-m^2)(\lambda_{mn}-m^2-6) \right. \\ \qquad \left. + 2m^2-2c^2]\right] + \xi\, R_{mn}^{(4)}{}'(-ic,i0)(\lambda_{mn}-m^2-2) + O(\xi^3) \end{cases} \tag{27}$$

Note that the coefficients of $R_{mn}^{(4)'}(-ic,io)$ in these equations are equal to those of $R_{mn}^{(1)'}(-ic,i0)$ in the corresponding equations of Formula (24).

3. Evaluation of $R_{mn}^{(4)}$ for large arguments

Equation (18) gives the large argument approximations

$$\begin{cases} R_{mn}^{(4)}(-ic,i\xi) \longrightarrow \dfrac{i^{n+1}}{c\xi}\ \exp(-ic\xi) \\ \dfrac{d}{d\xi}\ [R_{mn}^{(4)}](-ic,i\xi) \longrightarrow \dfrac{i^{n-1}}{c\xi}\ \left[ic + \dfrac{1}{\xi}\right]\ \exp(-ic\xi) \\ \dfrac{d^2}{d\xi^2}\ [R_{mn}^{(4)}](-ic,i\xi) \longrightarrow \dfrac{i^{n-1}}{c\xi}\left[c^2 - \dfrac{2ic}{\xi} - \dfrac{2}{\xi^2}\right] \exp(-ic\xi) \end{cases} \tag{28}$$

In the far field expansions, only the terms with $1/\xi$ dependence will be kept.

D. The Vector Wave Functions

Solenoidal solutions of the vector wave equation can be expanded as summations of spheroidal vector wave functions. Those will be defined, following Flammer's notation, by:

$$\begin{aligned} \bar{M}_{\substack{e\\o}mn}^{\alpha(i)}(\eta,\xi,\phi) &= \nabla \times [\psi_{\substack{e\\o}mn}^{(i)}(\eta,\xi,\phi)\hat{e}_\alpha] \\ \bar{N}_{\substack{e\\o}mn}^{\alpha(i)}(\eta,\xi,\phi) &= \frac{1}{k}\nabla \times \bar{M}_{\substack{e\\o}mn}^{\alpha(i)}(\eta,\xi,\phi) \end{aligned} \tag{29}$$

where $\hat{e}_\alpha$ is either a constant vector in Cartesian coordinates (α=x,y,z) or the position vector $\vec{r}=r\,\vec{e}_r(\alpha=r)$.

Extensive work has been done on these functions by Flammer, who lists them all in his book[10]. In contrast with the orthogonality of the scalar wave functions, the spheroidal vector wave functions are not orthogonal. They are not even independent as will be seen in Chapter IV-C. We will list here the behavior of those functions on the surface of the disk and for large radial arguments.

1. Behavior of the vector wave functions at $\xi=0$

We have seen Chapter III-C, Equation (21), that, on the surface of the disk, all radial functions and their derivatives can be expressed in terms of $R_{mn}^{(i)}(-ic,i0)$ and $R_{mn}^{(i)'}(-ic,i0)$. We can show that, on the surface of the disk, each component of any vector wave function defined by Equation (29) is proportional to only one of these values. We list the different cases.

a. Tangential components at $\xi=0$

$$[\bar{M}^{x(i)}_{\substack{e\\o}mn}]_\eta \ , \ [\bar{M}^{x(i)}_{\substack{e\\o}mn}]_\phi \ , \ [\bar{M}^{y(i)}_{\substack{e\\o}mn}]_\eta \ , \ [\bar{M}^{y(i)}_{\substack{e\\o}mn}]_\phi \ , [\bar{N}^{z(i)}_{\substack{e\\o}mn}]_\eta \text{ and}$$

$$[N^{z(i)}_{\substack{e\\o}mn}]_\phi \text{ are proportional to } R_{mn}^{(i)'}(-ic,i0). \tag{30}$$

$$[\bar{N}^{x(i)}_{\substack{e\\o}mn}]_\eta \ , \ [\bar{N}^{x(i)}_{\substack{e\\o}mn}]_\phi \ , \ [\bar{N}^{y(i)}_{\substack{e\\o}mn}]_\eta \ , \ [\bar{N}^{y(i)}_{\substack{e\\o}mn}]_\phi \ , \ [\bar{M}^{z(i)}_{\substack{e\\o}mn}]_\eta \ ,$$

$$[\bar{M}^{z(i)}_{\substack{e\\o}mn}]_\phi \text{ are proportional to } R_{mn}^{(i)}(-ic,i0). \tag{31}$$

b. Normal components at $\xi=0$

$$[\bar{N}^{x(i)}_{\substack{e\\o}mn}]_\xi \ , \ [\bar{N}^{y(i)}_{\substack{e\\o}mn}]_\xi \text{ are proportional to } R_{mn}^{(i)'}(-ic,i0) \tag{32}$$

$$[\bar{M}^{x(i)}_{\substack{e\\o}mn}]_\xi \ , \ [\bar{M}^{y(i)}_{\substack{e\\o}mn}]_\xi \ [\bar{N}^{z(i)}_{\substack{e\\o}mn}]_\xi \text{ are proportional to } R_{mn}^{(i)}(-ic,i0) \tag{33}$$

We notice that at the surface of the disk the tangential components of any of these vector wave functions, and the normal component of their curl - that is, for example, $[\bar{N}^\alpha]_{\eta,\phi}$ and $[\bar{M}^\alpha]_\xi$ or vice-versa - have the same radial dependence. That ensures that both boundary conditions on $\bar{E}$ and $\bar{H}$ at the surface of the disk are matched by the same expansion.

2. Behavior of the vector wave functions of index i=4 for large arguments of the radial part

In this section, we list the large radial argument approximations of the vector wave functions, keeping only the $1/\xi$ terms. From Equation (29),

$$
\begin{cases}
\bar{M}^{x(4)}_{\substack{e\\o}mn} = \dfrac{2}{d}\dfrac{i^n}{\xi} S_{mn}(-ic,\eta)\{-\sin\phi\ \hat{e}_\eta + \eta\cos\phi\ \hat{e}_\phi\} \begin{matrix}\cos\\ \sin\end{matrix} m\phi\ e^{-ic\xi} \\
\bar{M}^{y(4)}_{\substack{e\\o}mn} = \dfrac{2}{d}\dfrac{i^n}{\xi} S_{mn}(-ic,\eta)\{\cos\phi\ \hat{e}_\eta + \eta\sin\phi\ \hat{e}_\phi\} \begin{matrix}\cos\\ \sin\end{matrix} m\phi\ e^{-ic\xi} \\
\bar{M}^{z(4)}_{\substack{e\\o}mn} = -\dfrac{2}{d}\sqrt{1-\eta^2}\, S_{mn}(-ic,\eta)\dfrac{i^n}{\xi} \begin{matrix}\cos\\ \sin\end{matrix} m\phi\ e^{-ic\xi}\ \hat{e}_\phi \\
\bar{N}^{x(4)}_{\substack{e\\o}mn} = \dfrac{2}{d}\dfrac{i^{n-1}}{\xi} S_{mn}(-ic,\eta)\{\eta\cos\phi\ \hat{e}_\eta + \sin\phi\ \hat{e}_\phi\} \begin{matrix}\cos\\ \sin\end{matrix} m\phi\ e^{-ic\xi} \\
\bar{N}^{y(4)}_{\substack{e\\o}mn} = \dfrac{2}{d}\dfrac{i^{n-1}}{\xi} S_{mn}(-ic,\eta)\{\eta\sin\phi\ \hat{e}_\eta - \cos\phi\ \hat{e}_\phi\} \begin{matrix}\cos\\ \sin\end{matrix} m\phi\ e^{-ic\xi} \\
\bar{N}^{z(4)}_{\substack{e\\o}mn} = -\dfrac{2}{d}\sqrt{1-\eta^2}\, S_{mn}(-ic,\eta)\dfrac{i^{n-1}}{\xi} \begin{matrix}\cos\\ \sin\end{matrix} m\phi\ \hat{e}_\eta\ e^{-ic\xi}
\end{cases}
\tag{34}
$$

We now have enough tools to find the expansions of scalar and vector plane waves in terms of the spheroidal functions.

CHAPTER IV
PLANE WAVE EXPANSION

In order to expand the incident fields, we need the expansions of vector plane waves in terms of the spheroidal vector wave functions. First, we will derive the scalar plane wave expansion in terms of scalar wave functions. Taking its curl associated with different basis vectors will lead us to various vector plane wave expansions. The special cases of normal incidence to the disk are reviewed.

A. Scalar Plane Wave

By scalar plane wave we denote the function $\exp[ik(x \sin\theta_0 + z \cos\theta_0)]$ in our geometry. We do not know enough about the angular spheroidal functions to directly obtain the coefficients of the expansion of the scalar plane wave in terms of spheroidal functions by applying orthogonality on the trigonometric and angular functions. We will use another method as derived by Flammer[10]. The plane wave is considered to be due to a point source removed to infinity in the direction of arrival of the incident wave. The scalar plane wave will then be obtained from the asymptotic form of the free-space Green's function.

Because of our choice of the time dependence, $e^{i\omega t}$, the Green's function used here will be the complex conjugate of that obtained by Flammer[10]:

$$\frac{\exp(-ik|\bar{r}'-\bar{r}'|)}{4\pi|\bar{r}'-\bar{r}'|} = -\frac{ik}{2\pi}\sum_{m=0}^{\infty}\sum_{n=m}^{\infty}\frac{2-\delta_{0m}}{N_{mn}}S_{mn}(-ic,\eta)S_{mn}(-ic,\eta')$$
$$R_{mn}^{(4)}(-ic,i\xi')R_{mn}^{(1)}(-ic,i\xi)\cos m(\phi-\phi') \text{ when } \xi'>\xi, \tag{35}$$

where (η',ξ',ϕ') are the coordinates of the source point.

For a point source at infinity, we can use the approximations:

$$\frac{\exp(-ik|\bar{r}-\bar{r}'|)}{4\pi|\bar{r}-\bar{r}'|} \xrightarrow[c\xi'\to\infty]{} \frac{\exp(-ik(r'-\bar{r}\cdot\nabla' r'))}{4\pi r'} \tag{36}$$

$$R_{mn}^{(4)}(-ic,i\xi') \xrightarrow[c\xi'\to\infty]{} \frac{1}{c\xi'} \exp\left[-i\left(c\xi' - \frac{n+1}{2}\pi\right)\right] = \frac{i^{n+1}}{c\xi'} e^{-ic\xi'} \quad (37)$$

$$\begin{cases} \eta' \xrightarrow[c\xi'\to\infty]{} \cos\theta_o \\ c\xi' \xrightarrow[c\xi'\to\infty]{} kr' \qquad \text{as seen in Appendix B} \end{cases} \quad (38)$$

Finally

$$\exp(ik\bar{r}\cdot\nabla' r') = 2 \sum_{m=0}^{\infty} \sum_{n=m}^{\infty} \frac{(2-\delta_{0m})i^n}{N_{mn}} S_{mn}^{(1)}(-ic,\cos\theta_o) S_{mn}^{(1)}(-ic,\eta) \times R_{mn}^{(1)}(-ic,i\xi) \cos_m(\phi-\phi') \quad (39)$$

and

$$\bar{r}\cdot\nabla' r' = \bar{r}\cdot[\sin\theta_o\cos\phi'\,\hat{e}_x + \sin\theta_o\sin\phi'\,\hat{e}_y + \cos\theta_o\,\hat{e}_z]$$

$$\bar{r}\cdot\nabla' r' = x\sin\theta_o\cos\phi' + y\sin\theta_o\sin\phi' + z\cos\theta_o \quad . \quad (40)$$

For a wave incident from the positive x half x-z plane, $\phi'=0$ and we obtain the expansion

$$\exp[ik(x\sin\theta_o + z\cos\theta_o)] = 2 \sum_{m=0}^{\infty} \sum_{n=0}^{\infty} \frac{2-\delta_{0m}}{N_{mn}} i^n S_{mn}(-ic,\cos\theta_o) \times S_{mn}(-ic,\eta) R_{mn}^{(1)}(-ic,i\xi) \cos m\phi \quad . \quad (41)$$

We define the coefficients, $\gamma_{mn}(\theta_o)$, of the scalar wave functions, as in Flammer[10], Equation (7):

$$\gamma_{mn}(\theta_o) = 2 \frac{(2-\delta_{0m})}{N_{mn}} i^n S_{mn}(-ic,\cos\theta_o) \quad (42)$$

$$\exp[ik(x\sin\theta_o + z\cos\theta_o)] = \sum_{m=0}^{\infty} \sum_{n=m}^{\infty} \gamma_{mn}(\theta_o) \psi_{e_{mn}}^{(1)}(\eta,\xi,\phi) \quad . \quad (43)$$

B. Vector Plane Wave Expansion

The vector plane wave can then be expressed in terms of the vector wave functions by taking the curls of Formula (43) associated with a constant vector (see Equation (29)).

We list the obtained formulas, with the notations of Equation (29).

$$\hat{e}_y \exp[ik(x \sin\theta_0 + z \cos\theta_0)]$$

$$= \frac{1}{ik \cos\theta_0} \sum_{m=0}^{\infty} \sum_{n=m}^{\infty} \gamma_{mn}(\theta_0) \overline{M}_{e_{mn}}^{x(1)}(n,\xi,\phi) \tag{44}$$

$$(-\hat{e}_x \cos\theta_0 + \hat{e}_z \sin\theta_0)\exp[ik(x \sin\theta_0 + z \cos\theta_0)]$$

$$= \frac{1}{ik} \sum_{m=0}^{\infty} \sum_{n=m}^{\infty} \gamma_{mn}(\theta_0) \overline{M}_{e_{mn}}^{y(1)}(n,\xi,\phi) \tag{45}$$

$$\hat{e}_y \exp[ik(x \sin\theta_0 + z \cos\theta_0)]$$

$$= - \frac{1}{ik \sin\theta_0} \sum_{m=0}^{\infty} \sum_{n=m}^{\infty} \gamma_{mn}(\theta_0) \overline{M}_{e_{mn}}^{z(1)}(n,\xi,\phi) \tag{46}$$

$$(-\hat{e}_x \cos\theta_0 + \hat{e}_z \sin\theta_0)\exp[ik(x \sin\theta_0 + z \cos\theta_0)]$$

$$= - \frac{1}{k \cos\theta_0} \sum_{m=0}^{\infty} \sum_{n=m}^{\infty} \gamma_{mn}(\theta_0) \overline{N}_{e_{mn}}^{x(1)}(n,\xi,\phi) \tag{47}$$

$$\hat{e}_y \exp[ik(x \sin\theta_0 + z \cos\theta_0)] = \frac{1}{k} \sum_{m=0}^{\infty} \sum_{n=m}^{\infty} \gamma_{mn}(\theta_0) \overline{N}_{e_{mn}}^{y(1)}(n,\xi,\phi) \tag{48}$$

$$(-\hat{e}_x \cos\theta_0 + \hat{e}_z \sin\theta_0)\exp[ik(x \sin\theta_0 + z \cos\theta_0)]$$

$$= \frac{1}{k \sin\theta_0} \sum_{m=0}^{\infty} \sum_{n=m}^{\infty} \gamma_{mn}(\theta_0) \overline{N}_{e_{mn}}^{z(1)}(n,\xi,\phi) \tag{49}$$

C. Normal Incidence Case, θ_o=0

In this section, we will study the behavior of Equations (44) to (49) in the case of a plane wave normally incident on the top of the disk. As we have seen in Formula (15), the angular functions of order greater than zero are equal to zero for unity argument.

$$m \geq 1 \quad S_{mn}(-ic, \cos\theta_o) = 0 \quad \text{for } \theta_o = 0.$$

From Equation (42), we deduce that $\gamma_{0n}(0)$ is the only non-zero expansion coefficient. The expansions Equations (44), (45), (47) and (48) can be readily seen to be single summations on n, $0 \leq n < \infty$ with m=0. The expansions Equations (46) and (49), however, involve a $1/\sin\theta_o$ factor that leads to indeterminacy of the limit when θ_o tends towards zero.

As we can see from the definition of $S_{mn}(-ic,\eta)$, Equation (8), the angular function is led by a $(1-\eta^2)^{m/2}$ factor. Therefore, from Equation (42), we can write:

$$\gamma_{mn}(\theta_o) \propto (1-\cos^2\theta_o)^{m/2} = \sin^m\theta_o \tag{50}$$

or

$$\frac{1}{\sin\theta_o}\,\gamma_{mn}(\theta_o) \propto \sin^{m-1}\theta_o \quad .$$

We can then conclude that the value of the limit when θ_o goes to zero for the different values of m.

$$\text{For } m>1 \quad \lim_{\theta_o \to 0} \frac{\gamma_{mn}(\theta_o)}{\sin\theta_o} = 0$$

For m=1, we have seen in Equation (16) that:

$$\lim_{\theta_o \to 0} \frac{S_{1n}(-ic,\cos\theta_o)}{\sin\theta_o} = \frac{1}{2} \sum_{r=0,1}^{\infty} (r+1)(r+2)\, d_r^{1n}(-ic)$$

Thus,

$$\lim_{\theta_o \to 0} \frac{\gamma_{mn}(\theta_o)}{\sin\theta_o} = \frac{2\, i^n}{N_{1n}} \sum_{r=0,1}^{\infty} (r+1)(r+2) d_r^{1n}(-ic) \quad . \tag{51}$$

For m=0, $\gamma_{0n}(\theta_0)/\sin\theta_0$ goes to infinity when θ_0 approaches zero. We will show that, despite the fact that each coefficient diverges, the partial summations over n for m=0 in Equations (46) and (49) are globally equal to zero. This will lead to two dependence relationships for the spheroidal vector wave functions. Consider first the case of Equation (46). Because of an m coefficient, the η- and ξ-component of $\bar{M}_{e0n}^{z(1)}$ are equal to zero. We prove that the ϕ-component of the partial summation for m=0 in Equation (46) is also equal to zero; this is expressed in the following equation:

$$\sum_{n=0}^{\infty} \gamma_{0n}(0) \left[\eta \frac{d}{d\eta} S_{0n}(-ic,\eta)\, R_{0n}^{(1)}(-ic,i\xi) - \xi\, S_{0n}(-ic,\eta)\, \frac{d}{d\xi} R_{0n}^{(1)}(-ic,i\xi) \right] = 0 \qquad (52)$$

This must be valid for any pair (η,ξ). In order to prove this identity, we must go back to the scalar plane wave, Equation (41), and specialize to our normal incidence case.

$$\exp[ikz] = \sum_{n=0}^{\infty} \gamma_{0n}(0)\, S_{0n}(-ic,\eta)\, R_{0n}^{(1)}(-ic,i\xi) \qquad (53)$$

From Appendix B, we know that z can be expressed very simply in terms of η and ξ:

$$z = a\eta\xi \quad . \qquad (54)$$

Taking the derivative of Equation (53) with respect to η and ξ separately, we obtain two expansions as follows

$$\frac{\partial}{\partial\eta}[\exp(ikz)] = ika\xi \exp(ikz) = \sum_{n=0}^{\infty} \gamma_{0n}(0)\, S_{0n}'(-ic,\eta)\, R_{0n}^{(1)}(-ic,i\xi) \qquad (55)$$

$$\frac{\partial}{\partial\xi}[\exp(ikz)] = ika\eta \exp(ikz) = \sum_{n=0}^{\infty} \gamma_{0n}(0)\, S_{0n}(-ic,\eta)\, R_{0n}^{(1)'}(-ic,i\xi) \qquad (56)$$

Multiplying Equation (55) by η and Equation (56) by $-\xi$ and adding them leads directly to Formula (52). We have shown that, for any pair (η,ξ):

$$\sum_{n=0}^{\infty} \gamma_{0n}(0)\, \bar{M}_{e0n}^{z(1)}(\eta,\xi,\phi) = \vec{0} \qquad (57)$$

Taking the curl of this equation leads to:

$$\sum_{n=0}^{\infty} \gamma_{0n}(0)\, \bar{N}_{e_{0n}}^{z(1)}(\eta,\xi,\phi) = \dot{0} \tag{58}$$

To suppress the indeterminacy of the limit of the ratio of Equations (57) and (58) to $\sin\theta_0$ when θ_0 goes to zero, we will apply L'Hospital's rule to each component of those equations:

$$\lim_{\theta_0 \to 0} \left[\frac{1}{\sin\theta_0} \sum_{n=0}^{\infty} \gamma_{0n}(\theta_0)[\bar{F}]_\beta \right]$$

$$= \lim_{\theta_0 \to 0} \left[\sum_{n=0}^{\infty} \frac{2i^n}{N_{0n}} \frac{S_{0n}(ic,\cos\theta_0)(-\sin\theta_0)}{\cos\theta_0} [\bar{F}]_\beta \right] = 0 \tag{59}$$

where $[\bar{F}]_\beta$ represents the β-component of either $\bar{M}_{e_{0n}}^{z(1)}$ or $\bar{N}_{e_{0n}}^{z(1)}$, and $\beta=\eta,\xi,\phi$.

Thus we conclude that, in the normal incidence case, the expansions (46) and (49) can be expressed as single summations on n, $1 \le n < \infty$ with m=1. Flammer[7] gives a vectorial proof of Equation (57) by taking the curl of $\hat{e}_z \exp(ikz)$, Equation (53), which is zero as the curl of a z-directed vector whose component is a function of z only.

For convenience in the study of the normal incidence case, we define, as Flammer[10], the following coefficients:

$$a_{0n} = 2\, i^{n-1}\, N_{0n}^{-1} \sum_{r=0,1}^{\infty}{}' d_r^{0n}(-ic)$$

$$= 2\, i^{n-1}\, N_{0n}^{-1}\, S_{0n}(-ic,1)$$

$$= \frac{1}{i}\, \gamma_{0n}(0) \tag{60}$$

$$b_{1n} = 2\, i^{n+1}\, N_{1n}^{-1} \sum_{r=0,1}^{\infty}{}' \frac{(r+2)!}{r!}\, d_r^{1n}(-ic) \tag{61}$$

The vector wave expansions are then, for normal incidence:

$$\hat{e}_y \exp(ikz) = \frac{1}{k} \sum_{n=0}^{\infty} a_{0n}\, \bar{M}_{e_{0n}}^{x(1)} \tag{62}$$

$$\hat{e}_x \exp(ikz) = -\frac{1}{k} \sum_{n=0}^{\infty} a_{0n} \bar{M}_{e_{0n}}^{y(1)} \tag{63}$$

$$\hat{e}_y \exp(ikz) = \frac{1}{k} \sum_{n=1}^{\infty} b_{1n} \bar{M}_{e_{1n}}^{z(1)} \tag{64}$$

$$\hat{e}_x \exp(ikz) = \frac{i}{k} \sum_{n=0}^{\infty} a_{0n} \bar{N}_{e_{0n}}^{x(1)} \tag{65}$$

$$\hat{e}_y \exp(ikz) = \frac{i}{k} \sum_{n=0}^{\infty} a_{0n} \bar{N}_{e_{0n}}^{y(1)} \tag{66}$$

$$\hat{e}_x \exp(ika) = \frac{i}{k} \sum_{n=1}^{\infty} b_{1n} \bar{N}_{e_{1n}}^{z(1)} \tag{67}$$

D. Dependence Relations

In the previous two sections, we have derived various relationships between spheroidal scalar functions, and between spheroidal vector wave functions. Some limiting cases will allow us to show some dependence relationships, as follows.

Equations (55) for $\xi=0$ shows that the derivatives of $S_{0n}(-ic,\eta)$ are not independent and therefore not orthogonal as the original functions were.

Equations (57) and (58) show the lack of independence of the functions $\bar{M}_{e_{0n}}^{z(1)}$, and $\bar{N}_{e_{0n}}^{z(1)}$, respectively. Equations (44) and (47), multiplied by $\cos\theta_0$, lead to dependence relationships for $\bar{M}_{e_{mn}}^{x(1)}$, and $\bar{N}_{e_{mn}}^{x(1)}$ respectively, when θ_0 approaches $\pi/2$. That kind of relationship can be derived for each family of vector wave functions of index i=1. We do not deal with independent sets as in the spherical case. In the next two parts, we will derive two different solutions for the scattering problem. In both cases, the fields will be expanded in spheroidal vector wave functions. For the incident fields, we will use the expansions derived in the previous two sections. We will not be able to consider individual terms in the summation expressing the incident field to be modes as we do in simpler problems, where orthogonality properties exist. To each vector wave function of the expansion of the incident field will correspond not only one vector wave function in the scattered field but a summation of the scattered counterparts of all the vector wave functions appearing in the dependence relationship satisfied by the initial wave function. This will be shown in part VI-C. We have not, however, proved that the spheroidal vector wave function of index i=4 are

dependent since the relationships obtained for index 1 are not applicable to functions of index i=4.

In the following chapter, we will rederive Flammer's solution.

CHAPTER V
FLAMMER'S SOLUTION

Unlike Meixner, Flammer[7] deals directly with the electric and magnetic fields in order to find a solution to the scattering problem. This approach allows simpler, more physically interpretable boundary conditions, but at the expense of more complicated expansions. The major problem encountered in the scattering by a disk is that satisfying the boundary conditions on the surface of the disk leads to solutions that do not necessarily satisfy the edge condition. The edge condition puts restrictions on the behavior of the components of the total electromagnetic field in the vicinity of the edge as explained in Chapter II of this work. For the electromagnetic energy density to be integrable in the vicinity of the edge all components of the fields vary at most as $s^{-1/2}$ where s is the distance from the edge, while the ϕ-component of the total magnetic field remains finite and the ϕ-component of the total electric field goes to zero as $s^{1/2}$. A very remarkable point in Flammer's solution is that the satisfaction of the condition on the ϕ-component of the electric field directly ensures the satisfaction of the edge condition.

Whatever the expansion of the electric field of the incident plane wave in spheroidal vector wave functions of index 1, the summation of spheroidal vector wave functions of index 4 which satisfies the $\bar{E}$-field boundary conditions on the surface of the disk has a singularity of order $s^{-1/2}$ in its ϕ-component. Flammer chose to express the incident plane wave as sum of two different expansions. The relative weights of each expansion are then chosen in such a way that the coefficients of the singularity in the ϕ-component of the corresponding $\bar{E}$-field expansions of index 4 cancel each other. With the proper choice of the two plane wave expansions, the above procedure also leads to the satisfaction of the whole edge condition.

First we will study the normal incidence, perpendicular polarization bistatic case because of its greater simplicity. Perpendicular polarization is here understood as defined in Chapter II, considering the x-z plane as plane of incidence. The problems encountered in extending the method to the arbitrary incidence, arbitrary polarization bistatic case will be noted, and the results of a numerical test of the far-field for the normal incidence case will be presented.

A. Normal Incidence, Perpendicular Polarization Bistatic Case

This corresponds to the case $\alpha=\pi/2$, $\bar{E}^i||\hat{e}_y$, and $\bar{H}^i||\hat{e}_x$. The incident $\bar{E}$-field can be expanded according to Equations (62), (64) or (66) and the corresponding $\bar{H}$-field according to Equations (65), (67) or (63), respectively. To represent the outgoing scattered waves, we use vector wave functions of index 4 which match spherical waves when ξ becomes large.

We will successively consider the boundary conditions on the surface of the disk, an expansion of the ϕ-component of the electric field in the vicinity of the edge, the $[\bar{E}]_\phi$ condition, and the final solution where we will check the satisfaction of the edge condition.

1. Field boundary conditions on the surface of the disk

We will successively consider the three possible expansions and the scattered fields they lead to. Despite the lack of orthogonality of the spheroidal vector wave functions of index 1, we will use a term by term, function by function, matching technique to obtain the expansion of spheroidal vector wave functions of order 4 which satisfies the boundary condition on the surface of the disk for given incident wave expansion. These expansions will be called "reflected" fields $\bar{E}^r$ and $\bar{H}^r$. The reflected fields are not equal to the scattered fields unless the edge condition is satisfied by $\bar{E}^i+\bar{E}^r$ and $\bar{H}^i+\bar{H}^r$, but they satisfy the boundary conditions on the surface of the disk. The boundary condition is given in Equation (4):

$$[\bar{E}^i+\bar{E}^s]_\eta = [\bar{E}^i+\bar{E}^s]_\phi = [\bar{H}^i+\bar{H}^s]_\xi = 0$$

The term by term matching technique does not lead directly to the scattered field since the spheroidal vector wave functions of index 1 are not independent. We now express the reflected fields for the three possible expansions of the incident fields.

$\bar{M}_{e_{0n}}^{x(1)}$ expansion

From Equations (62) and (65),

$$\bar{E}^i = \frac{E_0}{k} \sum_{n=0}^{\infty} a_{0n} \bar{M}_{e_{0n}}^{x(1)} \quad , \quad \bar{H}^i = i \frac{H_0}{k} \sum_{n=0}^{\infty} a_{0n} \bar{N}_{e_{0n}}^{x(1)} \tag{68}$$

where $H_0=E_0/Z_0$ and Z_0 is the free space impedance.

From Equations (30) to (33), and Equation (22), we see that, for n even, the components of $\bar{M}_{e_{0n}}^{x(1)}$ tangential to the disk and the normal component of $\bar{N}_{e_{0n}}^{x(1)}$ are equal to zero. Therefore, in Equation (68), the vector wave functions for n even do not lead to any reflected field. For n odd, the above three components are all proportional to $R_{0n}^{(1)}(-ic, i0)$, and the same components of the functions of index 4 are proportional to $R_{0n}^{(4)}(-ic,i0)$. Since the only difference between a spheroidal vector wave function of index 1 and its counterpart of index 4 is their radial dependence, it is possible to cancel a component of one by that of the other on the surface of the disk with appropriate coefficients in order to satisfy the boundary condition.

$$F^{(1)}(\eta,0,\phi) - \frac{R_{0n}^{(1)'}(-ic,i0)}{R_{0n}^{(4)'}(-ic,i0)} F^{(4)}(\eta,0,\phi) = 0 \quad \text{for } 0<|\eta|\leq 0 \tag{69}$$

where

$$F^{(i)}(\eta,\xi,\phi) = [\bar{M}_{e_{0n}}^{x(i)}]_\eta \, , \, [\bar{M}_{e_{0n}}^{x(i)}]_\phi \, , \, [\bar{N}_{e_{0n}}^{x(i)}]_\xi \, .$$

The term by term cancellation method leads to the following reflected fields which satisfy the boundary conditions on the surface of the disk

$$\bar{E}^r = -\frac{E_0}{k} \sum_{n=1}^{\infty}{}' a_{0n} \frac{R_{0n}^{(1)'}(-ic,i0)}{R_{0n}^{(4)'}(-ic,i0)} \bar{M}_{e_{0n}}^{x(4)} \tag{70}$$

$$\bar{H}^r = -\frac{iH_0}{k} \sum_{n=1}^{\infty}{}' a_{0n} \frac{R_{0n}^{(1)'}(-ic,i0)}{R_{0n}^{(4)'}(-ic,i0)} \bar{N}_{e_{0n}}^{x(4)} \tag{71}$$

where the prime over the summation means that the index of the summation varies by increments of 2 from its initial value. This notation will be used throughout the rest of this work. In the same way, for the other two expansions, we obtain the following formulations.

$\bar{M}_{e_{1n}}^{z(1)}$ expansion

From Equations (64) and (67),

$$\overline{E}^i = \frac{E_o}{k} \sum_{n=1}^{\infty} b_{1n} \overline{M}_{e_{1n}}^{z(1)} \quad , \quad \overline{H}^i = \frac{iH_o}{k} \sum_{n=1}^{\infty} b_{1n} \overline{N}_{e_{1n}}^{z(1)} \tag{72}$$

From Equations (30) to (33), and Equation (22), we see that for n-1 odd, the components of $\overline{M}_{e_{1n}}^{z(1)}$ tangential to the disk and the normal component of $\overline{N}_{e_{1n}}^{z(1)}$ are equal to zero. For n-1 even, the same components are proportional to $R_{1n}^{(1)}(-ic,i0)$ and the corresponding components of the functions of index 4 to $R_{1n}^{(4)}(-ic,i0)$.

Using the same term by term matching technique, we obtain the following reflected fields:

$$\overline{E}^r = - \frac{E_o}{k} \sum_{n=1}^{\infty}{}' b_{1n} \frac{R_{1n}^{(1)}(-ic,i0)}{R_{1n}^{(4)}(-ic,i0)} \overline{M}_{e_{1n}}^{z(4)} \tag{73}$$

$$\overline{H}^r = - \frac{iH_o}{k} \sum_{n=1}^{\infty}{}' b_{1n} \frac{R_{1n}^{(1)}(-ic,i0)}{R_{1n}^{(4)}(-ic,i0)} \overline{N}_{e_{1n}}^{z(4)} \tag{74}$$

$\overline{N}_{e_{0n}}^{y(1)}$ expansion

From Equations (66) and (63),

$$\overline{E}^i = \frac{E_o i}{k} \sum_{n=0}^{\infty} a_{0n} \overline{N}_{e_{0n}}^{y(1)} \quad , \quad \overline{H}^i = - \frac{H_o}{k} \sum_{n=0}^{\infty} a_{0n} \overline{M}_{e_{0n}}^{y(1)} \tag{75}$$

From Equations (30) and (33), and Equation (22), we can see that for n odd, the components of $\overline{N}_{e_{0n}}^{y(1)}$ tangential to the disk and the normal component of $\overline{M}_{e_{0n}}^{y(1)}$ are equal to zero. For n even, the same components are proportional to $R_{0n}^{(1)}(-ic,i0)$ and the corresponding components of the functions of index 4 are proportional to $R_{0n}^{(4)}(-ic,i0)$.

Using the term by term matching technique, we obtain:

$$\overline{E}^r = - \frac{iE_o}{k} \sum_{n=0}^{\infty}{}' a_{0n} \frac{R_{0n}^{(1)}(-ic,i0)}{R_{0n}^{(4)}(-ic,i0)} \overline{N}_{e_{0n}}^{y(4)} \tag{76}$$

$$\bar{H}^r = \frac{H_o}{k} \sum_{n=0}^{\infty}{}' a_{On} \frac{R_{On}^{(1)}(-ic,i0)}{R_{On}^{(4)}(-ic,i0)} \bar{M}_{e_{On}}^{y(4)} \qquad (77)$$

All three pairs of incident and reflected fields satisfy the boundary condition on the disk, excluding the edge. We will study the behavior of $[\bar{E}^i+\bar{E}^r]_\phi$ at the edge in the following section for each case.

2. $[\bar{E}]_\phi$ condition at the edge

We will first give the expansion of $[\bar{E}^i+\bar{E}^r]_\phi$ in the vicinity of the edge, and then present Flammer's method.

a. Behavior of $[\bar{E}^i+\bar{E}^r]_\phi$ at the edge

The edge is located at the coordinates $\eta=0$ and $\xi=0$. We will use the small argument expansions for the angular and radial functions to obtain a power series expansion of $[\bar{E}^i+\bar{E}^r]_\phi$. In each summation, we will only retain the diverging and constant terms, when they exist, and the converging term of smallest order at the edge. We will use the following expansions:

$$\begin{aligned}
(1-\eta^2)^{1/2} &= 1 - \frac{1}{2}\eta^2 + O(\eta^4) && \text{for } \eta \text{ and } \xi \text{ small} \\
(1-\eta^2)^{-1/2} &= 1 + \frac{1}{2}\eta^2 + O(\eta^4) && |\eta| << 1 \\
(1+\xi^2)^{1/2} &= 1 + \frac{1}{2}\xi^2 + O(\xi^4) && \xi << 1 \\
(1+\xi^2)^{-1/2} &= 1 - \frac{1}{2}\xi^2 + O(\xi^4) \quad .
\end{aligned} \qquad (78)$$

We will now consider the three cases.

Case of the $\bar{M}_{e_{On}}^{x(1)}$ expansion

For this case only we will give the whole procedure:

$$[E^i+E^r]_\phi = \frac{1}{k}\sum_{n=0}^{\infty}{}' a_{0n}\frac{2}{d}\frac{1}{\xi^2+\eta^2}\left[\xi(1-\eta^2)\eta(-\lambda_{0n})\left(1+\lambda_{0n}\frac{\xi^2}{2}\right)\right.$$

$$\left.+\left(1-\frac{\eta^2}{2}\lambda_{0n}\right)\eta(1+\xi^2)\xi\lambda_{0n}\right]R_{0n}^{(1)}(-ic,i0)S_{0n}(-ic,0)\cos\phi$$

$$+\frac{1}{k}\sum_{n=1}^{\infty}{}' a_{0n}\frac{2}{d}\frac{1}{\xi^2+\eta^2}\left[\xi(1-\eta^2)\left(1-\frac{\eta^2}{2}(\lambda_{0n}-2)\right)\xi\right.$$

$$\left.+\eta(1+\xi^2)\eta\left(1+\frac{\xi^2}{2}(\lambda_{0n}-2)\right)\right]R_{0n}^{(1)}{}'(-ic,i0)S_{0n}'(-ic,0)\cos\phi$$

$$-\frac{1}{k}\sum_{n=1}^{\infty}{}' a_{0n}\frac{2}{d}\frac{R_{0n}^{(1)}{}'(-ic,i0)}{R_{0n}^{(4)}{}'(-ic,i0)}\frac{1}{\xi^2+\eta^2}\left\{\left[\xi(1-\eta^2)\left(1+\frac{\xi^2}{2}\lambda_{0n}\right)\right.\right.$$

$$\left.\left(1-\frac{\eta^2}{2}(\lambda_{0n}-2)\right)+\eta(1+\xi^2)\eta\xi\lambda_{0n}\right]\frac{i\,S_{0n}'(-ic,0)}{c\,R_{0n}^{(1)}{}'(-ic,i0)}$$

$$+\left[\xi(1-\eta^2)\left(1-\frac{\eta^2}{2}(\lambda_{0n}-2)\right)\xi+\eta(1+\xi^2)\eta\left(1+\frac{\xi^2}{2}(\lambda_{0n}-2)\right)\right]$$

$$\left.R_{0n}^{(4)}{}'(-ic,i0)\times S_{0n}'(-ic,0)\right\}\cos\phi \qquad (79)$$

We can see directly that the n=odd terms of the incident wave are cancelled by part of the terms of the "reflected" field in this expansion. Finally Equation (79) reduces to:

$$[\bar{E}^i+\bar{E}^r]_\phi = \frac{2}{kd}\left\{\eta\xi\sum_{n=0}^{\infty}{}' a_{0n}\lambda_{0n}\frac{2-\lambda_{0n}}{2}R_{0n}^{(1)}(-ic,i0)S_{0n}(-ic,0)\right.$$

$$\left.-\frac{\xi}{\eta^2+\xi^2}\sum_{n=1}^{\infty}{}' \frac{i\,a_{0n}}{c}\left[1+\frac{\lambda_{0n}}{2}(\eta^2+\xi^2)\right]\frac{S_{0n}'(-ic,0)}{R_{0n}^{(4)}{}'(-ic,i0)}\right\}$$

$$\times\cos\phi \qquad (80)$$

The singularity at the edge comes from the second term,

$$\frac{\xi}{\eta^2+\xi^2} \sum_{n=1}^{\infty}{}' \frac{i}{c} a_{0n} \frac{S'_{0n}(-ic,0)}{R^{(4)'}_{0n}(-ic,i0)} \quad ,$$

which does not converge when $\xi \to 0$ and $\eta \to 0$.

Case of the $\overline{M}_{e_{ln}}^{z(1)}$ expansion

The same procedure, taking into account the use of the approximations of Equation (78) leads to the following result.

$$[\overline{E}^i+\overline{E}^r]_\phi = -\frac{2}{kd} \left\{ \eta\, \xi \sum_{n=2}^{\infty} b_{1n} \frac{\lambda_{1n}^{-3}}{2} S'_{1n}(-ic,0) R^{(1)'}_{1n}(-ic,i0) + \frac{\xi}{\eta^2+\xi^2} \sum_{n=1}^{\infty}{}' i \frac{b_{1n}}{c} \left[1 + \frac{\lambda_{1n}^{-2}}{2}(\eta^2+\xi^2)\right] \frac{S_{1n}(-ic,0)}{R^{(4)}_{1n}(-ic,i0)} \right\} \cos\varphi \tag{81}$$

We notice that the singularities in Equations (80) and (81) are of the same order $\xi/(\eta^2+\xi^2)$. This is the reason why Flammer is able to cancel the singularity by taking the incident field as a linear combination of Equations (68) and (72) with proper relative weights of the two expansions.

Case of the $\overline{N}_{e_{0n}}^{y(1)}$ expansion

The $[\overline{N}_{e_{0n}}^{y(1)}]_\phi$ component involves second order derivatives of the angular and radial functions and are, therefore, more complicated to compute. We will use the following expression for that component:

$$[\overline{N}_{e_{0n}}^{y(i)}]_\phi = -\frac{k}{kd^2} \frac{\cos\phi}{\eta^2+\xi^2} \left[-\eta \frac{d}{d\eta}(S_{0n}) R^{(i)}_{0n} + (1-\eta^2) \frac{d^2}{d\eta^2}(S_{0n}) R^{(i)}_{0n} + \xi S_{0n} \frac{d}{d\xi}(R^{(i)}_{0n}) + (1+\xi^2) S_{0n} \frac{d^2}{d\xi^2} R^{(i)}_{0n} \right] \tag{82}$$

Using Equations (13), (14), (23), (24), (26) and (27), we finally obtain for the tangential electric field at the rim:

$$[\bar{E}^r+\bar{E}^i]_\phi = -\frac{4}{k^2d^2}\cos\phi\left\{+i\eta\sum_{n=1}'' a_{0n}\frac{3(\lambda_{0n}-2)}{2}S_{0n}(-ic,0)\right.$$

$$R_{0n}^{(1)'}(-ic,i0)+\frac{\xi}{\eta^2+\xi^2}\sum_{n=0}'\left[1+\eta^2(\lambda_{0n}+c^2)-\frac{3\xi^2}{2}\right.$$

$$\left.\left.(\lambda_{0n}-2)\right]\frac{a_{0n}}{c}\frac{S_{0n}(-ic,0)}{R_{0n}^{(4)}(-ic,i0)}\right\} \qquad (83)$$

These three expansions of the ϕ-component of $\bar{E}^i+\bar{E}^r$ for different incident plane wave expansions behave in the same way in the vicinity of the edge. They each have a singularity which comes from the ill-defined spheroidal vector wave functions at the edge. We have seen by comparing the power series expansions of $R_{mn}^{(1)}(-ic,i\xi)$ and its derivatives for small argument ξ, Equations (23) and (24), to those of $R_{mn}^{(4)}(-ic,i\xi)$, Equations (26) and (27), that part of the expansions of the functions of index 4 is identical to the whole expansion of the function of index 1 except for the change of index. The term by term matching technique exactly cancels these terms between the incident and reflected fields. Therefore, in Equations (80), (81) and (83), the second summation containing the singularity comes from the terms in the expansions of the radial functions of index 4 that do not disappear in the term by term matching. Their coefficient $\xi/(\eta^2+\xi^2)$ shows that, as expected, $\bar{E}^i+\bar{E}^r$ is equal to zero on the surface of the disk. Furthermore, the first summation in Equations (80), (81) and (83) corresponds to the part of the incident plane wave expansion that does not lead to a reflected field since it is equal to zero on the surface of the disk. This summation is also equal to zero at the rim as the factor $\eta\xi$ shows.

b. Flammer's method

In order to satisfy the $[\bar{E}]_\phi$ condition, Flammer[7] simply chose to express the incident wave as the sum of two different expansions whose weights would be adjusted so that the singularity in the ϕ-component of the electric field at the edge would disappear. In order to satisfy the whole edge condition by the procedure, it is necessary to choose the two expansions so that the other components of the fields have the right behavior near the edge. The η- and ξ-components of $\bar{N}_{e_{0n}}^{y(4)}$ have higher order singularities than those of $\bar{M}_{e_{0n}}^{x(1)}$ and $\bar{M}_{e_{1n}}^{z(1)}$, while the latter have the same singularities, and so do their magnetic field counterparts $\bar{N}_{e_{0n}}^{x(1)}$ and $\bar{N}_{e_{1n}}^{z(1)}$. We will show that the choice of

the two expansions in terms of $\bar{M}_{e_{0n}}^{x(1)}$, Equation (68), and $\bar{M}_{e_{1n}}^{z(1)}$, Equation (72), leads to a satisfactory solution.

$$\bar{E}^i = \frac{E_o}{k}\left\{\beta_x \sum_{n=0}^{\infty} a_{0n}\, \bar{M}_{e_{0n}}^{x(1)} + \beta_z \sum_{n=1}^{\infty} b_{1n}\, \bar{M}_{e_{1n}}^{z(1)}\right\} \tag{84}$$

with $\beta_x+\beta_z=1$ in order to have $|\bar{E}^i|=E_o$.

The scattered field will be:

$$\bar{E}^s = -\frac{E_o}{k}\left\{\beta_x \sum_{n=1}^{\infty}{}' a_{0n} \frac{R_{0n}^{(1)'}(-ic,i0)}{R_{0n}^{(4)'}(-ic,i0)}\, \bar{M}_{e_{0n}}^{x(4)} + \beta_z \sum_{n=1}^{\infty}{}' b_{1n} \frac{R_{1n}^{(1)}(-ic,i0)}{R_{1n}^{(4)}(-ic,i0)}\, \bar{M}_{e_{1n}}^{z(4)}\right\} \tag{85}$$

From Equations (80) and (81), we see that the coefficient of the singularity of the expansion of $[\bar{E}^i+\bar{E}^s]_\phi$ is:

$$\frac{2}{kd}\left\{\beta_x \sum_{n=1}^{\infty}{}' \frac{i}{c} a_{0n} \frac{S_{0n}'(-ic,0)}{R_{0n}^{(4)'}(-ic,i0)} + \beta_z \sum_{n=1}^{\infty}{}' \frac{i}{c} b_{1n} \frac{S_{1n}(-ic,0)}{R_{1n}^{(4)}(-ic,i0)}\right\}\cos\phi \tag{86}$$

In order to set this coefficient equal to zero, we must choose β_x and β_z as follows:

$$\begin{cases} \beta_x = -\dfrac{\displaystyle\sum_{n=1}^{\infty}{}' b_{1n} \dfrac{S_{1n}(-ic,0)}{R_{1n}^{(4)}(-ic,i0)}}{\displaystyle\sum_{n=1}^{\infty}{}' a_{0n} \dfrac{S_{0n}'(-ic,0)}{R_{0n}^{(4)'}(-ic,i0)} - \sum_{n=1}^{\infty}{}' b_{1n} \dfrac{S_{1n}(-ic,0)}{R_{1n}^{(4)}(-ic,i0)}} \\ \beta_z = 1-\beta_x \end{cases} \tag{87}$$

With β_x and β_z defined as above, $\bar{E}^i+\bar{E}^s$ satisfies the $[\bar{E}]_\phi$ condition at the edge. Equation (85) gives, then, the bistatic scattered field of the disk with normal incidence and perpendicular polarization (i.e., $\bar{E}^i||\hat{e}_y$). In the next section, we will verify that $\bar{E}^s$ satisfies the whole edge condition, underlining the convenience of Flammer's method which satisfies the edge condition by dealing only with the condition on the ϕ-component of the electric field.

3. The bistatic scattered field

The total scattered electromagnetic field obtained with Flammer's solution is, in the normal incidence case:

$$\overline{E}_{\perp}^{s} = -\frac{E_o}{k}\left\{\beta_x^{\perp}\sum_{n=1}^{\infty}{}' a_{0n}\frac{R_{0n}^{(1)'}(-ic,i0)}{R_{0n}^{(4)'}(-ic,i0)}\,\overline{M}_{e_{0n}}^{x(4)} + \beta_z^{\perp}\sum_{n=1}^{\infty}{}' b_{1n}\frac{R_{1n}^{(1)}(-ic,i0)}{R_{1n}^{(4)}(-ic,i0)}\,\overline{M}_{e_{1n}}^{z(4)}\right\}$$

$$\overline{H}_{\perp}^{s} = -\frac{iH_o}{k}\left\{\beta_x^{\perp}\sum_{n=1}^{\infty}{}' a_{0n}\frac{R_{0n}^{(1)'}(-ic,i0)}{R_{0n}^{(4)'}(-ic,i0)}\,\overline{N}_{e_{0n}}^{x(4)} + \beta_z^{\perp}\sum_{n=1}^{\infty}{}' b_{1n}\frac{R_{1n}^{(1)}(-ic,i0)}{R_{1n}^{(4)}(-ic,i0)}\,\overline{N}_{e_{1n}}^{z(1)}\right\} \qquad (88)$$

where $\beta_x^{\perp}$ and $\beta_z^{\perp}$ are defined by Equation (87).

First we will verify that the above fields satisfy the whole edge condition in the vicinity of the edge. The behavior of each component of the fields will be expressed in terms of local coordinates that have been defined in Appendix A. Second, the bistatic scattered far field will be computed in spherical coordinates.

a. Total field in the vicinity of the edge

The edge condition is expressed in terms of the distance from the edge to the observation point. We will introduce the local coordinate system, valid for η and ξ small, shown in Figure 5-1. We use the following notation:

s = distance from the edge, $s \ll a$

t = angle between the top surface of the disk, $\eta > 0$, and the direction from the edge to the observation point, $0 \le t \le 2\pi$.

ψ = same as in spheroidal coordinates.

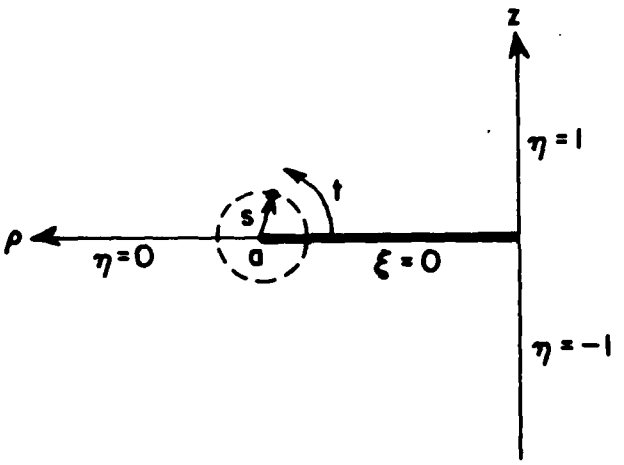

Figure 5-1. (s,t,ϕ) coordinate system.

The correspondance between spheroidal coordinates and these coordinates is derived in Appendix A.

$$\begin{cases} s = \frac{d}{4}(\eta^2+\xi^2) \\ \cos t = \frac{\eta^2-\xi^2}{\eta^2+\xi^2} \\ \sin t = \frac{2\eta\xi}{\eta^2+\xi^2} \end{cases} \tag{89}$$

or, conversely,

$$\begin{cases} \eta = 2\sqrt{\frac{s}{d}}\cos(t/2) \\ \xi = 2\sqrt{\frac{s}{d}}\sin(t/2) \end{cases} \tag{90}$$

The disk is characterized by t=0.

In order to obtain the components of the fields in the new coordinate system, we first expand the radial and angular functions using

their small argument approximations and then transform the terms of lower order with the above formulas.

For the η-component of $\bar{E}=\bar{E}^i+\bar{E}^r$, the singularity in $[\bar{M}_{e_{0n}}^{x(4)}]_\eta$ and $[\bar{M}_{e_{1n}}^{z(4)}]_\eta$ is $(\eta^2+\xi^2)^{-1/2}$, or $s^{-1/2}$, and $[\bar{E}]_\eta$ has a satisfactory behavior near the edge. More precisely, we have

$$[\bar{E}]_\eta = E_o \beta_x^1 \frac{1}{k} \sum_{n=0}^{\infty}{}' a_{0n} \left(-\frac{2}{d}\right) \text{sint}/2 \; S_{0n}(-ic,0) R_{0n}^{(1)''}(-ic,i0)\sin\phi$$

$$+ E_o \beta_x^1 \frac{1}{k} \sum_{n=1}^{\infty}{}' a_{0n} \left(-\frac{2}{d}\right) \sqrt{\frac{s}{d}} \; \text{sint} \; S_{on}'(-ic,0) \left[-\frac{R_{0n}^{(1)'}(ic,i0)}{R_{0n}^{(4)'}(-ic,i0)}\right]$$

$$\times R_{0n}^{(4)''}(-ic,i0)\sin\phi$$

$$+ E_o \beta_z^1 \frac{1}{k} \sum_{n=1}^{\infty}{}' b_{1n} \frac{2}{d} \sqrt{\frac{s}{d}} \; \text{sint} \; S_{1n}(-ic,0) \left[-\frac{R_{1n}^{(1)}(-ic,i0)}{R_{1n}^{(4)}(-ic,i0)}\right]$$

$$\times R_{1n}^{(4)'}(-ic,i0)\sin\phi \qquad (91)$$

The first summation is equal to zero on the surface of the disk but apparently only there. However, if we differentiate Equation (56) again by ξ, we obtain

$$\frac{\partial^2}{\partial\xi^2}[\exp(ikz)] = -k^2 a^2 \eta^2 \exp(ikz) = \sum_{n=0}^{\infty} \gamma_{0n}(0) \; S_{0n}(-ic,\eta) \times R_{0n}^{(1)''}(-ic,i\xi) \qquad (92)$$

At the edge, where $\xi=0$ and $\eta=0$, Equation (92) becomes:

$$\sum_{n=0}^{\infty}{}' \gamma_{0n}(0) \; S_{0n}(-ic,0) R_{0n}^{(1)''}(-ic,i0) = 0 \quad . \qquad (93)$$

The terms of this summation for n odd disappear since, for n odd, $S_{0n}(-ic,0)$ is equal to zero, Equation (14). Equation (93) is the coefficient of sint/2 in the first summation of Equation (91), recalling that by definition $a_{0n}=-i\lambda_{0n}(0)$. Finally we see that Equation (91) contains no term larger than $s^{1/2}$ and therefore, we have at the edge:

$$[\bar{E}]_\eta = O(s^{1/2}) \sin\phi \sin t \tag{94}$$

For the ξ-component of $\bar{E}$, we see that the singularity of $[\bar{M}_{e0n}^{x(4)}]_\xi$ and $[\bar{M}_{e1n}^{x(4)}]_\xi$ is due to a factor $(1/(\eta^2+\xi^2)^{1/2})$, or $s^{-1/2}$, (see the definition of the functions in Flammer[10]) and therefore $[\bar{E}]_\xi$ satisfy the edge condition for this component.

$$[\bar{E}]_\xi = E_o \frac{\beta_x^\perp}{k} \sum_{n=0}^{\infty}{}' a_{0n} \frac{2}{d} \cos t/2 \, S_{0n}(-ic,0) \, R_{0n}^{(1)}(-ic,i0)\sin\phi$$

$$+ E_o \frac{\beta_x^\perp}{k} \sum_{n=1}^{\infty}{}' \frac{i}{c} \frac{a_{0n}}{\sqrt{d}} \frac{S_{0n}'(-ic,0)}{R_{0n}^{(4)'}(-ic,i0)} \frac{(-1)}{\sqrt{s}} \sin\phi$$

$$+ E_o \frac{\beta_z^\perp}{k} \sum_{n=1}^{\infty}{}' b_{1n} \frac{4i}{cd^{3/2}} \sqrt{s} \sin^2 t/2 \frac{S_{1n}(-ic,0)}{R_{1n}^{(4)}(-ic,i0)} \sin\phi \tag{95}$$

The second term varies as $(s)^{-1/2}$ and is therefore predominant. Thus

$$[\bar{E}]_\xi = O(s^{-1/2}) \sin\phi \tag{96}$$

$[\bar{E}]_\phi$ has been computed to match the corresponding condition. We obtain from Equations (80) and (81):

$$[\bar{E}]_\phi = -2\sqrt{\frac{s}{d}} \sin t/2 \frac{E_o}{k} \left\{ \beta_x^\perp \sum_{n=1}^{\infty}{}' \frac{ia_{0n}}{c} \lambda_{0n} \frac{S_{0n}'(-ic,0)}{R_{0n}^{(4)'}(-ic,i0)} \right.$$

$$\left. + \beta_z^\perp \sum_{n=1}^{\infty} \frac{ib_{1n}}{c} (\lambda_{1n}-2) \frac{S_{1n}(-ic,0)}{R_{1n}^{(4)}(-ic,i0)} \right\} \cos\phi \tag{97}$$

Thus, as expected,

$$[\bar{E}]_\phi = O(s^{1/2}) \cos\phi \sin t/2 \tag{98}$$

The total electric field obtained from Equations (84) and (85) satisfies the edge condition. We now need to check the components of the total magnetic field, which are expressed in terms of the functions $\bar{N}_{e0n}^{x(i)}$ and $\bar{N}_{e1n}^{z(i)}$. Because of the greater complexity of these functions, we will only determine their order of variation. Since the order of the singularities of each component is not apparent directly from the definition of the functions, we will write out the diverging terms for each component as function of η and ξ, and then we can write the components of the total magnetic field $\bar{H}$. Since we will only be looking at singularities, we will not include in the following expressions, the summations corresponding to the incident waves since they are well defined at the edge, that is to say, of order 1 or smaller.

For the η-component of $\bar{H}$, we have the following singularities at the edge:

For n odd,

$$[\bar{N}_{e0n}^{x(4)}]_\eta(\eta,\xi,\phi) = \frac{4i\, S_{0n}'(-ic,0)}{ckd^2 R_{0n}^{(1)'}(-ic,i0)} \frac{\cos\phi}{(\eta^2+\xi^2)^{5/2}} [\eta^2-\xi^2+O(\eta^4,\eta^2\xi^2,\xi^4)]$$

$$[\bar{N}_{e1n}^{z(4)}]_\eta(\eta,\xi,\phi) = -\frac{i4}{ckd^2} \frac{S_{1n}(-ic,0)}{R_{1n}^{(1)}(-ic,i0)} \frac{\cos\phi}{(\eta^2+\xi^2)^{5/2}} [\xi^2-\eta^2+O(\eta^4,\eta^2\xi^2,\xi^4)] \tag{99}$$

From Equations (89) and (90) we find that:

$$\eta^2-\xi^2 = \frac{4s}{d}\cos t\ , \quad \frac{\eta^2-\xi^2}{(\eta^2+\xi^2)^{5/2}} = \left(\frac{4s}{d}\right)^{-3/2}\cos t \tag{100}$$

and

$$\frac{1}{(\eta^2+\xi^2)^{5/2}}\ O(\eta^4,\eta^2\xi^2,\xi^4) = O(s^{-1/2})$$

From the definition of the scattered magnetic field, Equation (88) and from Equations (99) to (100), we obtain the following expansion:

$$[\bar{H}]_\eta = \frac{H_o}{2ck^2d^{1/2}} \left\{ \beta_x^1 \sum_{n=1}^{\infty}{}' a_{0n} \frac{S'_{0n}(-ic,0)}{R^{(4)'}_{0n}(-ic,i0)} s^{-3/2} \cos t + \beta_z^1 \sum_{n=1}^{\infty}{}' b_{1n} \frac{S_{1n}(-ic,0)}{R^{(4)}_{1n}(-ic,i0)} s^{-3/2} \cos t \right\} \cos\phi + 0(s^{-1/2}) \tag{101}$$

By definition of β_x^1 and β_z^1, Equations (86) and (87), the coefficient of $s^{-3/2}$ in $[\bar{H}]_\eta$ is equal to zero. Thus,

$$[\bar{H}]_\eta = 0(s^{-1/2}) \cos\phi \tag{102}$$

For the ξ-component of $\bar{H}$, we have in the same way, for n odd:

$$[\bar{N}^{x(4)}_{e_{0n}}]_\xi = -\frac{4i}{ckd^2} \frac{S'_{0n}(-ic,0)}{R^{(1)'}_{0n}(-ic,i0)} \frac{\cos\phi}{(\eta^2+\xi^2)^{5/2}} [-2\eta\xi - \eta\xi^3(1-\lambda_{0n}) + 0(5)]$$

$$[\bar{N}^{z(4)}_{e_{1n}}]_\xi = -\frac{4i}{ckd^2} \frac{S_{1n}(-ic,0)}{R^{(1)}_{1n}(-ic,i0)} \frac{\cos\phi}{(\eta^2+\xi^2)^{5/2}} [-2\eta\xi - \eta\xi^3 + 0(5)] \tag{103}$$

where $0(5) = 0(\eta^5, \eta^4\xi, \eta^3\xi^2, \eta^2\xi^3, \eta^4\xi, \xi^5)$.

From Equations (89) and (90), we find:

$$\frac{2\eta\xi}{(\eta^2+\xi^2)^{5/2}} = \left(\frac{4s}{d}\right)^{-3/2} \sin t$$

$$\frac{\eta\xi^3}{(\eta^2+\xi^2)^{5/2}} = \frac{\sqrt{d}}{2\sqrt{s}} \sin t \sin^2 t/2 \tag{104}$$

and

$$\frac{0(5)}{(\eta^2+\xi^2)^{5/2}} = 0(1)$$

We have then the following expansion of the ξ-component of the total magnetic field, recalling that the terms coming from the incident field are of the order of 1 or smaller:

$$[\bar{H}]_\xi = \frac{H_o}{2ck^2d^{1/2}} \left\{ \beta_x^{\perp} \sum_{n=1}^{\infty} a_{0n} \frac{S'_{0n}(-ic,0)}{R^{(4)}_{0n}(-ic,i0)} \times \left(s^{-3/2+4} \frac{s^{-1/2}}{d} (1-\lambda_{0n}) \right) \sin^2 t/2 \sin t \right.$$

$$\left. + \beta_z^{\perp} \sum_{n=1}^{\infty} b_{1n} \frac{S_{1n}(-ic,0)}{R^{(4)}_{1n}(-ic,i0)} \times \left(s^{-3/2+} \frac{4}{d} s^{1/2} \right) \sin^2 t/2 \sin t \right\} \cos\phi + O(1) \tag{105}$$

Again by definition of $\beta_x^{\perp}$ and $\beta_z^{\perp}$, the coefficient of the improper singularity in $[\bar{H}]_\xi$, normal to the disk, disappears. Thus,

$$[\bar{H}]_\xi = O(s^{-1/2}) \cos\phi \sin t \tag{106}$$

For the ϕ-component of $\bar{H}$, the singularities of the vector wave function involved are of order $s^{-1/2}$. They are, however, cancelled by the coefficients introduced to satisfy the edge condition on $[\bar{E}]_\phi$.

For n odd,

$$[\bar{N}e^{x(4)}_{0n}]_\phi(\eta,\xi,\phi) = + \frac{4i}{ckd^2} \frac{S'_{0n}(-ic,0)}{R^{(1)'}_{0n}(-ic,i0)} \frac{\eta}{\eta^2+\xi^2} \sin\phi + O(1) \tag{107}$$

$$[\bar{N}e^{z(4)}_{1n}]_\phi(\eta,\xi,\phi) = - \frac{4i}{ckd^2} \frac{S_{1n}(-ic,0)}{R^{(1)}_{1n}(-ic,i0)} \frac{(-\eta)}{\eta^2+\xi^2} \sin\phi + O(1)$$

where $\frac{\eta}{\eta^2+\xi^2} = \frac{1}{2}\sqrt{\frac{d}{s}} \cos t/2$

From the definition of the scattered magnetic field and from Equation (107), we obtain for the total field:

$$[\bar{H}]_\phi = \frac{2H_o}{ck^2d^{3/2}} \left\{ \beta_x^1 \sum_{n=1}^{\infty}{}' a_{0n} \frac{S'_{0n}(-ic,0)}{R^{(4)'}_{0n}(-ic,i0)} s^{-1/2} \cos t/2 \right.$$

$$\left. + \beta_z^1 \sum_{n=1}^{\infty}{}' b_{1n} \frac{S_{1n}(-ic,0)}{R^{(4)'}_{1n}(-ic,i0)} s^{-1/2} \cos t/2 \right\} \sin\phi + O(1) \tag{108}$$

By definition of β_x^1 and β_z^1, the coefficient of $s^{-1/2}$ disappears and finally

$$[\bar{H}]_\phi = O(1) \sin\phi \tag{109}$$

Therefore, the total magnetic field $\bar{H}$ satisfies the edge condition. We have thus verified that the scattered field obtained by Flammer by matching the ϕ-component of the electric field at the rim satisfies the whole edge condition.

We summarize the different results:

$$\begin{aligned} &[\bar{E}]_\eta = O(s^{1/2}),\ [\bar{E}]_\xi = O(s^{-1/2}),\ [\bar{E}]_\phi = O(s^{1/2}) \\ &[\bar{H}]_\eta = O(s^{-1/2}),\ [\bar{H}]_\xi = O(s^{-1/2}),\ [\bar{H}]_\phi = O(1) \end{aligned} \tag{110}$$

The formal solution for the bistatic, normal incidence, perpendicular polarization case satisfies the boundary conditions on the disk including the edge and is therefore proved. In the next section we will compute the scattered far-field for the above case.

b. Bistatic scattered far-field in normal incidence

The bistatic scattered electric far-field for normal incidence and perpendicular polarization can be obtained from Equation (88) by replacing the vector wave functions by their large radial argument approximations, listed in Equation (34). From Appendix A, we will use the approximation of the coordinate system for large ξ.

When $c\xi \to -1$,

$$\hat{e}_\eta \to -\hat{e}_\theta$$

$$\hat{e}_\xi \to \hat{e}_r$$

$$\eta \to \cos\theta$$

$$\sqrt{1-\eta^2} \to \sin\theta \qquad (111)$$

$$c\xi \to kr$$

$$\frac{2}{\xi d} \to \frac{1}{r}$$

Thus the scattered field becomes:

$$\overline{E}_\perp^s = -\frac{E_o}{k}\left\{ \hat{e}_\theta \beta_x^\perp \sum_{n=1}^{\infty}{}' a_{0n} \frac{R_{0n}^{(1)'}(-ic,i0)}{R_{0n}^{(4)'}(-ic,i0)} i^n \; S_{0n}(-ic,\cos\theta)\sin\phi \right.$$
$$+ \hat{e}_\phi \left[\beta_x^\perp \sum_{n=1}^{\infty}{}' a_{0n} \frac{R_{0n}^{(1)'}(-ic,i0)}{R_{0n}^{(4)'}(-ic,i0)} i^n \; S_{0n}(-ic,\cos\theta)\cos\theta \right.$$
$$\left. \left. - \beta_z^\perp \sum_{n=1}^{\infty}{}' b_{1n} \frac{R_{1n}^{(1)}(-ic,i0)}{R_{1n}^{(4)}(-ic,i0)} i^n \; S_{0n}(-ic,\cos\theta)\sin\theta \right] \right.$$
$$\left. \times \cos\phi \right\} \frac{\exp(-ikr)}{r} \qquad (112)$$

$$\overline{H}_\perp^s = i\frac{H_o}{k}\left\{ \hat{e}_\theta \left[\beta_x^\perp \sum_{n=1}^{\infty}{}' a_{0n} \frac{R_{0n}^{(1)'}(-ic,ic)}{R_{0n}^{(4)'}(-ic,i0)} i^{n-1} \; S_{0n}(-ic,\cos\theta)\cos\theta \right.\right.$$
$$\left. \left. - \beta_z^\perp \sum_{n=1}^{\infty}{}' b_{1n} \frac{R_{1n}^{(1)}(-ic,i0)}{R_{1n}^{(4)}(-ic,i0)} i^{n-1} \; S_{1n}(-ic,\cos\theta)\sin\theta \right] \cos\phi \right.$$
$$\left. - \hat{e}_\phi \beta_x^\perp \sum_{n=1}^{\infty}{}' \frac{R_{0n}^{(1)'}(-ic,i0)}{R_{0n}^{(4)'}(-ic,i0)} i^{n-1} \; S_{0n}(-ic,\cos\theta)\sin\phi \right\} \times \frac{e^{-ikr}}{r}$$
$$(113)$$

We can easily check that $\overline{E}^s \times \overline{H}^s$ is parallel to $\vec{e}_r$ since we are in the far field region.

The electric field given by Equation (112) has been programmed, and the results are compared with those obtained from the program derived by Hodge[9] with Meixner's solution in a later section. We will now study Flammer's approach to the arbitrary incidence, arbitrary polarization bistatic case.

B. Arbitrary Incidence

In the previous section the disk scattering for a normally incident plane wave with perpendicular polarization has been solved. The general solution for arbitrary incidence can be attempted following the same approach.

The general formula for the incident field, Equation (3), can be separated into two components

$$\overline{E}^i = E_0(\cos\alpha\ \overline{E}^{i\parallel} + \sin\alpha\ \overline{E}^{i\perp})$$

where

$$\begin{aligned} \overline{E}^{i\parallel} &= (\cos\theta_0\ \hat{a}_x - \sin\theta_0\ \hat{a}_z)e^{-i\overline{k}^i\cdot\overline{r}} \\ \overline{E}^{i\perp} &= \hat{a}_y\ e^{-i\overline{k}^i\cdot\overline{r}} \end{aligned} \tag{114}$$

Let us define $\overline{E}^{s\parallel}_{\perp}$ as the scattered field corresponding to the incident field $\overline{E}^{i\parallel}_{\perp}$. The general scattered field will be obtained from $\overline{E}^{s\perp}$ and $\overline{E}^{s\parallel}$ as follows:

$$\overline{E}^s = E_0(\cos\alpha\ \overline{E}^{s\parallel} + \sin\alpha\ \overline{E}^{s\perp}) \tag{115}$$

In order to follow the method of the previous sections, we will expand $\overline{E}^{i\parallel}$ and $\overline{E}^{i\perp}$ as sums of two different expansions. We will use Equations (44) and (46) for $\overline{E}^{i\perp}$, and Equations (47) and (49) for $\overline{E}^{i\parallel}$. The H-fields can be expressed with the corresponding spheroidal wave functions.

$$\bar{E}^{i\perp} = \frac{\beta_x^{\perp}}{ik\cos\theta_o} \sum_{m=0}^{\infty} \sum_{n=m}^{\infty} \gamma_{mn}(\theta_o)\, \bar{M}_{e_{mn}}^{x(1)}$$

$$- \frac{\beta_z^{\perp}}{ik\sin\theta_o} \sum_{m=0}^{\infty} \sum_{n=m}^{\infty} \gamma_{mn}(\theta_o)\, \bar{M}_{e_{mn}}^{z(1)} \qquad (116)$$

$$\bar{E}^{i\parallel} = \frac{\beta_x^{\parallel}}{k\cos\theta_o} \sum_{m=0}^{\infty} \sum_{n=m}^{\infty} \gamma_{mn}(\theta_o)\, \bar{N}_{e_{mn}}^{x(1)}$$

$$- \frac{\beta_z^{\parallel}}{k\sin\theta_o} \sum_{m=0}^{\infty} \sum_{n=m}^{\infty} \gamma_{mn}(\theta_o)\, \bar{N}_{e_{mn}}^{z(1)} \qquad (117)$$

where $\beta_x^{\perp} + \beta_z^{\perp} = 1$, $\beta_x^{\parallel} + \beta_z^{\parallel} = 1$.

Unlike the case of normal incidence these expansions involve all the values of m and, therefore, all the different ϕ-dependences. The reflected fields are calculated using the same term by term matching technique as in the normal incidence case. From Equations (30) to (33), we obtain the following expansions.

$$\bar{E}^{r\perp} = -\frac{\beta_x^{\perp}}{ik} \sum_{m=0}^{\infty} \sum_{n=m+1}^{\infty}{}' \frac{\gamma_{mn}(\theta_o)}{\cos\theta_o} \frac{R_{mn}^{(1)'}(-ic,i0)}{R_{mn}^{(4)'}(-ic,i0)}\, \bar{M}_{e_{mn}}^{x(4)}$$

$$+ \frac{\beta_z^{\perp}}{ik} \sum_{m=0}^{\infty} \sum_{n=m}^{\infty}{}' \frac{\gamma_{mn}(\theta_o)}{\sin\theta_o} \frac{R_{mn}^{(1)}(-ic,i0)}{R_{mn}^{(4)}(-ic,i0)}\, \bar{M}_{e_{mn}}^{z(4)} \qquad (118)$$

$$\bar{E}^{r\parallel} = -\frac{\beta_x^{\parallel}}{k} \sum_{m=0}^{\infty} \sum_{n=m}^{\infty}{}' \frac{\gamma_{mn}(\theta_o)}{\cos\theta_o} \frac{R_{mn}^{(1)}(-ic,i0)}{R_{mn}^{(4)}(-ic,i0)}\, \bar{N}_{e_{mn}}^{x(4)}$$

$$+ \frac{\beta_z^{\parallel}}{k} \sum_{m=0}^{\infty} \sum_{n=m+1}^{\infty}{}' \frac{\gamma_{mn}(\theta_o)}{\sin\theta_o} \frac{R_{mn}^{(1)'}(-ic,i0)}{R_{mn}^{(4)'}(-ic,i0)}\, \bar{N}_{e_{mn}}^{z(4)} \qquad (119)$$

For arbitrary values of $\beta_x^{\perp\!\!\!\perp}$ and $\beta_z^{\perp\!\!\!\perp}$, the edge conditions is not satisfied. As in the normal incidence case, we will try to satisfy the edge condition by simply satisfying the $[\bar{E}]_\phi$ condition at the edge. We will study the perpendicular polarization case in more detail. The method can be exactly paralleled for the parallel polarization case. We will now expand the ϕ-component of the total electric field in the vicinity of the edge for the perpendicular polarization case. We need the expansion of the summations on $\bar{M}_{emn}^{x(i)}$ and $\bar{M}_{emn}^{z(i)}$ in terms of η and ξ.

In the same way that we derived the expansions of $[\bar{E}^i+\bar{E}^r]_\phi$ in the vicinity of the edge for the normal incidence, perpendicular polarization case for plane wave expansions in terms of $\bar{M}_{e0n}^{x(1)}$, Equation (80), and $\bar{M}_{e1n}^{z(1)}$, Equation (81), we obtain here in the arbitrary incidence case:

$$
\begin{aligned}
[\bar{E}^i+\bar{E}^r]_\phi = \frac{1}{kd}\,\beta_x^{\perp}\sum_{m=0}^{\infty}\Bigg\{ & \eta\xi \sum_{n=m}^{\infty}{}' \frac{i\gamma_{mn}(\theta_0)}{\cos\theta_0}\,(\lambda_{mn}-m^2-2)\,\frac{\lambda_{mn}-m^2-2}{2} \\
& \times R_{mn}^{(1)}(-ic,i0)\,S_{mn}^{(1)}(-ic,0) \\
& - \frac{\xi}{\eta^2+\xi^2}\sum_{n=m+1}^{\infty}{}' \frac{\gamma_{mn}(\theta_0)}{c\,\cos\theta_0}\left(1+\frac{\lambda_{mn}-m^2}{2}\,(\eta^2+\xi^2)\right) \\
& \times \frac{S'_{mn}(-ic,0)}{R_{mn}^{(4)'}(-ic,i0)}\Bigg\} \times [(1+\delta_{0m})\cos(m+1)\phi+(1-\delta_{0m})\cos(m-1)\phi] + \\
& + \frac{2}{kd}\,\beta_z^{\perp}\sum_{m=0}^{\infty}\Bigg\{ -\eta\xi \sum_{n=m+1}^{\infty}{}' i\,\frac{\gamma_{mn}(\theta_0)}{\sin\theta_0}\,\frac{\lambda_{mn}-m^2-2}{2} \\
& \times S'_{mn}(-ic,0)\,R_{mn}^{(1)'}(-ic,i0) \\
& + \frac{\xi}{\eta^2+\xi^2}\sum_{n=m}^{\infty}{}' \frac{\gamma_{mn}(\theta_0)}{c\,\sin\theta_0}\left(1+\frac{\lambda_{mn}-m^2-1}{2}\,(\eta^2+\xi^2)\right)\frac{S_{mn}(-ic,0)}{R_{mn}^{(4)}(-ic,i0)}\Bigg\} \times \\
& \times \cos m\phi \qquad (120)
\end{aligned}
$$

where δ_{mn} is the standard Kronecker symbol.

The condition on $[E^i+E^r]_\perp$ is that it be zero on the rim. $\beta_x^\perp$ and $\beta_z^\perp$ must then cancel the coefficient of the singularity $\xi/(\rho^2+\xi^2)$ in Equation (120). If we reorder the coefficient of the singularity and equate it to zero, we obtain the following equation:

$$\frac{1}{kd}\sum_{m=0}^{\infty}\left\{-\beta_x^\perp\left[\sum_{n=m}^{\infty}{}' \frac{\gamma_{m-1n}(\theta_o)}{c\cos\theta_o}\frac{S'_{m-1n}(-ic,0)}{R^{(4)'}_{m-1n}(-ic,i0)}(1-\delta_{0m})(1+\delta_{1m})\right.\right.$$

$$\left.+\sum_{n=m+2}^{\infty}{}' \frac{\gamma_{m+1n}(\theta_o)}{c\cos\theta_o}\frac{S'_{m+1n}(-ic,0)}{R^{(4)'}_{m+1n}(-ic,i0)}\right]$$

$$\left.+2\beta_z^\perp\sum_{n=m}^{\infty}{}' \frac{\gamma_{mn}(\theta_o)}{c\sin\theta_o}\frac{S_{mn}(-ic,0)}{R^{(4)}_{mn}(-ic,i0)}\right\}\cos m\phi = 0 \qquad (121)$$

Note that the coefficients $\beta_x^\perp$ and $\beta_z^\perp$ have been taken inside of the summation of index m.

Because of the ϕ-orthogonality, the coefficient of each factor $\cos m\phi$ must be equal to zero. Because of the relation $\beta_x^\perp+\beta_z^\perp=1$, we obtain for $\beta_x^\perp$ and $\beta_z^\perp$ the various following relationships that must be satisfied simultaneously.

For m=0

$$\beta_x^\perp = \frac{2\sum_{n=0}^{\infty}{}' \frac{\gamma_{0n}(\theta_o)}{c\sin\theta_o}\frac{S_{0n}(-ic,0)}{R^{(4)}_{0n}(-ic,i0)}}{\sum_{n=2}^{\infty}{}' \frac{\gamma_{1n}(\theta_o)}{c\cos\theta_o}\frac{S'_{1n}(-ic,0)}{R^{(4)'}_{1n}(-ic,i0)}+2\sum_{n=0}^{\infty}{}' \frac{\gamma_{0n}(\theta_o)}{c\sin\theta}\frac{S_{0n}(-ic,0)}{R^{(4)}_{0n}(-ic,i0)}} \qquad (122)$$

$$\beta_z^\perp = 1-\beta_x^\perp$$

for m=1

$$\beta_x^{\perp} = \left(2 \sum_{n=1}^{\infty}{}' \frac{\gamma_{1n}(\theta_o)}{c \sin\theta_o} \frac{S_{1n}(-ic,0)}{R_{1n}^{(4)}(-ic,i0)} \right) \Bigg/ \left(2 \sum_{n=1}^{\infty}{}' \frac{\gamma_{0n}(\theta_o)}{c \cos\theta_o} \frac{S_{0n}'(-ic,0)}{R_{0n}^{(4)'}(-ic,i0)} \right.$$

$$\left. + \sum_{n=3}^{\infty}{}' \frac{\gamma_{2n}(\theta_o)}{c \cos\theta_o} \frac{S_{2n}'(-ic,0)}{R_{2n}^{(4)'}(-ic,i0)} + 2 \sum_{n=1}^{\infty}{}' \frac{\gamma_{1n}(\theta_o)}{c \sin\theta_o} \frac{S_{1n}(-ic,0)}{R_{1n}^{(4)}(-ic,i0)} \right) \tag{123}$$

$$\beta_z^{\perp} = 1 - \beta_x^{\perp} .$$

In the limit when θ_o tends to zero, these coefficients lead to those of the normal incidence case.

For m>1

$$\beta_x^{\perp} = \left(\sum_{n=m}^{\infty}{}' \frac{\gamma_{mn}(\theta_o)}{c \sin\theta_o} \frac{S_{mn}(-ic,0)}{R_{mn}^{(4)}(-ic,i0)} \right) \Bigg/ \left(\sum_{n=m}^{\infty}{}' \frac{\gamma_{mn}(\theta_o)}{c \sin\theta_o} \frac{S_{mn}(-ic,0)}{R_{mn}^{(4)}(-ic,i0)} \right.$$

$$+ \frac{1}{2} \sum_{n=m}^{\infty}{}' \frac{\gamma_{m-1n}(\theta_o)}{c \cos\theta_o} \frac{S_{m-1n}'(-ic,0)}{R_{m-1n}^{(4)'}(-ic,i0)}$$

$$\left. + \frac{1}{2} \sum_{n=m+2}^{\infty}{}' \frac{\gamma_{m+1n}(\theta_o)}{c \cos\theta_o} \frac{S_{m+1n}'(-ic,0)}{R_{m+1n}^{(4)'}(-ic,i0)} \right) \tag{124}$$

$$\beta_z^{\perp} = 1 - \beta_x^{\perp} .$$

In order to satisfy the $[\overline{E}]_{\phi}$ condition at the edge, $\beta_x^{\perp}$ and $\beta_z^{\perp}$ must satisfy Equations (122), (123) and (124) for every value of m. According to our definition in Equation (116), $\beta_x^{\perp}$ and $\beta_z^{\perp}$ are independent of m since they represent the relative weights of the two different incident plane wave expansions. To see if a pair $(\beta_x^{\perp}, \beta_z^{\perp})$ can

satisfy the $[\bar{E}]_\phi$ condition at the edge, the different expressions of $\beta_x^\perp$, for example, in Equations (122) to (124) should be computed for various values of m. However, since the vector wave functions of index i=1 are not independent, the fact that the coefficients should take different values for each m is not a proof that the solution is invalid. If this happens, another approach introduced by Flammer[7] can be used. Instead of one pair $(\beta_x^\perp, \beta_z^\perp)$, Flammer uses a whole set of pairs $(\beta_{x_m}^\perp, \beta_{z_m}^\perp)$ where $\beta_{x_m}^\perp$ and $\beta_{z_m}^\perp$ satisfy the Equations (122) to (124) corresponding to the value of m. Note that while $\beta_{z_m}^\perp$ will then be the coefficient of the summation over n of $\bar{M}_{e_{mn}}^{z(1)}$ in the incident field, $\beta_{x_m}^\perp$ is not the weight of the summation over n of $\bar{M}_{e_{mn}}^{x(1)}$ but of other functions whose ϕ-dependence is due to one trinogometric function only per component, instead of product of trigonometric functions in the case of $\bar{M}_{e_{mn}}^{x(1)}$. This is due to the reordering necessary to obtain Equation (121). The new functions $\bar{M}_{e_{m+1n}}^{+(i)}$ and $\bar{M}_{e_{m-1n}}^{-(i)}$ are defined in Flammer's book[10]. Their m-index, m+1 and m-1 respectively, represent the order of their ϕ-dependence. In order to write the incident field used by Flammer, we introduce the relation

$$\text{for } m \geq 1 \quad \bar{M}_{e_{mn}}^{x(i)} = \bar{M}_{e_{m+1n}}^{+(i)} + \bar{M}_{e_{m-1n}}^{-(i)}$$

$$\text{for } m=0 \quad \bar{M}_{e_{0n}}^{x(i)} = 2\,\bar{M}_{e_{1n}}^{+(i)} \tag{125}$$

The incident field is then equal to the following formula:

$$\bar{E}^{i\perp} = \frac{E_o}{ik} \sum_{m=0}^{\infty}{}' \left\{ (1-\delta_{0m})\, \beta_{xm-1}^\perp \sum_{n=m}^{\infty} \frac{\gamma_{mn}(\theta_o)}{\cos\theta_o}\, \bar{M}_{e_{m-1,n}}^{-(1)} \right.$$

$$+ (1+\delta_{0m})\, \beta_{x_{m+1}}^\perp \sum_{n=m}^{\infty} \frac{\gamma_{mn}(\theta_o)}{\cos\theta_o}\, \bar{M}_{e_{m+1,n}}^{+(1)}$$

$$\left. - \beta_{z_m}^\perp \sum_{n=m}^{\infty} \frac{\gamma_{mn}(\theta_o)}{\sin\theta_o}\, \bar{M}_{e_{mn}}^{z(1)} \right\} \tag{126}$$

where $\beta_{x_m}^\perp$ and $\beta_{z_m}^\perp$ satisfy the corresponding condition, Equations (122) to (124)^m.

A term by term matching technique leads to a reflected field which satisfies the boundary conditions on the surface of the disk and the $[\bar{E}]_\phi$ condition at the edge. But, when these coefficients are utilized in Equation (126), it is not clear whether these expansions still represent plane waves. This question remains to be answered.

By introducing different coefficients for each value of m, we have modified the initial plane wave expansions. Since the vector wave functions of index 1 are not independent, the incident field of Equation (126) may still be a plane wave. This needs to be checked for every value of θ_0. Computations of Equation (126) on the surface of the disk should be made to verify whether or not Flammer's solution is valid for arbitrary incidence. In his paper[7], Flammer does not mention the problem. It is in no way proven and a computational verification, though not a proof, should be made in future work.

C. Numerical Test of the Normal Incidence Case

A computer program based on Equation (112) computes the scattered electric far field in the normal incidence, perpendicular polarization, bistatic case. We will successively introduce the variables computed by the program, present the computed data, and discuss the results.

1. Computer program

The program, presented in Appendix D, computes the value of $\hat{E}$, where $\hat{E}$ is defined by:

$$\bar{E}_\perp^s = \frac{E_0}{k} \frac{\exp(-ikr)}{kr} \hat{E} \tag{127}$$

The functions and subroutines presented in Reference[9] were used for this purpose. The output data are, as in Hodge's program for Meixner's solution[9]:

the magnitude and phase of the θ- and ϕ- components of $\hat{E}$,

the normalized cross sections of the disk corresponding to the θ- and ϕ-components of $\hat{E}$ as follows:

$$\sigma_\alpha(\theta_s,\phi_s) = \frac{1}{\pi a^2} \lim_{r\to\infty} \left[4\pi r^2 \frac{|[\bar{E}_\perp^s]_\alpha|^2}{E_0^2} \right] = \frac{4}{k^2 a^2} |[\hat{E}]_\alpha|^2$$

$$\sigma_\alpha(\theta_s,\phi_s) = \frac{4}{c^2} |[\hat{E}]_\alpha(\theta_s,\phi_s)|^2 \tag{128}$$

where $\alpha = \theta,\phi$.

The normalization is obtained by dividing the scattering cross section by the surface area of the disk. The magnitude of the cross section in the scattering direction defined by (θ_s,ϕ_s) is equal to $[\sigma_\theta^2(\theta_s,\phi_s)+\sigma_\phi^2(\theta_s,\phi_s)]^{1/2}$.

2. Data

The results obtained from Equation (112) will be compared to computations made with Meixner's solution. Meixner's far-field solution has been studied extensively by Hodge[9], who wrote a computer program which calculates the electric far-field for arbitrary incidence and polarization. The results of Hodge's program show very favorable agreement with measurements, with calculations based on the small disk approximation, and with Geometrical Theory of Diffraction (GTD) computations. We will accept that program as a comparison source for the results obtained from Flammer's solution.

Various plots of both solutions have been made and we will use the following notation for the curves, except where otherwise stated:

———— continuous line for Flammer's solution

-------- dashed line for Meixner's solution.

In the cases where $\phi_s=0°$, $\bar{H}$-plane, or $\phi_s=90°$, $\bar{E}$-plane, the normalized cross section and the phase will be that of the non-zero component of $\hat{E}$, σ_ϕ when $\phi_s=0°$ or σ_θ when $\phi_s=90°$, respectively. For other values of ϕ_s, the cross sections corresponding to the two components of $\hat{E}$ will be plotted.

3. Results

From the plots drawn, we can see generally good agreement between both theories. We notice the following tendencies:

The concordance between the two solutions is very good for small disks - $ka\leq 2$ -. In Figures 5.2 to 5.4, the low frequency ends of the curves match very well. Figures 5.5, 5.8, 5.11 and 5.13 show a very good agreement for both magnitude and phase in the case ka=2. For ka=4, Figures 5.6 and 5.14 show a reasonably good agreement for the $\bar{E}$-plane cross section and for the phase of $\hat{E}$ in the $\bar{H}$-plane, but the values of the $\bar{H}$-plane cross sections differ greatly as θ_1 approaches 90°, Figure 5.9. ka=2 seems a reasonable limit for the low frequency region where the two solutions match well.

As can be seen from Figures 5.2, 5.3 and more from Figure 5.4, the oscillations of the cross section as a function of ka do not match

very well. Actually, the tendency is the same but the minima and maxima are shifted as ka increases when compared with the GTD solution in the backscatter case, Meixner's solution gives a much better result for large disks.

For a disk of given size, ka, the agreement of the $\overline{E}$ plane cross section is rather good even for large values of ka as shown in Figure 5.5, 5.6 and 5.7. The greater difference between the two solutions in this E plane appears to be the value of the minima.

On the other hand, the ϕ-components do not match very well for values of θ_s greater than 20° for large values of ka. Figure 5.8, for ka=2, shows good agreement but, Figure 5.10, for ka=10, shows $\overline{H}$-plane values obtained from Flammer's solution much larger than those obtained from Meixner's as θ_s approaches 90°. The difference almost reaches a factor 2.5 (i.e., $\sim$4 dB) for θ_s=90°.

We have seen that this difference appears also in the $\overline{H}$-plane cross section for ka=4 and in the ϕ-part of Figure 5.12. The good agreement for ka=2 makes less likely an error in the programming of Flammers solution, but nevertheless, that possibility cannot be rejected. When ϕ_s=0° and θ_s=90°, $[\hat{E}]_\phi$ is proportional to β_7^1. An error due to a truncation or a precision problem may appear in the computation of β_7^1 for large values of ka. In our program we used the same criterion to truncate the infinite summations as Hodge's[9], and, therefore, one would not expect that this should lead to a difference.

The phases, Figures 5.13 to 5.18, seem in general on good agreement for all values of θ_s, except for an evident problem in Figures 5.13, 5.14 and 5.18. The phase of the θ-component of the field obtained from Meixner's solution is consistently 180° out of phase with that obtained by Flammer. Thus there is apparently a sign problem in one of the components of Hodge's since he does not obtain the same phase for the backscatter case, θ_s=0°, for ϕ_s=0° and ϕ_s=90° as can be seen by comparing Figures 5.13 and 5.15, for ka=2, and Figures 5.14 and 5.17 for ka=10. We verify that the scattered electric field must have the same phase for ϕ_s=0° and ϕ_s=90° when θ_s=0°:

$$\begin{aligned} \phi_s=0° \quad & \overline{E}^s = E_\phi^s \hat{e}_\phi = E_\phi^s \hat{e}_y \\ \phi_s=90° \quad & \overline{E}^s = E_\theta^2 \hat{e}_\theta = E_\theta^s \hat{e}_y \end{aligned} \tag{129}$$

Flammer's solution, as calculated, satisfies this condition.

From the data, we see that we have an overall correspondence between Flammer's and Meixner's solutions for the bistatic normal

incidence, parallel polarization case. However, except in the case of small electric circumference, ka, the curves are never quite equal. The weakest point of the solution is apparently the behavior of the ϕ-component of the scattered far-field in the $\overline{H}$ plane in the neighborhood of the plane of the disk.

D Conclusion

In this part, we have rederived Flammer's solution for the normal incidence, perpendicular polarization, bistatic case. We have shown that, with an appropriate choice of the two expansions of the incident plane wave, the condition on the ϕ-component of the total electric field at the edge is equivalent to the whole edge condition. This remarkable property will not appear in Meixner's solution as we will see in the next section. It is a characteristic of Flammer's approach. No answer has been given to the question of the validity of the general solution for arbitrary incidence and polarization. The computational checks explained in Section B should allow a better understanding of Flammer's approach. The numerical test of Flammer's electric scattered far-field has led to mixed conclusions. Despite an overall agreement with Meixner's solution, Flammer's fields, show some important deviations. These might be due to computer problems.

We will now consider Meixner's considerably different approach to the problem of the scattering by a disk.

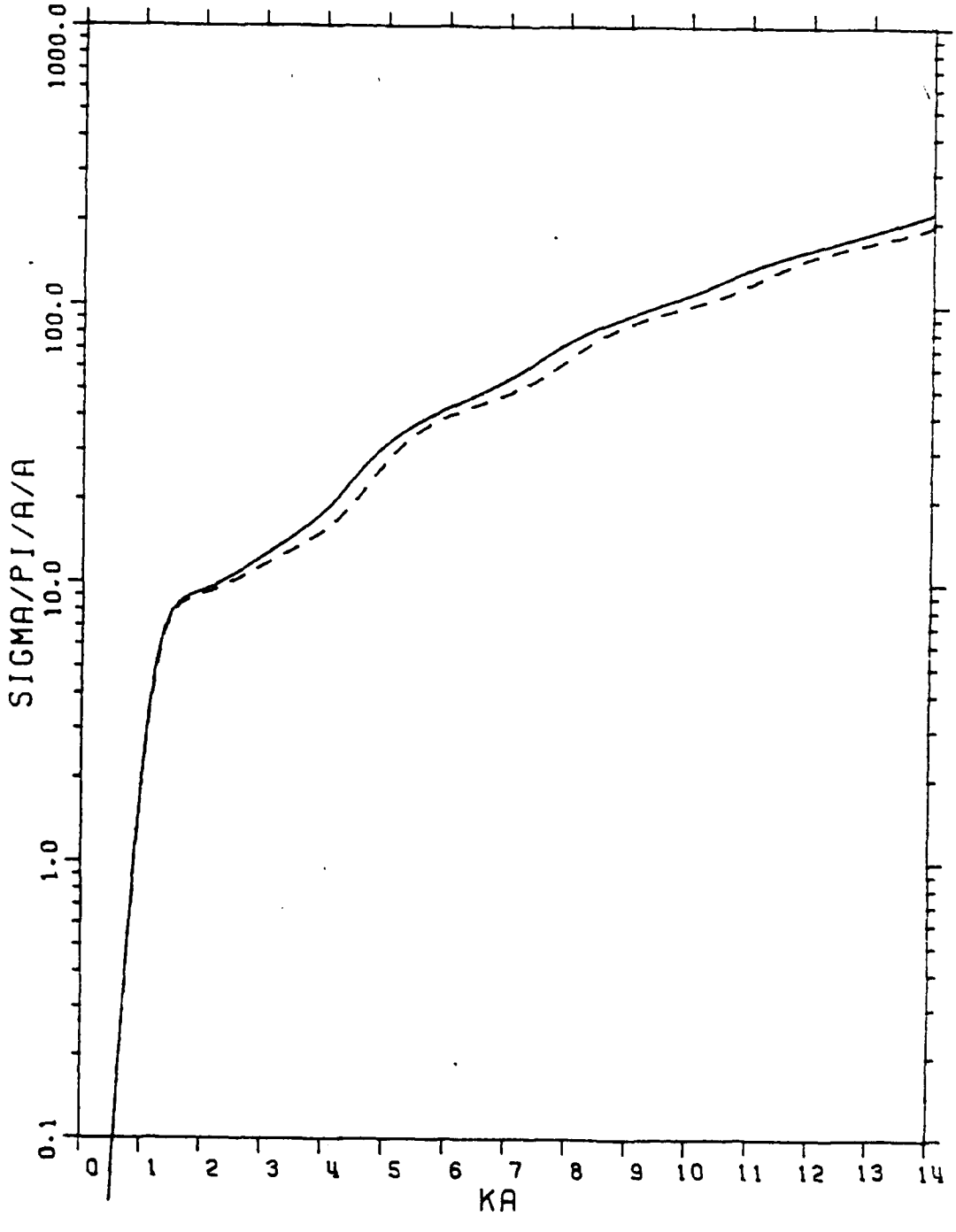

Figure 5.2. Backscatter normalized cross section as a function of ka.

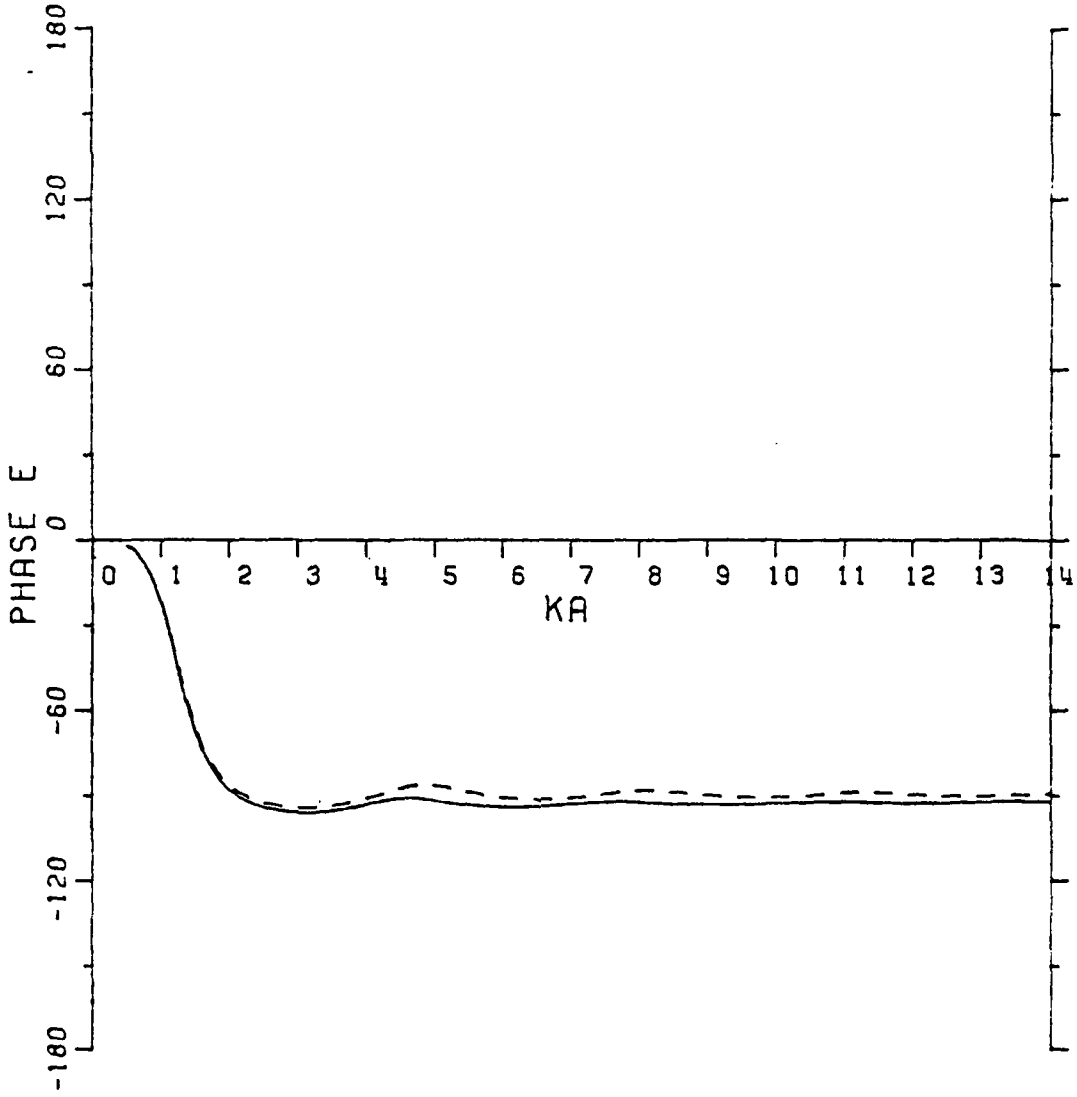

Figure 5.3. Backscatter phase of $\overline{E}^s$.

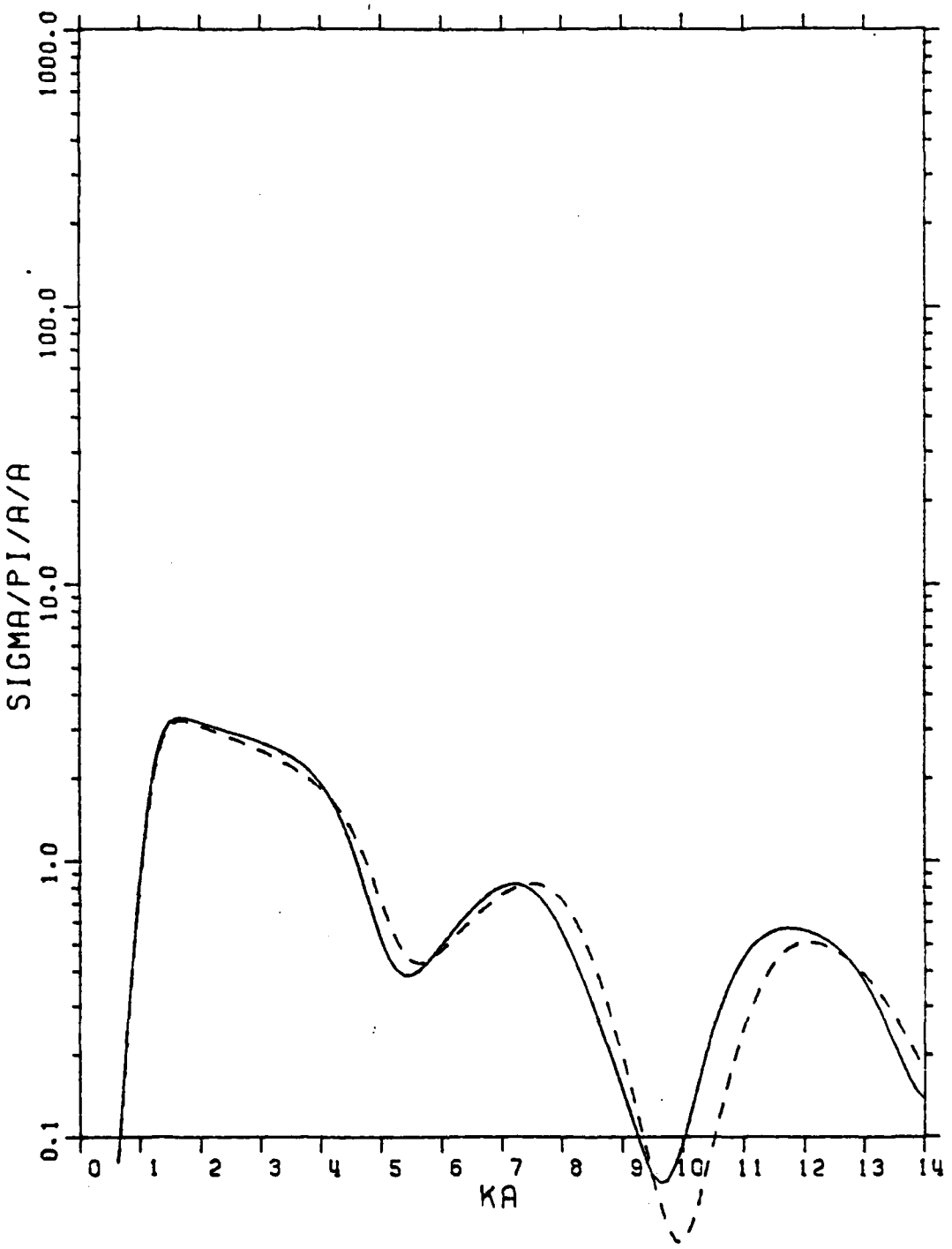

Figure 5.4. Normalized cross section as function of ka for ϕ_S=90°; θ_S=45°.

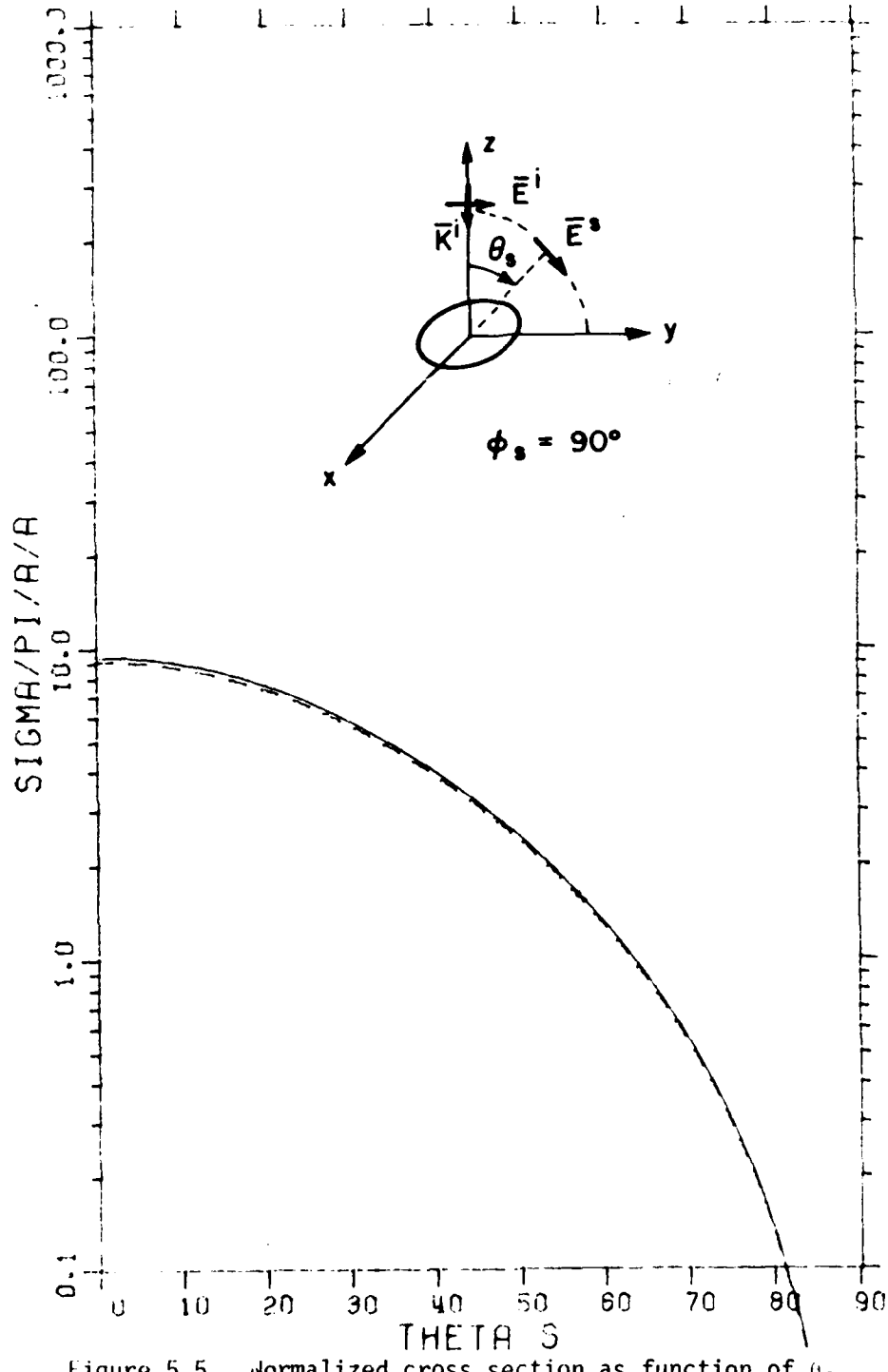

Figure 5.5. Normalized cross section as function of θ_s for ka=2; ϕ_s=90° (E-plane).

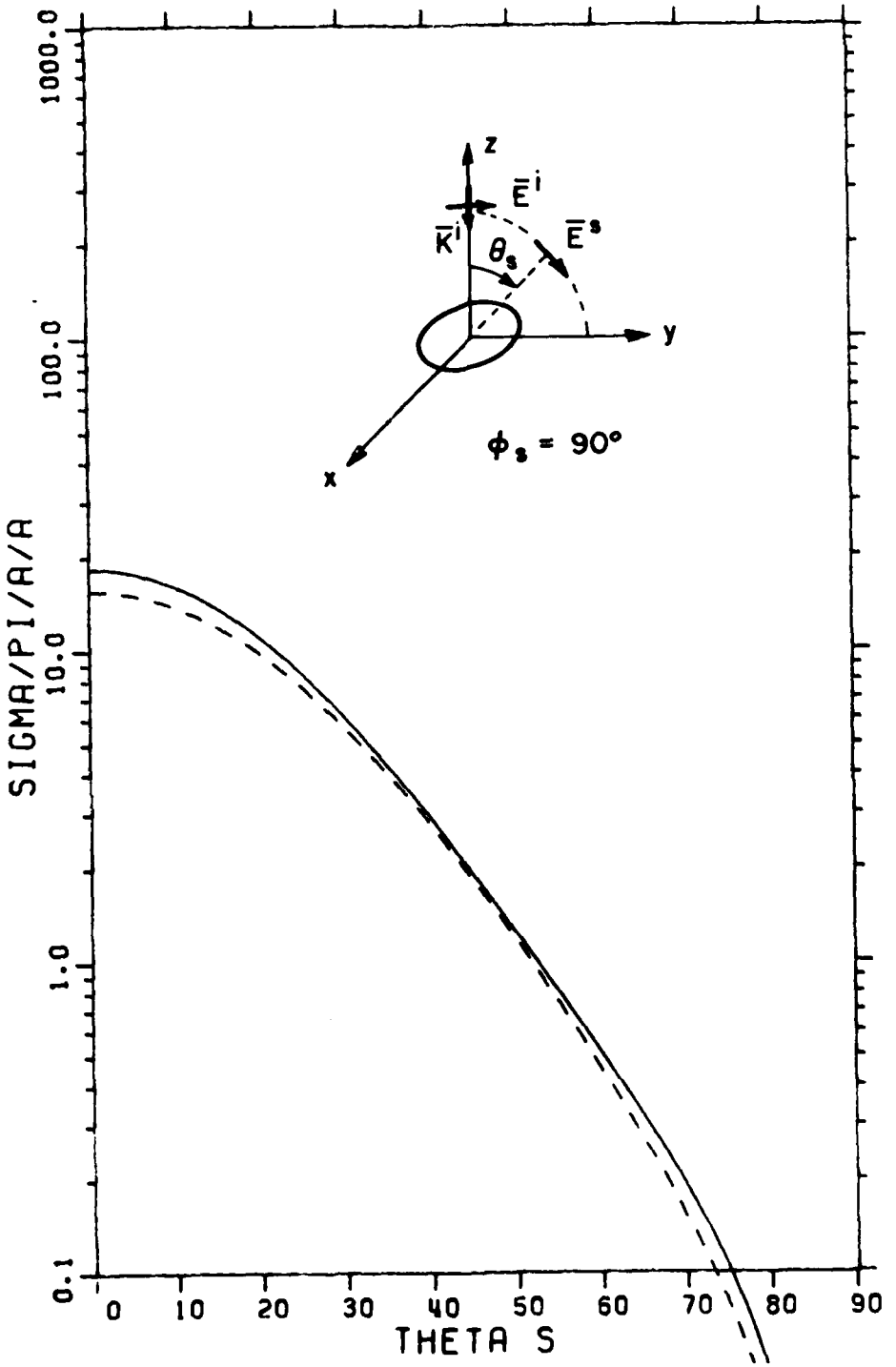

Figure 5.6. Normalized cross section as function of θ_S for ka=4; ϕ_S=90° (E-plane).

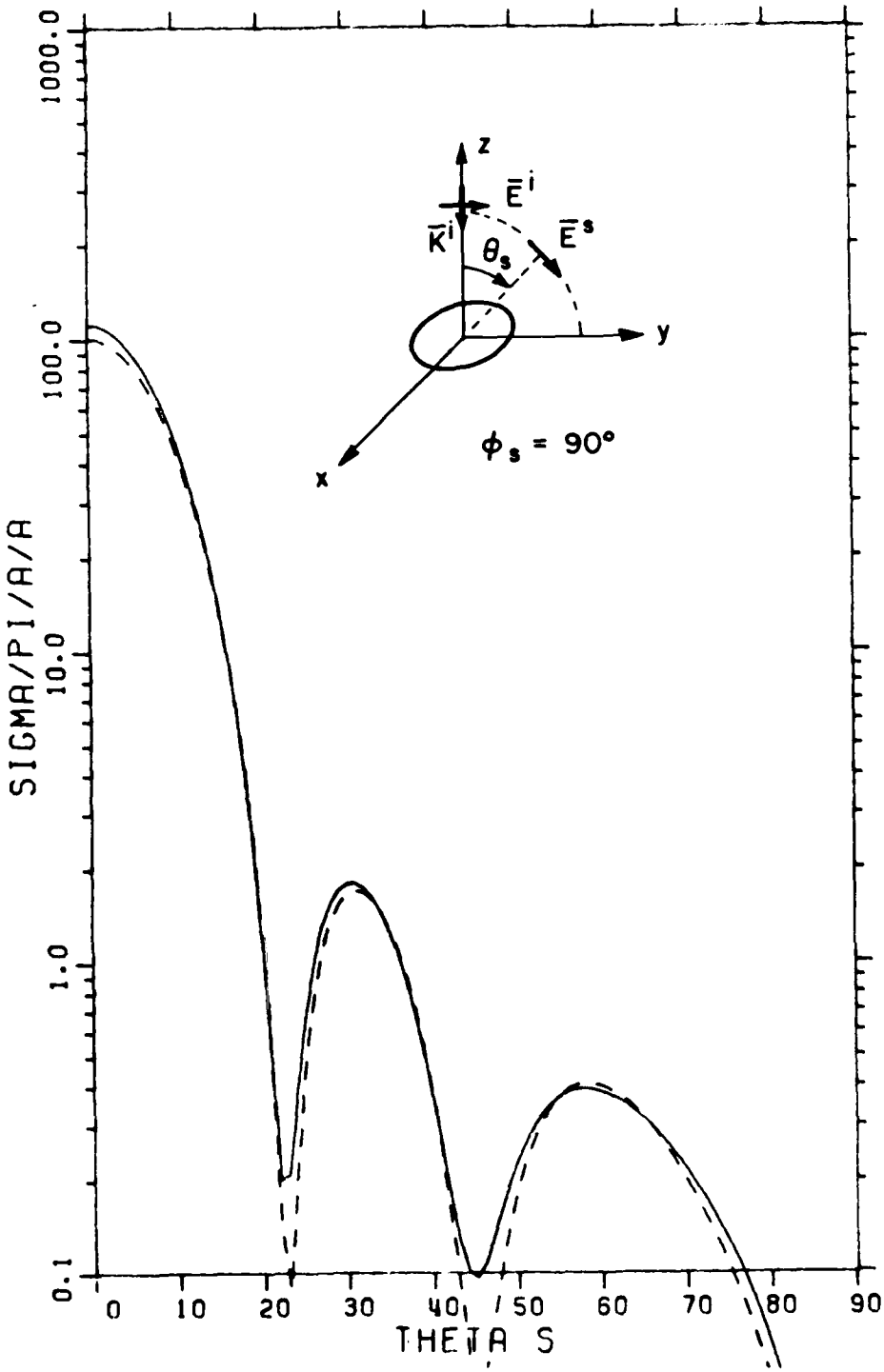

Figure 5.7. Normalized cross section as function of θ_s for ka=10; ϕ_s=90° (E-plane).

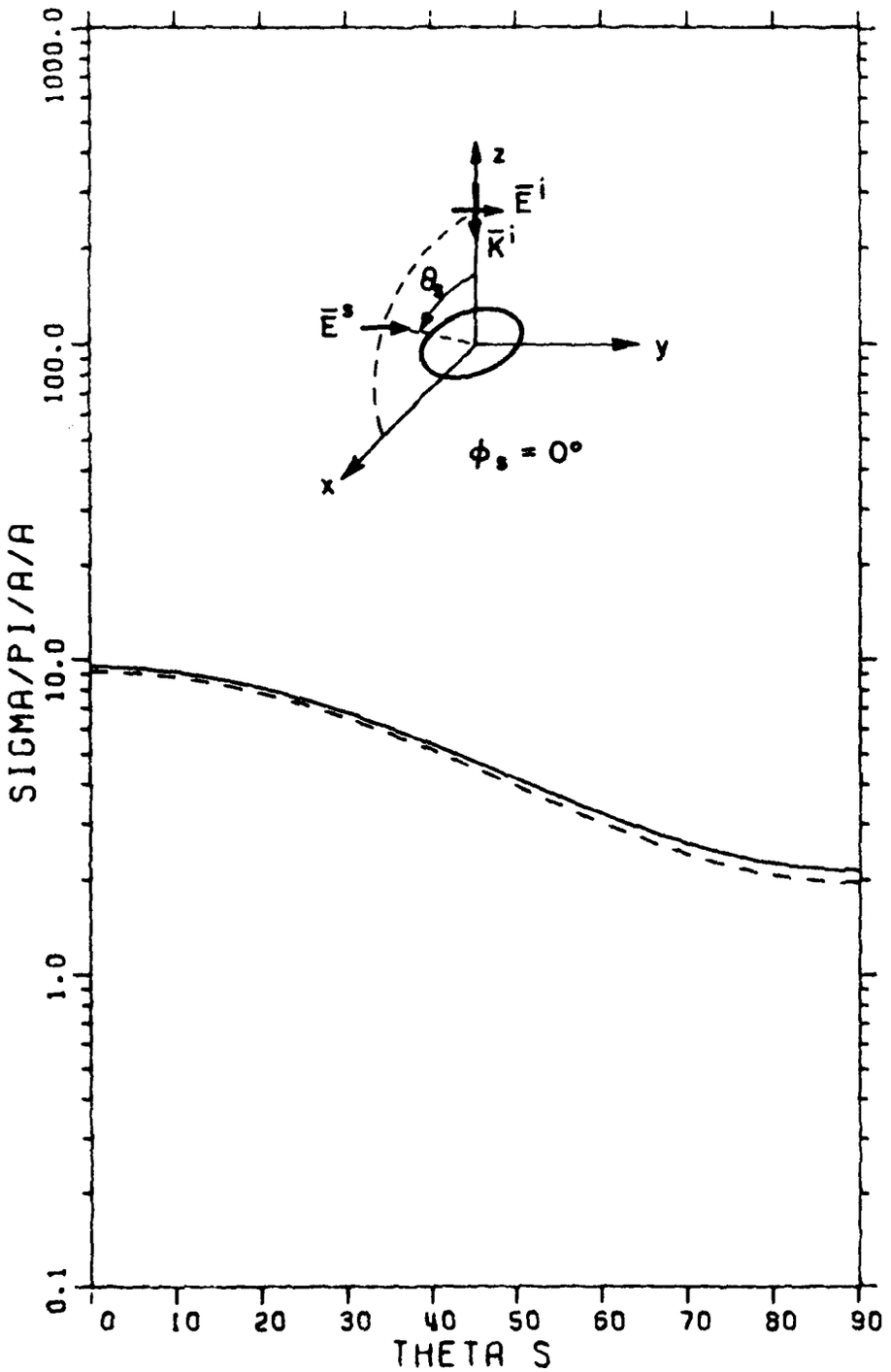

Figure 5.8. Normalized cross section as function of θ_S for ka=2; ϕ_S=0 (H-plane).

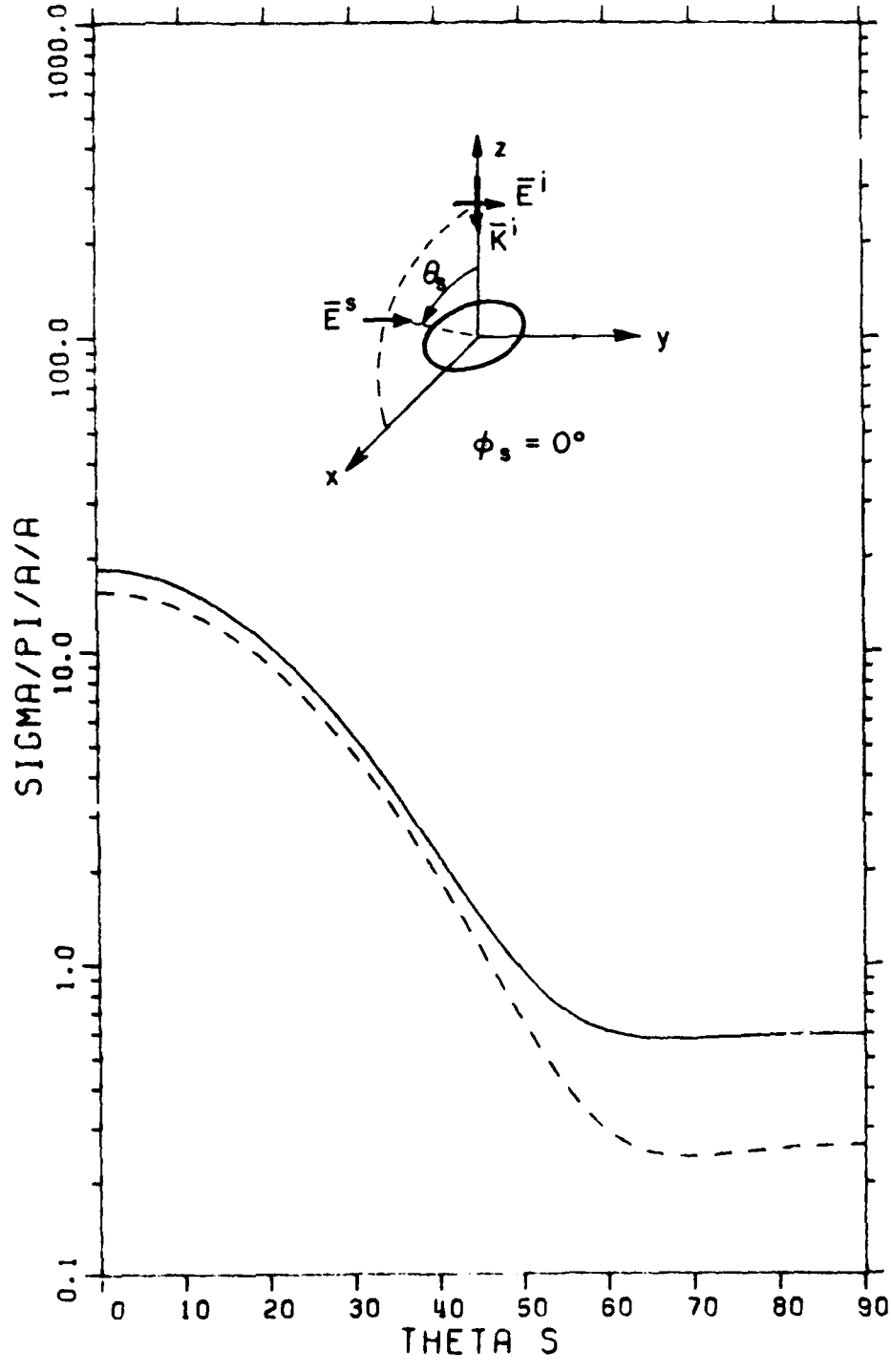

Figure 5.9. Normalized cross section as function of θ_s for ka=4; ϕ_s=0 (H-plane).

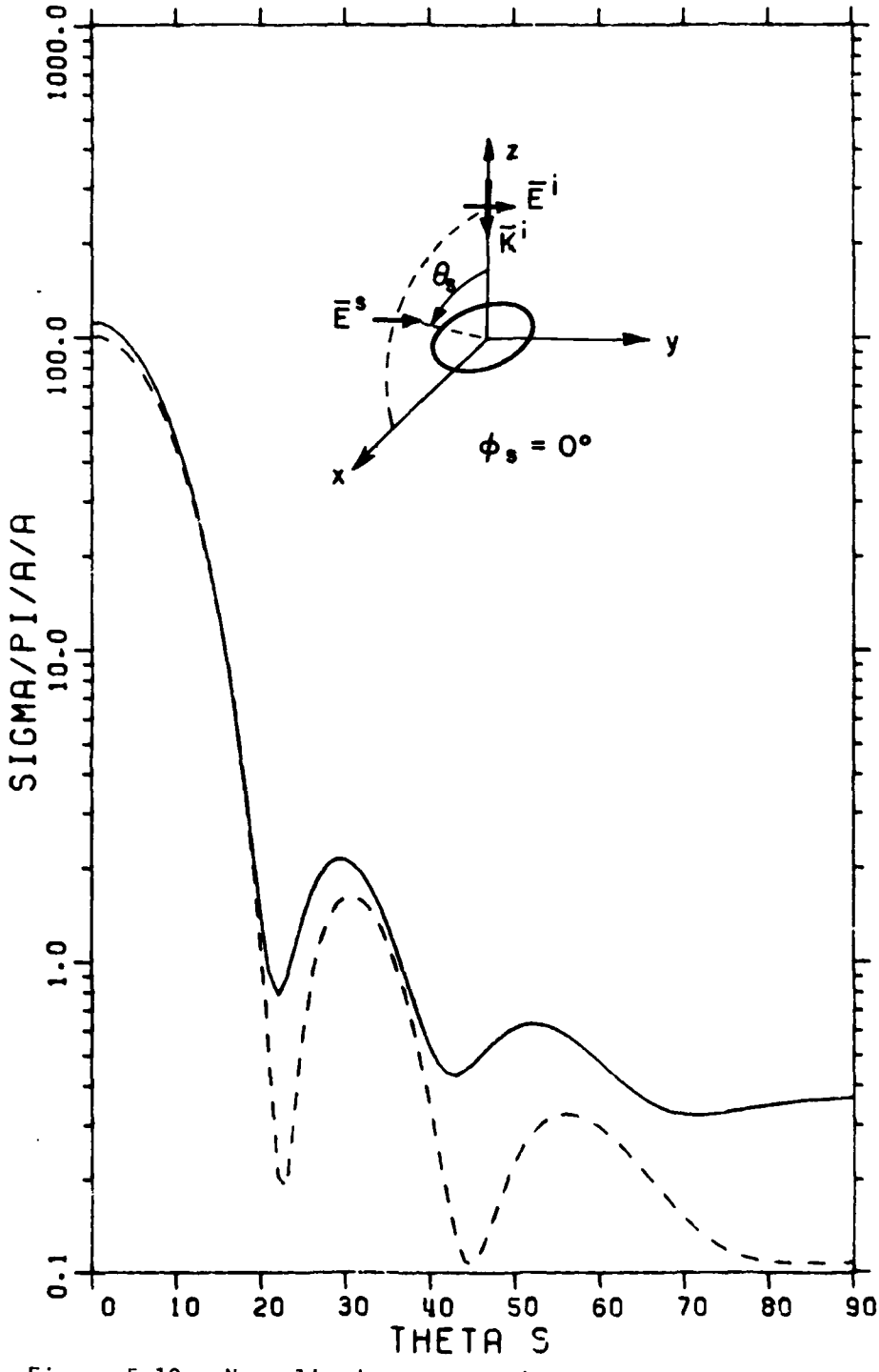

Figure 5.10. Normalized cross section as a function of θ_S for ka=10; ϕ_S=0 (H-plane).

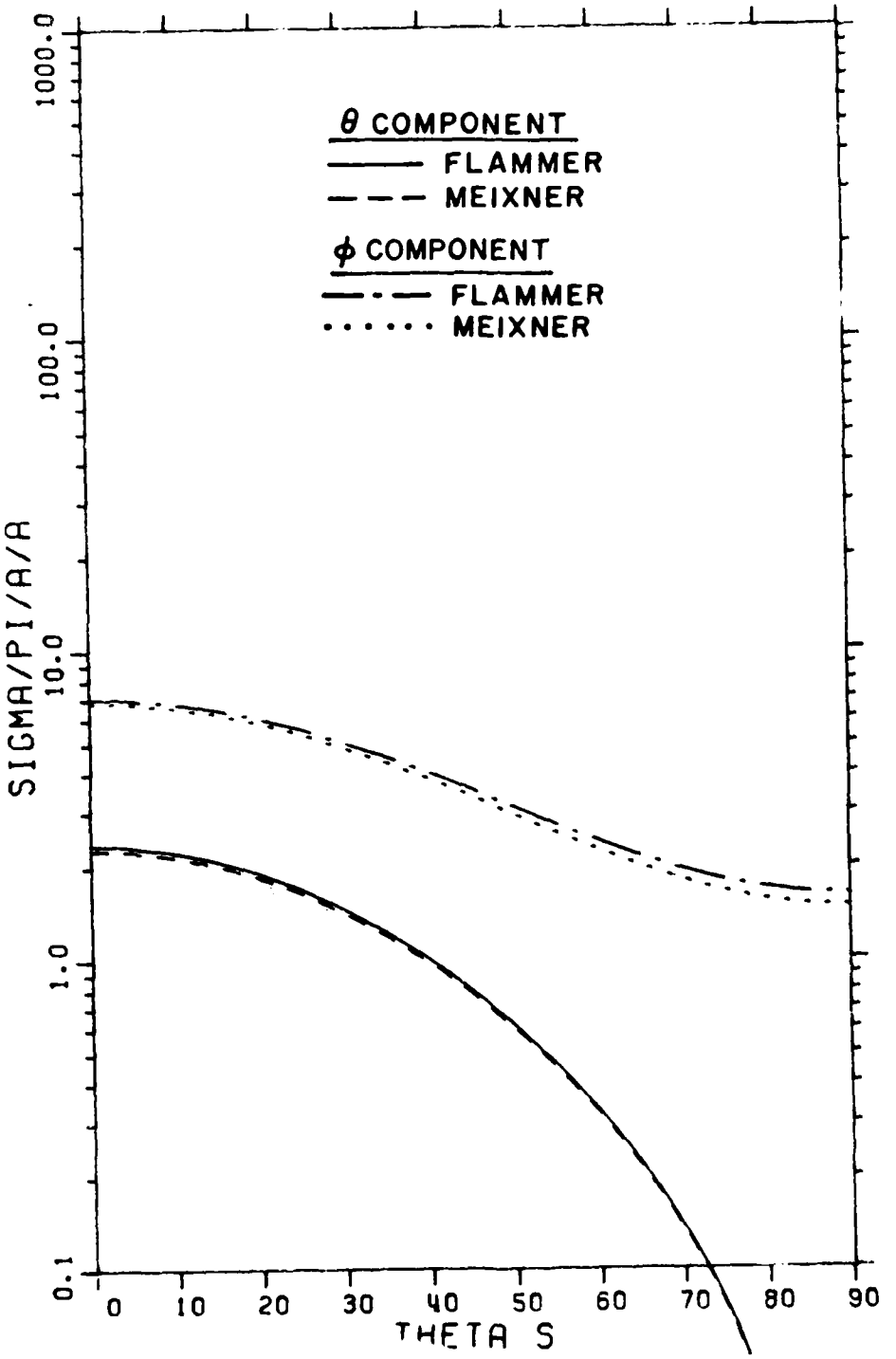

Figure 5.11. Normalized cross section as a function of θ_S for ka=2; ϕ_S=30°.

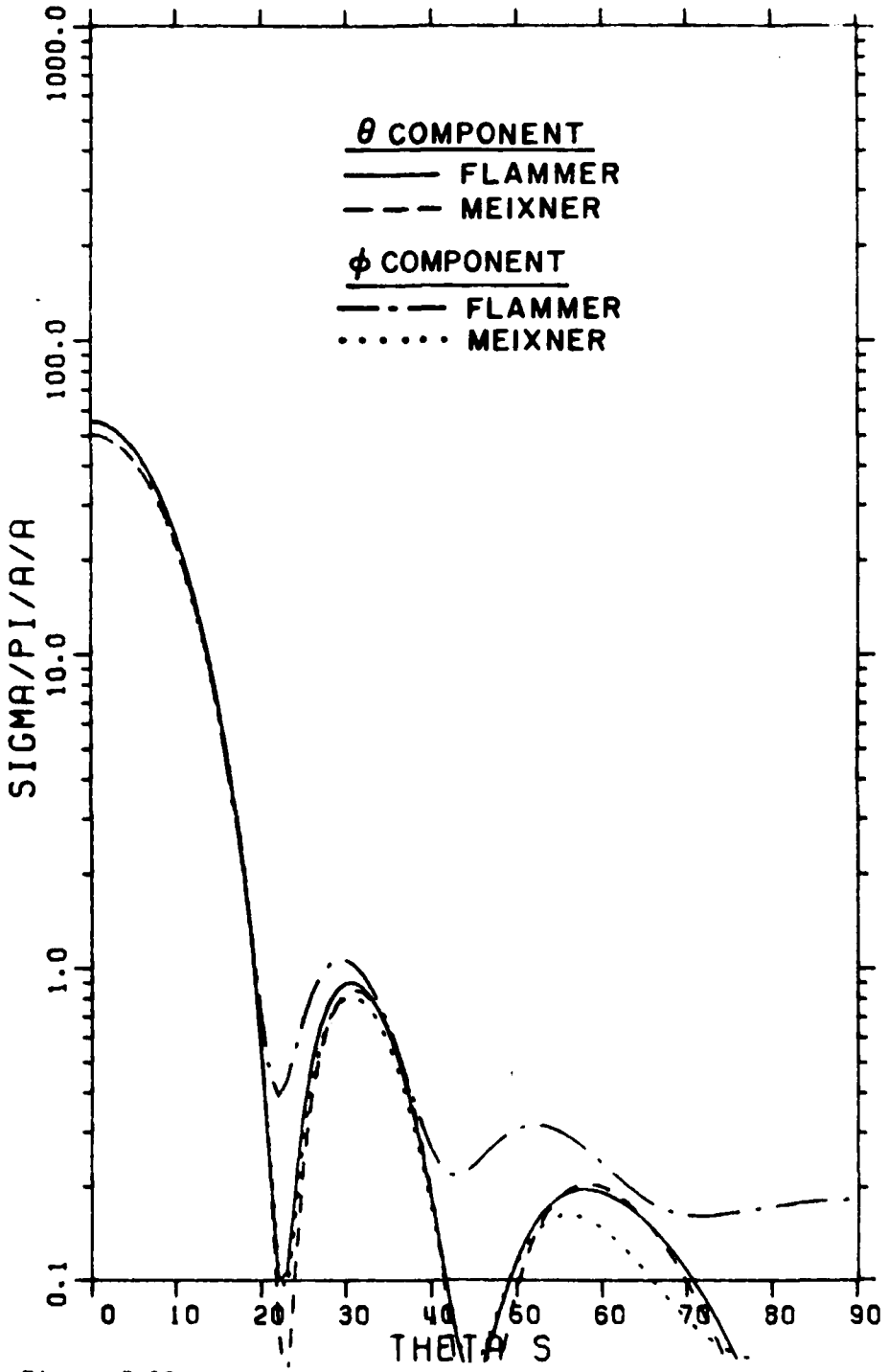

Figure 5.12. Normalized cross section as a function of θ_S for ka=10; ϕ_S=45°.

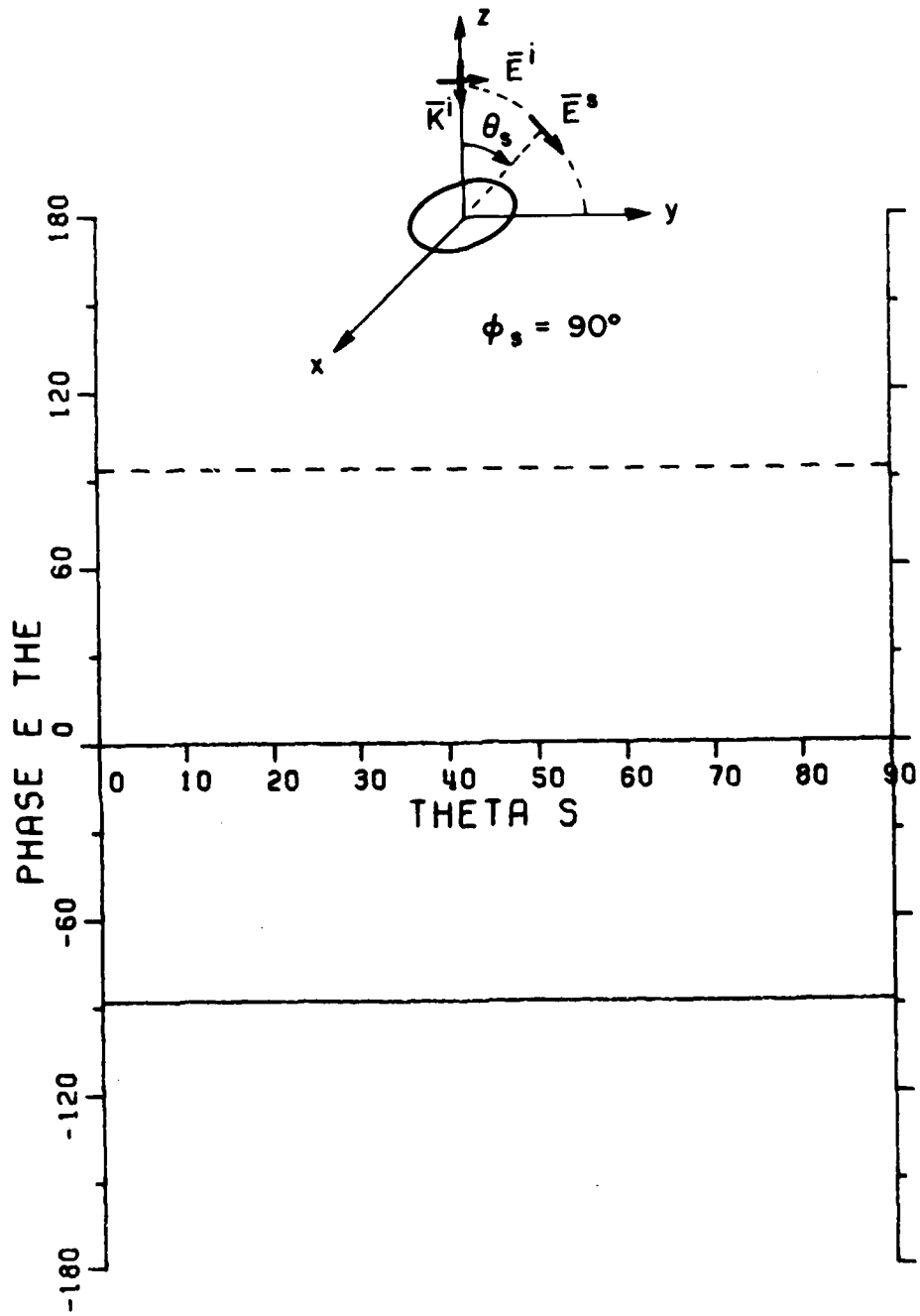

Figure 5.13. Phase of E_θ^s as a function of θ_s for ka=2; ϕ_s=90°.

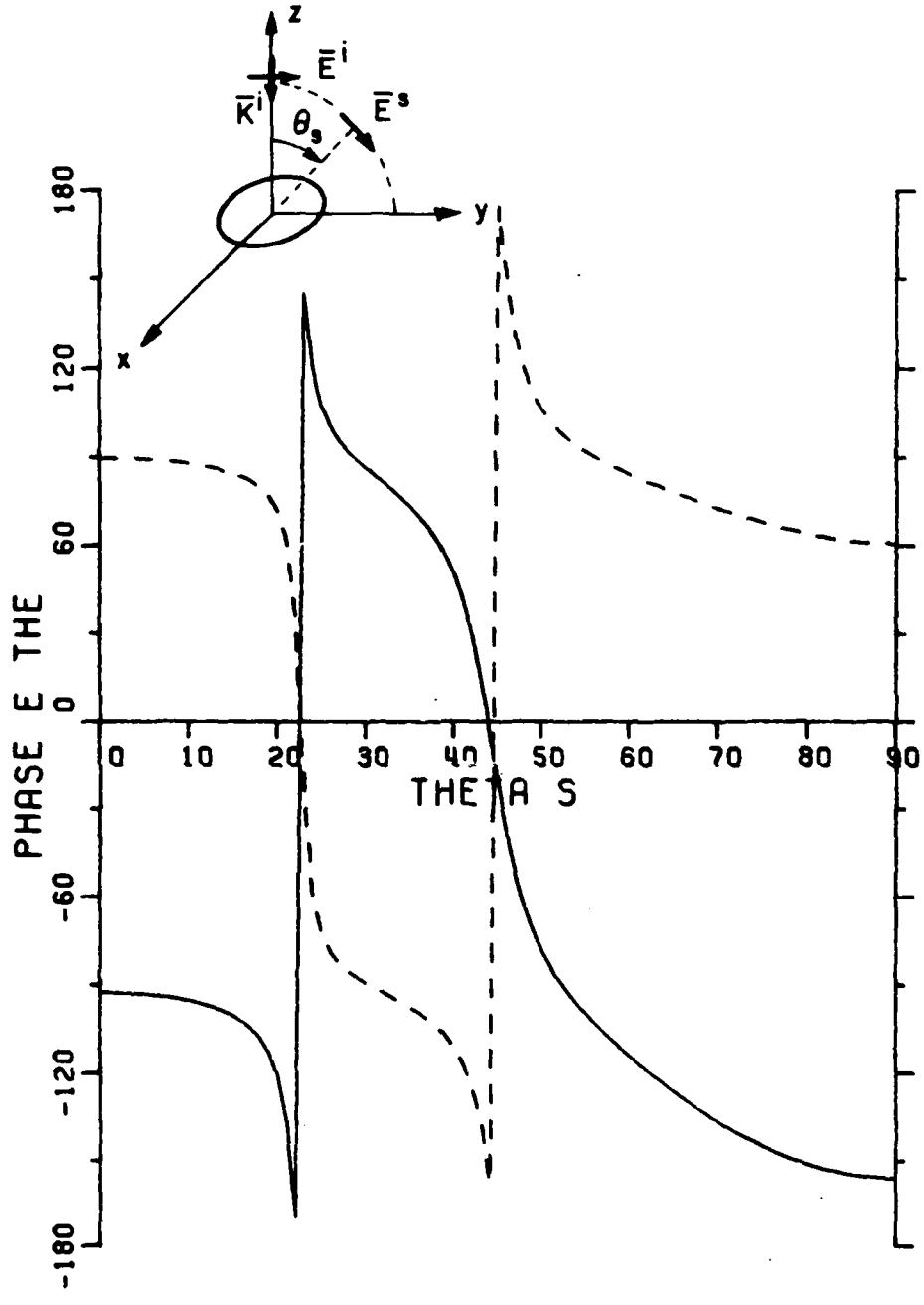

Figure 5.14. Phase of E_θ^s as a function of θ_s for ka=10; ϕ_s=90°.

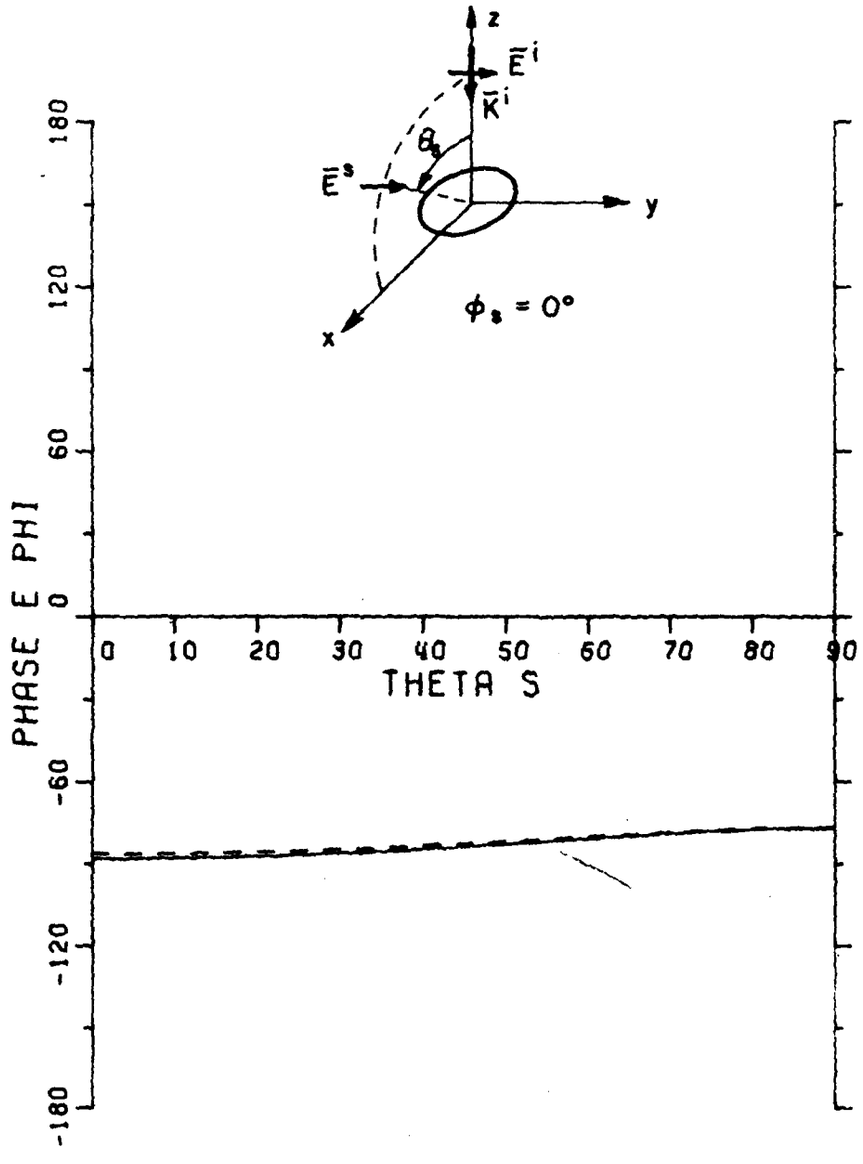

Figure 5.15. Phase of E_ϕ^s as a function of θ_s for ka=2; ϕ_s=0° (H-plane).

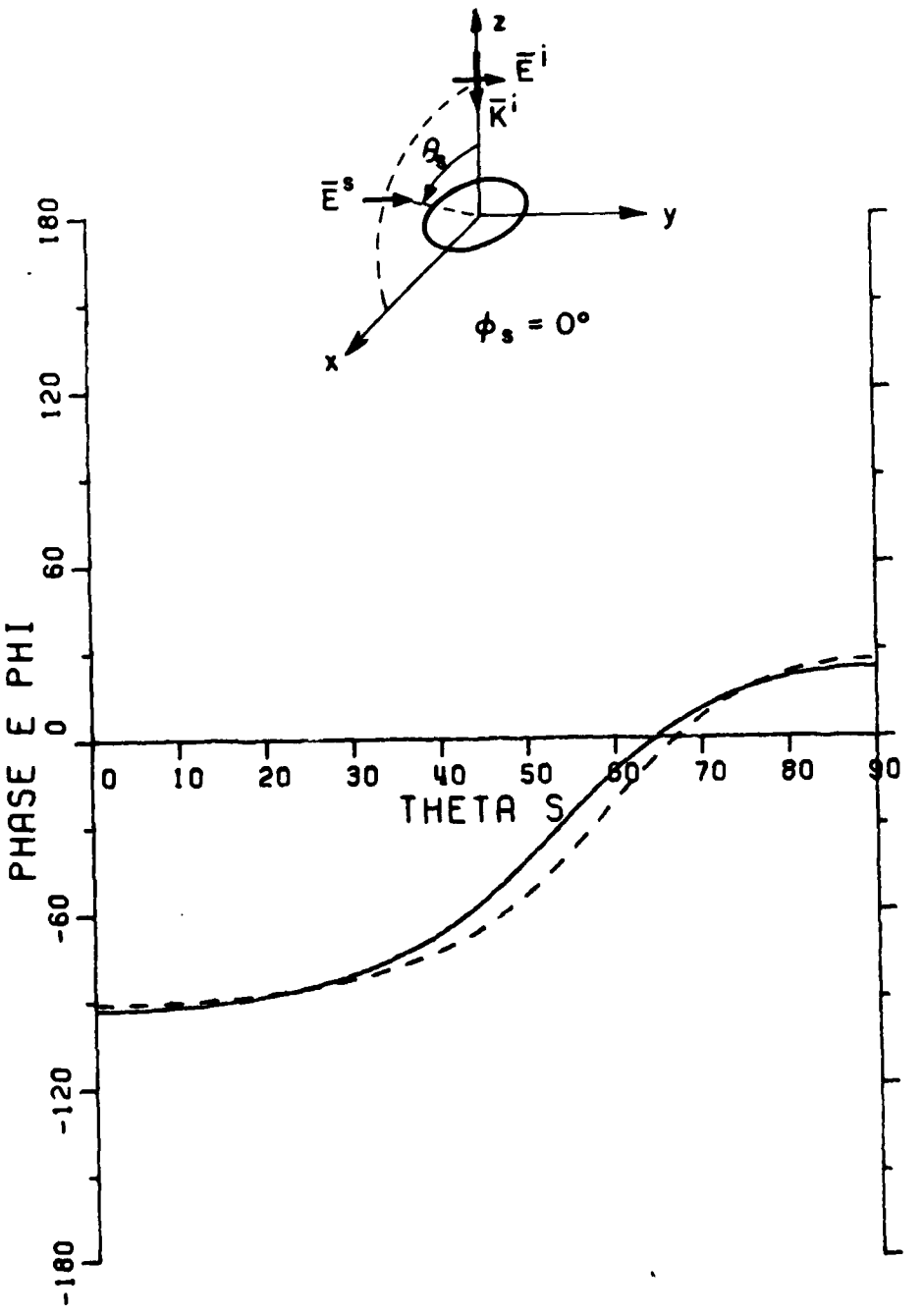

Figure 5.16. Phase of E_ϕ^s as a function of θ_s for ka=4; ϕ_s=0° (H-plane).

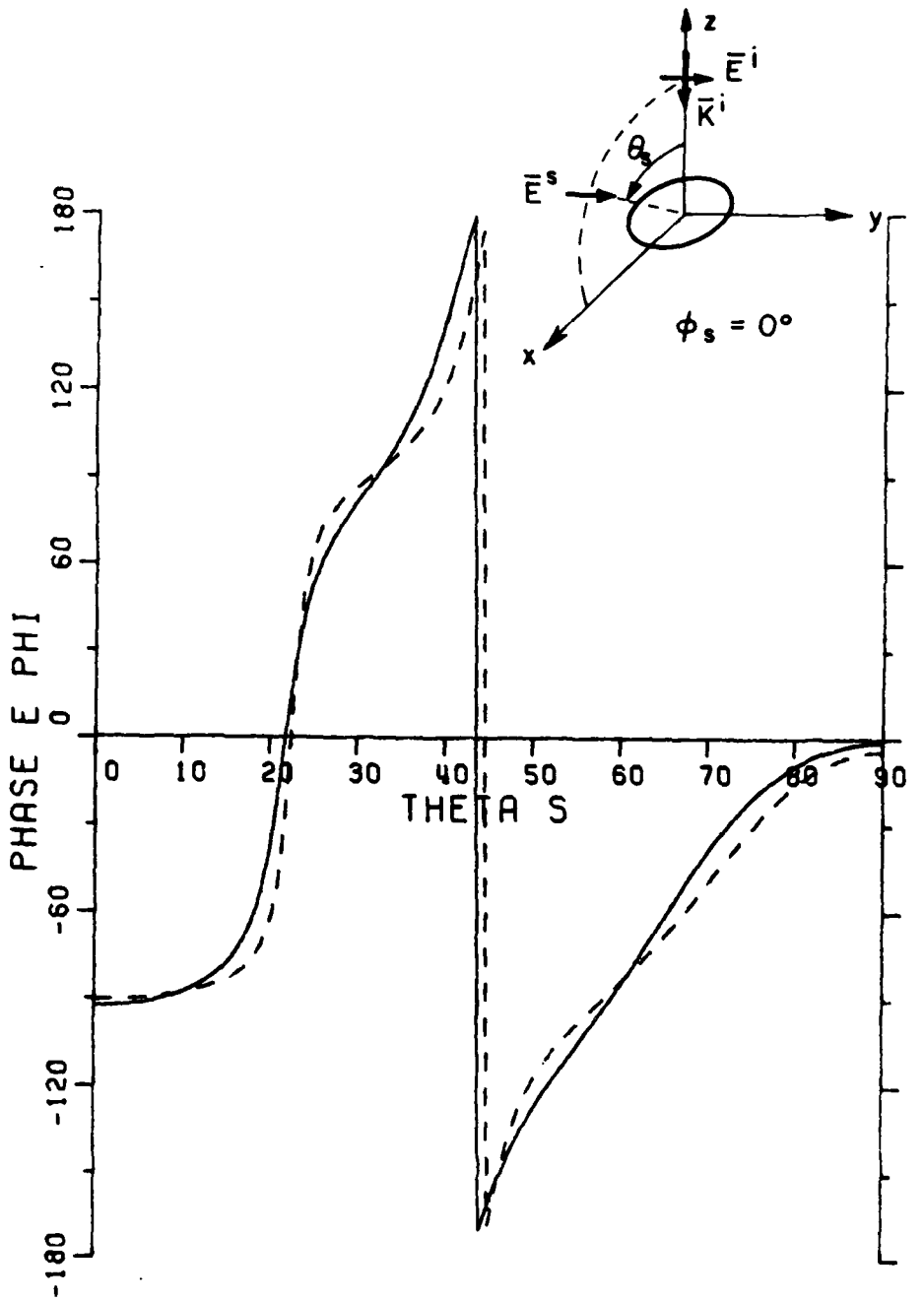

Figure 5.17. Phase of E_ϕ^s as a function of θ_s for ka=10; ϕ_s=0 (H-plane)

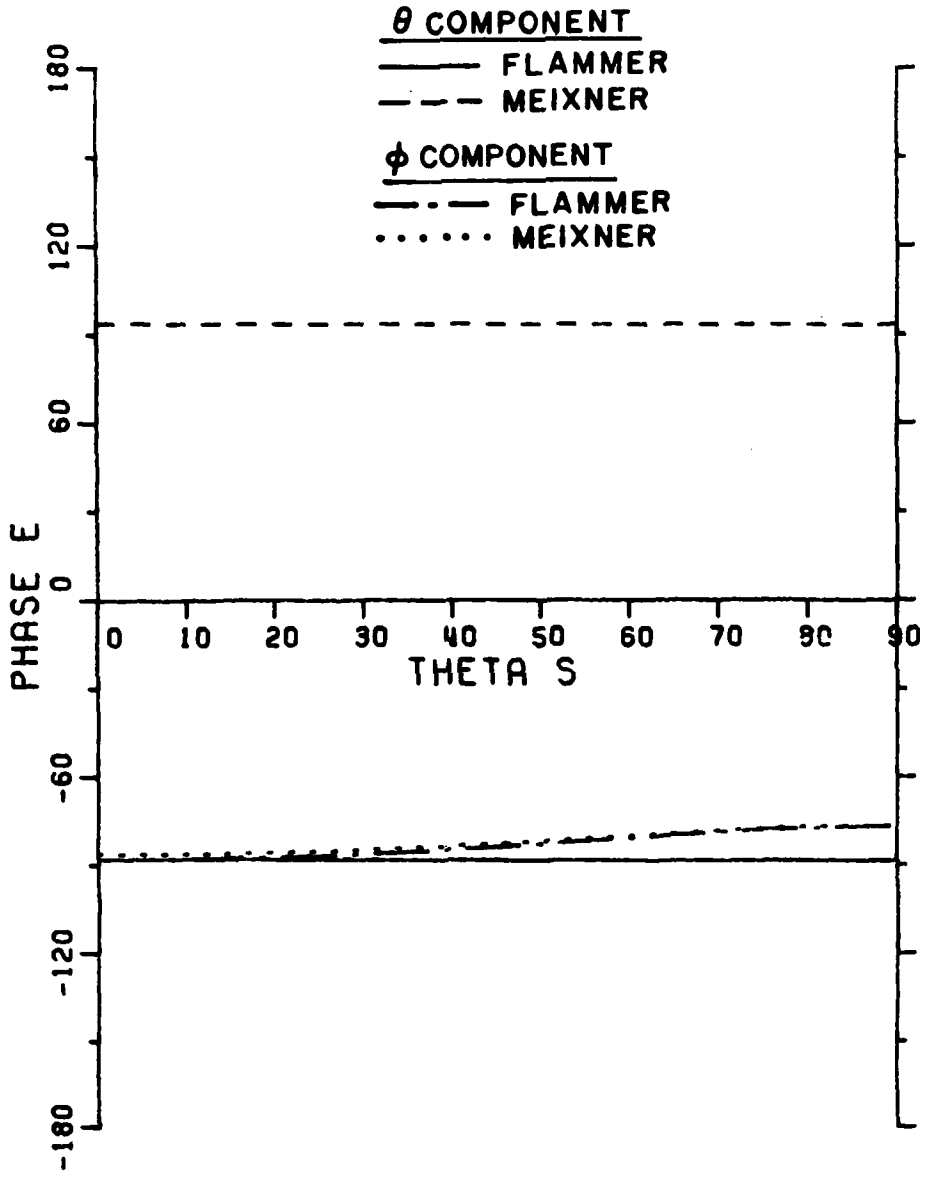

Figure 5.18. Phase of E_θ^s and E_ϕ^s as a function of θ_s for ka=2; ϕ_s=30°.

CHAPTER VI
MEIXNER'S SOLUTION

The validity of Meixner's solution has been established. Theoretical and numerical checks have been conducted in recent years, and they have shown very good agreement between computations and experimental data. In this Chapter, we will not repeat Meixner's solution, since the derivation is available in the literature. The reference work used for Meixner's solution is Hodge's version[8]. Here we will derive the expansions of the fields in terms of spheroidal vector wave functions and show a proof of the solution using only vector wave functions without refering to vector potentials.

A. The Vector Potentials

Meixner used Hertz vector potentials to solve the scattering problem. In this section we will give the expressions of the components of those potentials in terms of the scalar wave functions, Equation (7). This formulation is much more convenient than Meixner's for the computation of the fields. Meixner's solution computes the potential of the scattered field for arbitrary incidence and polarization. We will use here the notation defined in Chapter V-B, Equation (114), for the incident field.

$$\bar{E}^{i} = E_0(\cos\alpha\ \bar{E}^{i\parallel} + \sin\alpha\ \bar{E}^{i\perp}) \tag{130}$$

The definitions of $\bar{E}^{i\parallel}$, Equation (114), in this work and in Hodge's work[8] have opposite signs. Our definition was chosen to avoid a supplementary minus sign in the expansion of $\bar{E}^{i\parallel}$ in vector wave functions in Flammer's solution. This will lead us to introduce a minus sign in front of the scattered vector potentials corresponding to parallel polarization. As in Flammer's solution, we can obtain the scattered field in any arbitrary case if we know $\bar{E}^{s\parallel}$ and $E^{s\perp}$, scattered fields corresponding to the incident fields $\bar{E}^{i\parallel}$ and $\bar{E}^{i\perp}$, respectively. We will define the vector potentials in order to obtain $\bar{E}^{s\parallel}$ directly.

Meixner's solution involves three different potentials. $\bar{\pi}^{i}$ is the potential of the incident plane wave, $\bar{\pi}^{s\parallel}$ is the "reflected"

potential defined so that $\pi^{i}+\pi^{s1}$ has its components tangential to the disk equal to zero. Because of the shape of $\bar{\pi}^{i}$, the components of the electric field corresponding tangential to the disk to $\bar{\pi}^{i}+\bar{\pi}^{s}$ are then equal to zero. $\bar{\pi}^{s2}$ is a second scattered potential defined so that $\bar{\pi}=\bar{\pi}^{i}+\bar{\pi}^{s1}+\bar{\pi}^{s2}$ satisfies the edge condition derived by Meixner:

$$\frac{\partial}{\partial\xi}(\pi_\rho) = 0 = \frac{\partial}{\partial\eta}(\pi_\rho) \text{ at } \eta=\xi=0 \tag{131}$$

π_x and π_y finite at the edge.

where $\pi_\rho = \pi_x \cos\phi + \pi_y \sin\phi$.

$\bar{\pi}^{s2}$ also leads to an electric field whose components tangential to the disk are equal to zero. We list here the vector potentials for $\bar{E}^{s}$ as defined above, using Hodge's notation

$$\bar{\pi}^{s} = \bar{\pi}^{s1} + \bar{\pi}^{s2} \tag{132}$$

$$\pi^{s1}_{\parallel x} = -\frac{2\varepsilon_o}{k^2\cos\theta_o}\sum_{m=0}^{\infty}(2-\delta_{0m})V_m \cos m\phi \tag{133}$$

$$\pi^{s1}_{\parallel y} = 0 \tag{134}$$

$$\pi^{s1}_{\perp x} = 0 \tag{135}$$

$$\pi^{s1}_{\perp y} = -\frac{2\varepsilon_o}{k^2}\sum_{m=0}^{\infty}(2-\delta_{0m})V_m \cos m\phi \tag{136}$$

$$\pi^{s2}_{\parallel\perp x} = \frac{\varepsilon_o}{k^2}\sum_{m=0}^{\infty} i^{-m}\left\{\frac{\left[U^{\parallel}_{\perp m+1}-(1+\delta_{m1})U^{\parallel}_{\perp m-1}\right]}{\cos\theta_o}\cos m\phi + \left[X^{\parallel}_{\perp m+1}-(1-\delta_{m,1})X^{\parallel}_{\perp m-1}\right]\sin m\phi\right\}\phi_m \tag{137}$$

$$\pi^{s2}_{ij} = \frac{\varepsilon_o}{k^2} \sum_{m=0}^{\infty} i^{-m} \left\{ \left[X^{\perp}_{m+1}{}^{\parallel} + (1-\delta_{m,1}) X^{\perp}_{m-1}{}^{\parallel} \right] \cos m\phi \right.$$

$$\left. - \frac{1}{\cos\theta_o} \left[U^{\perp}_{m+1}{}^{\parallel} + (1+\delta_{m,1}) U^{\perp}_{m-1}{}^{\parallel} \right] \sin m\phi \right\} \phi_m \quad (138)$$

The different functions used in those potentials are:

$$V_m(\xi,\eta,c,\theta_o) = \sum_{n=m}^{\infty}{}' \frac{i^n}{N_{mn}(-ic)} \frac{R^{(1)}_{mn}(-ic,i0)}{R^{(4)}_{mn}(-ic,i0)} R^{(4)}_{mn}(-ic,i\xi)$$

$$\cdot S_{mn}(-ic,\cos\theta_o) S_{mn}(-ic,\eta) \quad (139)$$

$$\phi_m(\xi,\eta,c,\theta_o) = \sum_{n=m}^{\infty}{}' \frac{i^n}{N_{mn}(-ic)} \frac{R^{(1)}_{mn}(-ic,i0)}{R^{(4)}_{mn}(-ic,i0)} R^{(4)}_{mn}(-ic,i\xi)$$

$$\cdot S_{mn}(-ic,0) S_{mn}(-ic,\eta) \quad (140)$$

$$\begin{cases} U^{\parallel}_m = \dfrac{2i^{m-1}}{(1+\delta_{m,0})} \dfrac{W_{m-1}+W_{m+1}}{\psi_{m-1}+\psi_{m+1}} \quad , \quad U^{\perp}_m = 0 \quad , \quad m \geq 0 \\ U^{\perp}_m{}^{\parallel} = 0 \quad , \quad m < 0 \end{cases} \quad (141)$$

$$\begin{cases} X^{\perp}_m = 2\, i^{m-1} \dfrac{W_{m-1}-W_{m+1}}{\psi_{m-1}+\psi_{m+1}} \quad , \quad X^{\parallel}_m = 0 \quad , \quad m > 0 \\ X^{\perp}_m{}^{\parallel} = 0 \quad , \quad m \leq 0 \end{cases} \quad (142)$$

$$\begin{cases} W_m(c,\theta_o) = \sum_{n=m}^{\infty}{}' \dfrac{i^n}{N_{mn}} \dfrac{S_{mn}(-ic,\cos\theta_o)S_{mn}(-ic,0)}{R^{(4)}_{mn}(-ic,i0)} , & m \geq 0 \\ W_m(c,\theta_o) = 0, \quad m < 0 \end{cases} \tag{143}$$

$$\begin{cases} \psi_m(c,\theta_o) = \sum_{n=m}^{\infty}{}' \dfrac{i^n}{N_{mn}} \dfrac{[S_{mn}(-ic,0)]^2}{R^{(4)}_{mn}(-ic,i0)} , & m \geq 0 \\ \psi_m(c,\theta_o) = 0 , \quad m < 0 \end{cases} \tag{144}$$

As previously mentioned, the sign of $\pi^{s1}_{\parallel x}$, Equation (133), is the opposite of Hodge's result in order to match the different definitions of $\vec{E}^{i\parallel}$. However, the signs of the coefficients of $U^{\parallel}_m$ and $X^{\parallel}_m$ have not been modified in Equations (137) and (138) in order to keep the parallelism between the parallel and perpendicular cases. The sign difference will appear inside $U^{\parallel}_m$ and $X^{\parallel}_m$ instead. We, however, have the same $U^{\parallel}_m$ and $X^{\parallel}_m$ as in Hodge's results. This is due to a sign error in the derivation of $U^{\parallel}_m$ in Hodge's solution and to the fact that the $X^{\parallel}_m$ are all zero. In order to simplify $U^{\parallel}_m$ and $X^{\perp}_{m3}$, their coefficients in $\vec{\pi}^{s2}$ differ by the factors $(\varepsilon_o/k^3\cos\theta_o)$ and (ε_o/k^3) respectively from Hodge's expression. We now can express these potentials in terms of the scalar spheroidal wave functions.

From Equations (7), (42) and (139) we can express $V_m \cos m\phi$ as a summation of $\psi e^{(4)}_{mn}$ functions:

$$V_m \cos m\phi = \frac{1}{2(2-\delta_{0m})} \sum_{n=m}^{\infty}{}' \gamma_{mn}(\theta_o) \frac{R^{(1)}_{mn}(-ic,i0)}{R^{(4)}_{mn}(-ic,i0)} \psi e^{(4)}_{mn}(\eta,\xi,\phi) \tag{145}$$

In the same way, from Equations (7) and (140), we have for ϕ_m:

$$\psi_m \begin{Bmatrix} \cos \\ \sin \end{Bmatrix} m\phi = \sum_{n=m}^{\infty}{}' \frac{i^n}{N_{mn}} S_{mn}(-ic,0) \frac{R_{mn}^{(1)}(-ic,i0)}{R_{mn}^{(4)}(-ic,i0)} \psi_{e_{o}^{o}mn}^{(4)}(\eta,\xi,\phi) \tag{146}$$

By using these expansions in the expressions of the scattered potentials, Equations (133) to (138), we obtain the following scattered vector potentials.

1. Perpendicular polarization

$$\pi_x^{s\perp} = \frac{\varepsilon_o}{k^2} \sum_{m=0}^{\infty} i^{-m} \left\{ [X_{m+1}^{\perp} - (1-\delta_{m1}) X_{m-1}^{\perp}] \times \sum_{n=m}^{\infty}{}' \frac{i^n}{N_{mn}} S_{mn}(-ic,0) \frac{R_{mn}^{(1)}(-ic,i0)}{R_{mn}^{(4)}(-ic,i0)} \psi_{o_{mn}}^{(4)} \right\} \tag{147}$$

$$\pi_y^{s\perp} = -\frac{\varepsilon_o}{k^2} \sum_{m=0}^{\infty} \sum_{n=m}^{\infty}{}' \gamma_{mn}(\theta_o) \frac{R_{mn}^{(1)}(-ic,i0)}{R_{mn}^{(4)}(-ic,i0)} \psi_{e_{mn}}^{(4)}$$

$$+ \frac{\varepsilon_o}{k^2} \sum_{m=0}^{\infty} i^{-m} \left\{ [X_{m+1}^{\perp} + (1-\delta_{m1}) X_{m-1}^{\perp}] \times \sum_{n=m}^{\infty}{}' \frac{i^n}{N_{mn}} S_{mn}(-ic,0) \frac{R_{mn}^{(1)}(-ic,i0)}{R_{mn}^{(4)}(-ic,i0)} \psi_{e_{mn}}^{(4)} \right\} \tag{148}$$

2. Parallel polarization

$$\pi_x^{s\parallel} = -\frac{\varepsilon_o}{k^2 \cos\theta_o} \sum_{m=0}^{\infty} \sum_{n=m}^{\infty} \gamma_{mn}(\theta_o) \frac{R_{mn}^{(1)}(-ic,i0)}{R_{mn}^{(4)}(-ic,i0)} \psi_{e_{mn}}^{(4)}$$

$$+ \frac{\varepsilon_o}{k^2 \cos\theta_o} \sum_{m=0}^{\infty} \left\{ i^{-m} [U_{m+1}^{\parallel} - (1+\delta_{1m}) U_{m-1}^{\parallel}] \times \sum_{n=m}^{\infty}{}' \frac{i^n}{N_{mn}} S_{mn}(-ic,0) \frac{R_{mn}^{(1)}(-ic,i0)}{R_{mn}^{(4)}(-ic,i0)} \psi_{e_{mn}}^{(4)} \right\} \tag{149}$$

$$\pi_y^{s\parallel} = -\frac{\varepsilon_0}{k^2\cos\theta_0}\sum_{m=0}^{\infty}\left\{i^{-m}\left[U_{m+1}^{\parallel}+(1+\delta_{1m})U_{m-1}^{\parallel}\right]\times\right.$$

$$\left.\times\sum_{n=m}^{\infty}{}'\ \frac{i^n}{N_{mn}}\ S_{mn}(-ic,0)\ \frac{R_{mn}^{(1)}(-ic,i0)}{R_{mn}^{(1)}(-ic,i0)}\ \psi_{o_{mn}}^{(4)}\right\} \qquad (150)$$

Those formulas will allow us to compute the fields simply by taking their curls. This formulation is very convenient for this purpose since to each scalar wave function in a given component, x or y, of the potential corresponds a vector wave function of vector $\hat{e}_x$ or $\hat{e}_y$, respectively, when the curl of the vector potential is taken. The expressions for the electric and magnetic field will then be obtained in a very straight forward manner.

B. Meixner's Fields

In this section, we will derive the expressions of $\bar{E}^{s\parallel}$ and $\bar{E}^{s\perp}$ as summations of vector wave function. The fields are computed from the Hertz vector potential using the following general relations:

$$\bar{H} = i\omega\,\nabla\times\bar{\pi}$$
$$\bar{E} = \frac{1}{\varepsilon}\,\nabla\times\nabla\times\bar{\pi} \qquad (151)$$

Using Maxwell's equations, we also have the relation:

$$\bar{H} = \frac{i}{kZ_0}\,\nabla\times\bar{E} \qquad (152)$$

where Z_0 is the free space wave impedance.

Equation (152) will allow us to compute the magnetic fields from the electric fields. The scattered magnetic fields will not be listed because of the simplicity of the transformation. In order to compute the fields, we will use the following identity:

$$\nabla\times\hat{e}_i\,\psi_{e_{\delta mn}}^{(4)} = k\,N_{e_{\delta mn}}^{(4)}, \quad \text{where } i = x \text{ or } y. \qquad (153)$$

The final form of the expansion of the fields will be obtained by replacing the vector wave functions $\bar{N}^{x}_{\substack{e\\o}mn}$ and $\bar{N}^{y}_{\substack{e\\o}mn}$ by their expressions in terms of $\bar{N}^{+}_{\substack{e\\o}m+1n}$ and $\bar{N}^{-}_{\substack{e\\o}m-1n}$. This way the electric field will be expanded in terms of functions whose ϕ-dependence is indicated by their m index. These transformations are given by Flammer[10]:

$$\bar{N}^{x(i)}_{\substack{e\\o}mn} = \bar{N}^{+(i)}_{\substack{e\\o}m+1n} + \bar{N}^{-(i)}_{\substack{e\\o}m-1n} \quad , \qquad m>0$$

$$\bar{N}^{x(i)}_{e_{0n}} = 2\bar{N}^{+(i)}_{e_{1n}} \quad , \quad \bar{N}^{x(i)}_{o_{0n}} = \bar{0}$$

$$\bar{N}^{y(i)}_{\substack{e\\o}mn} = \pm [\bar{N}^{+(i)}_{\substack{o\\e}m+1n} - \bar{N}^{-(i)}_{\substack{o\\e}m-1n}] \quad , \quad m>0$$

$$\bar{N}^{y(i)}_{e_{0n}} = + 2\bar{N}^{+(i)}_{o_{1n}} \quad , \quad \bar{N}^{y(i)}_{o_{0n}} = \bar{0} \tag{154}$$

We will now list $\bar{E}^{s\perp}$ and $\bar{E}^{s\parallel}$, obtained by applying Equations (151) and (153) to the corresponding vector potential, respectively, Equations (147) and (148) and Equations (149) and (150).

1. Perpendicular polarization

$$\begin{aligned}\bar{E}^{s\perp} = & -\frac{1}{k}\sum_{m=0}^{\infty}\sum_{n=m}^{\infty'} \gamma_{mn}(\theta_o)\,\frac{R^{(1)}_{mn}(-ic,i0)}{R^{(4)}_{mn}(-ic,i0)}\,\bar{N}^{y(4)}_{e_{mn}} \\ & + \frac{1}{k}\sum_{m=0}^{\infty} i^{-m}\Bigg\{(X^{\perp}_{m+1}-(1-\delta_{m1})X^{\perp}_{m-1}) \times \\ & \times \sum_{n=m}^{\infty'} \frac{i^n}{N_{mn}}\,S_{mn}(-ic,0)\,\frac{R^{(1)}_{mn}(-ic,i0)}{R^{(4)}_{mn}(-ic,i0)}\,\bar{N}^{x(4)}_{e_{mn}} \\ & + (X^{\perp}_{m+1}+(1-\delta_{m1})X^{\perp}_{m-1}) \sum_{n=m}^{\infty'} \frac{i^n}{N_{mn}}\,S_{mn}(-ic,0)\,\frac{R^{(1)}_{mn}(-ic,i0)}{R^{(4)}_{mn}(-ic,i0)}\,\bar{N}^{y(4)}_{e_{mn}}\Bigg\}\end{aligned} \tag{155}$$

We notice that the first summation is a "reflected" field as defined in Chapter V.

Using Equation (154) in the above formula and rearranging in terms of $X_m^{\perp}$, we obtain:

$$\overline{E}^{s\perp} = -\frac{1}{k}\sum_{m=0}^{\infty}\sum_{n=m}^{\infty}{}' \gamma_{mn}(\theta_o)\,\frac{R_{mn}^{(1)}(-ic,i0)}{R_{mn}^{(4)}(-ic,i0)}\,\left[(1+\delta_{0m})\overline{N}_{o_{m+1n}}^{+(4)} - (1-\delta_{0m})\overline{N}_{o_{m-1n}}^{-(4)}\right]$$

$$+\frac{2}{k}\sum_{m=0}^{\infty} i^{-m}\left\{\sum_{n=m}^{\infty}{}' \frac{i^n}{\overline{N}_{mn}} S_{mn}(-ic,0)\,\frac{R_{mn}^{(1)}(-ic,i0)}{R_{mn}^{(4)}(-ic,i0)}\left[X_{m+1}^{\perp}\,\overline{N}_{o_{m+1n}}^{+(4)} - X_{m-1}^{\perp}\,\overline{N}_{o_{m-1}}^{-(4)}\right]\right\} \qquad (156)$$

with $X_m^{\perp} = 0$ for $m \leq 0$.

2. Parallel polarization

$$\overline{E}^{s\parallel} = -\frac{1}{k\cos\theta_o}\sum_{m=0}^{\infty}\sum_{n=m}^{\infty}{}' \gamma_{mn}(\theta_o)\,\frac{R_{mn}^{(1)}(-ic,i0)}{R_{mn}^{(4)}(-ic,i0)}\,\overline{N}_{e_{mn}}^{x(4)}$$

$$+\frac{1}{k\cos\theta_o}\sum_{m=0}^{\infty} i^{-m}\left\{\left[U_{m+1}^{\parallel} - (1+\delta_{1m})U_{m-1}^{\parallel}\right]\times\right.$$

$$\times\sum_{n=m}^{\infty}{}' \frac{i^n}{\overline{N}_{mn}} S_{mn}(-ic,0)\,\frac{R_{mn}^{(1)}(-ic,i0)}{R_{mn}^{(4)}(-ic,i0)}\,\overline{N}_{e_{mn}}^{x(4)}$$

$$\left.-\left[U_{m+1}^{\parallel} + (1+\delta_{1m})U_{m-1}^{\parallel}\right]\sum_{n=m}^{\infty}{}' \frac{i^n}{\overline{N}_{mn}} S_{mn}(-ic,0)\,\frac{R_{mn}^{(1)}(-ic,i0)}{R_{mn}^{(4)}(-ic,i0)}\,\overline{N}_{o_{mn}}^{y(4)}\right\} \qquad (157)$$

In the same way, using Equation (154) in the above formula and rearranging in terms of U_m'', we obtain:

$$E^{s\prime\prime} = -\frac{1}{k\cos\theta_o}\sum_{m=0}^{\infty}\sum_{n=m}^{\infty'} \gamma_{mn}(\theta_o)\frac{R_{mn}^{(1)}(-ic,i0)}{R_{mn}^{(4)}(-ic,i0)}\left[(1+\delta_{0m})\,\bar{N}_{e_{m+1n}}^{+(4)} + (1-\delta_{0m})\,\bar{N}_{e_{m-1n}}^{-(4)}\right]$$

$$+\frac{2}{k\cos\theta_o}\sum_{m=0}^{\infty} i^{-m}\left\{\sum_{n=m}^{\infty'}\frac{i^n}{N_{mn}} S_{mn}(-ic,0)\frac{R_{mn}^{(1)}(-ic,i0)}{R_{mn}^{(4)}(-ic,i0)}\right.$$

$$\left.\left[U_{m+1}''\,\bar{N}_{e_{m+1n}}^{+(4)} - (1+\delta_{1m})\,U_{m-1}''\,\bar{N}_{e_{m-1n}}^{-(4)}\right]\right\}$$

with $U_m'' = 0$ for $m < 0$.

3. Conclusion

For an incident field of arbitrary incidence and polarization, the total scattered $\bar{E}$-field can be expressed in terms of $\bar{E}^{s\perp}$ and $\bar{E}^{s\prime\prime}$ as shown in Equation (115):

$$\begin{aligned}\bar{E}^s &= E_o(\cos\alpha\,\bar{E}^{s\prime\prime} + \sin\alpha\,\bar{E}^{s\perp})\\ \bar{H}^s &= E_o(\cos\alpha\,\bar{H}^{s\prime\prime} + \sin\alpha\,\bar{H}^{s\perp})\end{aligned} \qquad (159)$$

where, from Equation (152), $\bar{H}^{s\perp}_{\prime\prime} = (i/kZ_o)\,\nabla\times\bar{E}^{s\prime\prime}_{\perp}$.

In this section we have found the expression for the scattered electromagnetic field in terms of the spheroidal vector wave functions. This allows us to deal with the fields directly instead of the vector potentials, and it therefore offers the same possibilities as Flammer's solution for studying the near-field problem in a much simpler manner. In the normal incidence case, we now have two different formulas, Flammer's and Meixner's formal solutions, giving the bistatic scattered field. A term by term comparison of the two solutions should be carried out to see how it is possible to match the results. A first step however would be to compare the scattered electric fields in the far-field region. This would be much easier since the remaining components of

$\bar{E}^s$ are, in each solution, equal to single summations of scalar spheroidal functions over n. The task of reordering those far-field components as summations of the Legendre associated functions has not yet been completed. The Legendre associated functions are the natural functions since they are orthogonal in the far-field region and since the spheroidal coordinate system approaches the spherical coordinate system in this limit. This orthogonality will lead to an infinite number of relations between the expansion coefficients $d_r^{mn}(-ic)$ and values of the radial functions at $\xi=0$. The validity of these relations could easily be checked on the computer since the different functions are readily available in Hodge's program[9] and in the one used in Chapter V of this work. A study of those relations as function of the variable $c=(kd/2)$ might explain the discrepancy obtained in Figure 5.1 for the backscattering cross-section. It would determine whether the differences are due to some inaccuracy in the computations of the coefficients or to improper truncations of the infinite summations in one of the solutions. The far-field of Meixner's solution can easily be computed by inserting the large argument approximations of the spheroidal wave functions, Equation (34), in the formulas for these fields. This showed a sign error in the θ-component of the scattered field in the perpendicular polarization case as computed by Hodge[9]. A sign error also appears in the θ-component of the scattered field in the parallel polarization case in Hodge's work.

In the next section, we will derive Meixner's solution with another method using vector wave functions exclusively. The edge condition will involve all the components of the electric field unlike Flammer's solution where the ϕ-component only was needed.

C. Another Proof of Meixner's Solution

As can be seen from the previous section, Meixner develops a solution to the scattering problem by using only one expansion for the incident plane wave in each polarization case - parallel or perpendicular. His method is equivalent to adding to the incident and reflected field a summation of vector wave functions whose tangential components are zero on the surface of the disk but which has a singularity at the edge. The variable coefficients of that summation are then adjusted to cancel the singularities in the ϕ-component of the total electric and magnetic fields, and to insure a proper behavior of their other components near the edge. This is exactly the method that we are going to use to prove Meixner's solution.

In this section we will first derive some useful vector wave functions expansions which are equal to zero on the surface of the disk. We will summarize the power series approximations of their components in terms of η and ξ in the vicinity of the edge. We will then be able to prove Meixner's solution, using the above expansions to match the edge condition.

1. Vector wave expansion

This section is mainly based on the properties of the N^x_{emn} expansion of a plane wave, Equation (47), for an angle of incidence θ_0 equal to 90^0.

a. Derivation of the vectorial relations

We will first establish some dependence relations for the $\overline{N}^{x(1)}_{e_{mn}}$ vector wave function and use the ϕ-orthogonality to obtain relations for each value of m. We will then show that those relations apply equally to the odd vector wave functions. We can then find vector wave expansions whose tangential components are equal to zero on the surface of the disk and that behave like outward travelling waves in the far-field region by using a term by term matching technique identical to that used for the calculation of the reflected field in Flammer's solution.

For $\theta_0 = 90^0$, Equation (47) multiplied by $\cos\theta_0$ can be written as

$$\sum_{m=0}^{\infty} \sum_{n=m}^{\infty}{}' \gamma_{mn}(\pi/2)\, \overline{N}^{x(1)}_{e_{mn}}(\eta,\xi,\phi) = \vec{0} \qquad (160)$$

From Equation (42) and Equation (14), we have, for n-m odd, $\gamma_{mn}(\pi/2)=0$ and, therefore, in the previous summation only the terms for n-m even will remain.

$$\sum_{m=0}^{\infty} \sum_{n=m}^{\infty}{}' \gamma_{mn}(\pi/2)\, \overline{N}^{x(1)}_{e_{mn}}(\eta,\xi,\phi) = \vec{0} \qquad (161)$$

We will introduce here the functions $\overline{N}^{+(4)}_{mn}$ and $\overline{N}^{-(4)}_{mn}$ which have a convenient ϕ-dependence, Equation (154).

Equation (161) can be rewritten as follows

$$\sum_{n=1}^{\infty}{}' \gamma_{1n}(\pi/2)\, \overline{N}^{-(1)}_{e_{on}}$$

$$+ \sum_{m=1}^{\infty} \left\{ \sum_{n=m-1}^{\infty}{}' (1+\delta_{1m})\gamma_{m-1,n}(\pi/2)\, \overline{N}^{+(1)}_{e_{mn}} \right.$$

$$\left. + \sum_{n=m+1}^{\infty}{}' \gamma_{m+1,n}(\pi/2)\, \overline{N}^{-(1)}_{e_{mn}} \right\} = \vec{0} \qquad (162)$$

where corresponding components of $\overline{N}^{+(1)}_{e_{mn}}$ and $\overline{N}^{-(1)}_{e_{mn}}$ have the same ϕ-dependence.

A difficulty encountered with the use of this notation is the difference in the parity of n-m between Equation (161) and (162). Equation (161) is a summation of $\overline{N}^{x(1)}_{e_{mn}}$ for n-m even, while Equation (162) is a summation of $\overline{N}^{+(1)}_{e_{mn}}$ and $\overline{N}^{-(1)}_{e_{mn}}$ for n-m odd. In order to avoid a possible confusion, the index p will be used instead of n in $\overline{N}^{+(1)}_{e_{mn}}$ and $\overline{N}^{-(1)}_{e_{mn}}$ during the rest of this section. With that notation, the ϕ-orthogonality applied to Equation (162) leads for every value of m to the relation:

$$\sum_{p=m-1}^{\infty'} (1+\delta_{1m})(1-\delta_{0m})\gamma_{m-1p}(\pi/2)\overline{N}^{+(1)}_{e_{mp}} + \sum_{p=m+1}^{\infty'} \gamma_{m+1p}(\pi/2)\overline{N}^{-(1)}_{e_{mp}} = \vec{0} \qquad (163)$$

Equation (163) means that the coefficient of cos $m\phi$ in the η- and ξ-components of the above summation and the coefficient of sin $m\phi$, except for $m=0$, in its ϕ-component are equal to zero.

We can then substitute, for m greater than zero, sin $m\phi$ for cos $m\phi$ and cos $m\phi$ for -sin $m\phi$ without changing the value of the summation. This transformation leads to the following equation for the odd functions:

$$\sum_{p=m-1}^{\infty'} (1+\delta_{1m})(1-\delta_{0m})\gamma_{m-1p}(\pi/2)\overline{N}^{+(1)}_{o_{mp}} + \sum_{p=m+1}^{\infty'} \gamma_{m+1p}(\pi/2)\overline{N}^{-(1)}_{o_{mp}} = \vec{0} \qquad (164)$$

for every value of $m \geq 1$ and (η, ξ, ϕ). Note that Equations (163) and (164) are also valid for $\overline{M}^{\pm(1)}_{e_{mp}}$. This is proved by simply taking the curl of these equations. In order to match the behavior of out-wave travelling waves at infinity and still keep the behavior of the tangential components at $\xi=0$, we will make a term by term transformation.

From Equation (154) and Equation (30) to (33), we can see that, on the surface of the disk, the η- and ϕ-components of $\overline{N}^{+(i)}_{e_{\delta mp}}$, or $\overline{N}^{-(i)}_{e_{\delta mp}}$, are proportional to $R^{(i)}_{m-1}(-ic,io)$, or $R^{(i)}_{m+1}(-ic,io)$ respectively. We will therefore make the following substitution in Equation (164):

$$\overline{N}^{+(1)}_{e_{\delta mp}} \rightarrow \frac{R^{(1)}_{m-1p}(-ic,io)}{R^{(4)}_{m-1p}(-ic,io)} \overline{N}^{+(4)}_{e_{\delta mp}}$$

$$\overline{N}^{-(1)}_{e_{\delta mp}} \rightarrow \frac{R^{(1)}_{m+1p}(-ic,io)}{R^{(4)}_{m+1p}(-ic,io)} \overline{N}^{-(4)}_{e_{\delta mp}} \qquad (165)$$

We will denote by $\overline{F}_{e_{\delta m}}(\eta,\xi,\phi)$ the value of the transformed summation. From Equations (164) and (165), we have for every value of η:

$$\overline{F}_{e_{\delta m}}(\eta,\xi,\phi) = \sum_{p=m-1}^{\infty}{}' (1+\delta_{1m})(1-\delta_{0m})\gamma_{m-1p}(\pi/2)\frac{R^{(1)}_{m-1p}(-ic,io)}{R^{(4)}_{m-1p}(-ic,io)} \times$$

$$\times \overline{N}^{+(4)}_{e_{\delta mp}}(\eta,\xi,\phi) + \sum_{p=m+1}^{\infty}{}' \gamma_{m+1p}(\pi/2)\frac{R^{(1)}_{m+1p}(-ic,io)}{R^{(4)}_{m+1p}(-ic,io)} \overline{N}^{-(4)}_{e_{\delta mp}}(\eta,\xi,\phi) \qquad (166)$$

$\overline{F}_{e_{\delta m}}$ satisfies for $|\eta| > 0$:

$$[\overline{F}_{e_o}]_\alpha(\eta,0,\phi) = 0$$

$$\text{where } \alpha = \eta,\phi \ . \qquad (167)$$

$$[\overline{F}_{e_{\delta m}}]_\alpha(\eta,0,\phi) = 0 \text{ for } m \geq 1.$$

In contrast to Equation (161) and (163) these $\overline{F}_{e_{\delta m}}$ functions are not zero everywhere. Note that $\overline{F}_{e_{\delta m}}$ is the reflected field corresponding to the zero incident field of Equation (164). Since the reflected field is not zero, we immediately realize that the reflected

field is not equal to the scattered field in that case. We will need the expansion of the components of $\bar{F}_{e_{\delta m}}$ in terms of η and ξ near the edge. In the following subsection, we list the expansion of the necessary vector wave functions.

b. $\bar{N}^{+(1)}_{e_{\delta mn}}$ and $\bar{N}^{-(i)}_{e_{\delta m-1n}}$ near the edge

---

We do not need very complete expansions of the vector wave functions in the neighborhood of the edge since we are only looking for the terms that do not have the behavior required by the edge condition for each component. The other terms will not lead to any problem in satisfying the edge condition. We will first consider the case of $\bar{N}^{+(i)}_{e_{\delta m+1n}}$, component by component. $\bar{N}^{+(1)}_{e_{\delta mn}}$ has no singularity. Since Equation (161) involves the functions $\bar{N}^{x(1)}_{e_{mn}}$ for n-m even only, we will need $\bar{N}^{+(i)}_{e_{\delta m+1n}}$ and $\bar{N}^{-(i)}_{e_{\delta m-1n}}$ for n-m even only for the computation of $\bar{F}_{e_{\delta m}}$.

For the η-component, we only need the terms of singularity greater than $s^{-\frac{1}{2}}$, where s is the distance from the edge as defined in Equation (89).

n-m even, $|\eta| \ll 1$ and $c\xi \ll 1$

$$[\bar{N}^{+(4)}_{e_{\delta m+1n}}]_\eta = \frac{4i}{ckd^2} \frac{S_{mn}(-ic,o)}{R^{(1)}_{mn}(-ic,io)} \frac{\eta\xi}{(\eta^2+\xi^2)^{5/2}} \begin{Bmatrix}\cos\\ \sin\end{Bmatrix}(m+1)\phi + O(s^{-\frac{1}{2}}) \tag{168}$$

For the ξ-component of $\bar{N}^{+(4)}_{e_{\delta m+1n}}$, we only need the terms of singularity greater than $s^{-\frac{1}{2}}$

n-n even, $|\eta| \ll 1$ and $c\xi \ll 1$

$$[\bar{N}^{+(i)}_{e_{\delta m+1n}}]_\xi = \frac{2i}{ckd^2} \frac{S_{mn}(-ic,o)}{R^{(1)}_{mn}(-ic,io)} \frac{\xi^2-\eta^2}{(\eta^2+\xi^2)^{5/2}} \begin{Bmatrix}\cos\\ \sin\end{Bmatrix}(m+1)\phi + O(s^{-\frac{1}{2}}) \tag{169}$$

For the ϕ-component, we need the terms up to the order of $s^{\frac{1}{2}}$ to test the edge condition on the ϕ-component.

For n-m even, $n \geq 1$, $c \neq 1$

$$[\overline{N}^{+(4)}_{\substack{e\\o}m+1,n}]_\phi = \frac{2}{kd^2}\,\frac{S_{mn}(-ic,o)}{\eta^2+\xi^2}\begin{Bmatrix}\sin(m+1)\phi\\ -\cos(m+1)\phi\end{Bmatrix} \times$$

$$\times \left\{(\eta^2+\xi^2)[-(m+1)\lambda_{mn}+m(m+1)-c^2]\,R^{(4)}_{mn}(-ic,io)\right.$$

$$+ \left[1+m+\eta^2\left[c^2+\frac{\lambda_{mn}}{2}(m+1)-\frac{m}{2}(m+1)(m+2)\right]\right.$$

$$\left.\left.+\xi^2\left[\frac{1}{2}(m-3)(\lambda_{mn}-m^2)-2m+3\right]\right]\frac{i\xi}{cR^{(1)}_{mn}(-ic,io)}\right\}+O(s) \quad (170)$$

We will need the expansion of $[\overline{N}^{+(1)}_{\substack{e\\o}m+1,n}]_\phi$ for n-m odd.

For n-m odd

$$[\overline{N}^{+(1)}_{\substack{e\\o}m+1n}]_\phi = \frac{2}{kd^2}\,\eta\xi\left[\frac{3}{2}(\lambda_{mn}-m^2-2)+m\,\frac{4-\lambda_{mn}+m^2}{2}\right]\begin{Bmatrix}\sin(m+1)\phi\\ -\cos(m+1)\phi\end{Bmatrix}$$

$$\times S'_{mn}(-ic,o)R^{(1)'}_{mn}(-ic,io)+O(s^{3/2}) \quad (171)$$

It is well behaved at the edge since it goes to zero as s does. The case of $\overline{N}^{-(4)}_{\substack{e\\o}m-1n}$ can easily be derived from that of $\overline{N}^{+(4)}_{\substack{e\\o}m+1n}$. $\overline{N}^{-(1)}_{\substack{e\\o}m-1n}$ has no singularity. The η- and ξ-components of $\overline{N}^{-(4)}_{\substack{e\\o}m-1n}$ can be obtained from Equations (168) and (169) by replacing m+1 by m-1 in the ϕ-dependence. The expansions of the ϕ-component of $\overline{N}^{-}_{\substack{e\\o}m-1n}$ are obtained from Equation (170) and (171) by replacing m by -m except in the indexes, $\sin(m+1)\phi$ by $-\sin(m-1)\phi$ and $-\cos(m+1)\phi$ by $\cos(m-1)\phi$.

In order to compute the complete electromagnetic field, we will also need the functions $\overline{M}^{+(i)}_{\substack{e\\o}m+1n}$ and $\overline{M}^{-(i)}_{\substack{e\\o}m-1n}$ as defined below:

$$\overline{M}^{+(i)}_{\substack{e\\o}m+1n} = \frac{1}{k}\nabla \times \overline{N}^{+(i)}_{\substack{e\\o}m+1n} \quad (172)$$

As seen from their expressions in Flammer's book[10], the η- and ξ-components of these functions have a singularity of order at most $s^{-\frac{1}{2}}$ and therefore satisfy the edge condition. The expansion of ϕ-component of $\overline{M}^{+(4)}_{\substack{e\\o}mn}$ is listed below for n-m even.

n-m even

$$[\overline{M}^{+(4)}_{\substack{e\\o}m+1n}]_\phi = \frac{1}{kd}\ \frac{S_{mn}(-ic,o)}{\eta^2+\xi^2}\ \left\{\begin{matrix}\cos\\ \sin\end{matrix}(m+1)\phi\right\} x$$

$$\left\{\eta\xi\ (\eta^2+\xi^2)(m^2-\lambda_{mn})\ \frac{\lambda_{mn}-m^2-2}{2}\ R^{(4)}_{mn}(-ic,io)\right.$$

$$\left. x\ \left[1+\eta^2\ \frac{\lambda_{mn}-m^2}{2}+\xi^2\ \frac{\lambda_{mn}-m^2}{2}\right]\ \frac{(-i\ )}{cR^{(1)}_{mn}(-ic,io)}\right\}+O(s) \qquad (173)$$

We will also need $[\overline{M}^{+(1)}_{\substack{e\\o}m+1n}]_\phi$ for n-m odd:

n-m odd

$$[\overline{M}^{+(1)}_{\substack{e\\o}m+1n}]_\phi = \frac{1}{kd}\ S'_{mn}(-ic,o)\ R'_{mn}(-ic,io)\left\{\begin{matrix}\cos\\ \sin\end{matrix}(m+1)\phi\right\} = O(s) \qquad (174)$$

The corresponding expansions for $\overline{M}^{-}_{\substack{e\\o}m-1n}$ are obtained by replacing m+1 by m-1 in the trigonometric functions. We note that the components of the functions of index 4 listed in Equations (168) to (170) and (173) have singularities that do not satisfy the edge condition, but that all the components of the vector wave functions of index 1 do satisfy it.

$\overline{F}^{+}_{\substack{e\\o}m}$ is expanded in terms of $\overline{N}^{\pm(4)}_{\substack{e\\o}mp}$ instead of $\overline{N}^{+(4)}_{\substack{e\\o}m+1n}$ or $\overline{N}^{-(4)}_{\substack{e\\o}m-1n}$. From $\overline{N}^{+(i)}_{\substack{e\\o}m+1n}$, n-m even or odd, we can derive the expression of $\overline{N}^{+(i)}_{\substack{e\\o}mp}$ for p-m odd or even, respectively, by replacing m by m-1 even in the indexes and n by p. From $\overline{N}^{-(1)}_{\substack{e\\o}m-1}$, n-m even or odd, we can derive the expansion of $\overline{N}^{-(i)}_{\substack{e\\o}mp}$ for p-m odd or even, respectively, by replacing m by m+1 and n by p.

c. $\overline{F}_{e_{\delta m}}$ at the edge

Here we will compute the coefficients of the improper singularities of the components of $\overline{F}_{e_{\delta m}}$ and $1/k\nabla \times \overline{F}_{e_{\delta m}}$. The coefficient of $\frac{\eta\zeta}{(\eta^2+\zeta^2)^{5/2}}$ in $[\overline{F}_{e_{\delta m}}]_\eta$ is, from Equation (168) and (166):

$$\frac{4i}{ckd^2}\left\{\sum_{p=m-1}^{\infty}{}' (1+\gamma_{1m})(1-\delta_{om})\gamma_{m-1p}(\pi/2)\frac{S_{m-1p}(-ic,o)}{R^{(4)}_{m-1p}(-ic,io)} + \sum_{p=m+1}^{\infty}{}' \gamma_{m+1p}(\pi/2)\frac{S_{m+1p}(-ic,o)}{R^{(4)}_{m+1p}(-ic,io)}\right\}\begin{Bmatrix}\cos\\ \sin\end{Bmatrix} m\phi \qquad (175)$$

The coefficient of $\frac{\zeta^2-\eta^2}{(\eta^2+\zeta^2)^{5/2}}$ in $[\overline{F}_{e_{\delta m}}]_\zeta$ is half of equation (175).

Those two components will, therefore, enforce the same condition.

The coefficient of $\frac{\zeta}{\eta^2+\zeta^2}$ in $[\overline{F}_{e_{\delta m}}]_\zeta$ is, from Equation (166) and (170):

$$\frac{2i}{ckd^2}\left[\left\{\sum_{p=m-1}^{\infty}{}' (1+\delta_{1m})(1-\delta_{om})\gamma_{m-1p}(\pi/2)\frac{S_{m-1p}(-ic,o)}{R^{(4)}_{m-1p}(-ic,io)}\right\} m\begin{Bmatrix}\sin m\phi\\ -\cos\end{Bmatrix} + \sum_{p=m+1}^{\infty}{}' \gamma_{m+1p}(\pi/2)\frac{S_{m+1p}(-ic,o)}{R^{(4)}_{m+1p}(-ic,o)}(-m)\begin{Bmatrix}-\sin m\\ \cos\end{Bmatrix}\right] \qquad (176)$$

It can be rewritten as follows:

$$\frac{2im}{ckd^2}\left\{\sum_{p=m-1}^{\infty} (1+\delta_{1m})(1+\delta_{om})\gamma_{m-1p}(\pi/2)\frac{S_{m-1p}(-ic,o)}{R^{(4)}_{m-1p}(-ic,io)} + \sum_{p=m+1}^{\infty} \gamma_{m+1p}(\pi/2)\frac{S_{m+1p}(-ic,o)}{R^{(4)}_{m+1p}(-ic,o)}\right\}\begin{Bmatrix}\sin\\ -\cos\end{Bmatrix} m\phi \qquad (177)$$

This coefficient has a different ϕ-dependence than the other two. The coefficient of $\frac{\eta}{\eta^2+\xi^2}$ in $[\frac{1}{k} \nabla x \overline{F}_{e_{om}}]_\phi$ is obtained from Equation (166), (172) and (173). It is equal to Equation (175) multiplied by $-\frac{d}{2}$. Equation (175) and (177) differ only by their ϕ-dependence and a factor m in Equation (177).

Equation (175) and (177) give the coefficients of the terms in the components of $\overline{F}_{e_{om}}$ and $1/k \nabla x \overline{F}_{e_{om}}$ that do not behave as required by the edge condition in the vicinity of the edge. Note that for m=0, the coefficient in Equation (177) is always equal to zero while only the odd case of Equation (175) disappears. Thus $\overline{F}_{o_{o}}$ and $1/k \nabla x \overline{F}_{o_{o}}$ behave as required by the edge condition and, therefore, the missing relation in Equation (167) will not be needed since the functions $\overline{N}^{(4)}_{o_{op}}$ and $\overline{M}^{(4)}_{o_{op}}$ are well behaved at the edge.

We now have the necessary tools to solve the scattering problem.

2. Solution

The solution will be derived for the general case of arbitrary incidence and polarization. We will use the same notation as in part V for the electric and magnetic field.

$$\overline{E}^i = E_o(\cos\alpha\, \overline{E}^{i''} + \sin\alpha\, \overline{E}^{i\perp}) \tag{178}$$

We expand $\overline{E}^{i''}$ and $\overline{E}^i$ from Equations (47) and (48)

$$\overline{E}^{i''} = \frac{1}{k\cos\theta_o} \sum_{m=0}^{\infty} \sum_{n=m}^{\infty} \gamma_{mn}(\theta_o)\, \overline{N}^{x(1)}_{e_{mn}}$$

$$\overline{E}^{i\perp} = \frac{1}{k} \sum_{m=0}^{\infty} \sum_{n=m}^{\infty} \gamma_{mn}(\theta_o)\, \overline{N}^{y(1)}_{e_{mn}} \tag{179}$$

From Equations (30) to (33), we see that, for n-m odd, the incident vector wave functions have null taggential components on the disk. Therefore the reflected fields are:

$$\overline{E}^{r''} = -\frac{1}{k\cos\theta_o} \sum_{m=0}^{\infty} \sum_{n=m}^{\infty}{}' \gamma_{mn}(\theta_o) \frac{R^{(1)}_{mn}(-ic,io)}{R^{(4)}_{mn}(-ic,io)} \overline{N}^{x(4)}_{e_{mn}}$$

$$\overline{E}^{i\perp} = -\frac{1}{k} \sum_{m=0}^{\infty} \sum_{n=m}^{\infty}{}' \gamma_{mn}(\theta_o) \frac{R^{(1)}_{mn}(-ic,io)}{R^{(4)}_{mn}(-ic,io)} \overline{N}^{y(4)}_{e_{mn}} \tag{180}$$

Once again the "reflected" fields as defined here are not equal to the scattered fields since they do not satisfy the edge condition. We can now add to the reflected field any summation of functions $\bar{F}_{e_m}$ and still have a reflected field. The coefficients of that summation will be adjusted so that the fields satisfy the edge condition.

From Equation (154), we see that $\bar{N}^{x(i)}_{e_{mn}}$ involves only even functions $\bar{N}^{+(i)}_{e_{m+1n}}$ and $\bar{N}^{-(i)}_{e_{m-1n}}$ while $\bar{N}^{y(i)}_{e_{mn}}$ involves only odd functions $\bar{N}^{+(i)}_{o_{m+1n}}$ and $\bar{N}^{-(i)}_{o_{m+1n}}$. Therefore to match the edge condition, we need only add a summation of $\bar{F}_{e_m}$ to $\bar{E}^{r''}$ and $\bar{F}_{om}$ to $E^{r\perp}$, since $\bar{F}_{e_{\delta m}}$ satisfies the boundary condition on the surface of the disk. The scattered field will be:

$$\bar{E}^{s''} = \bar{E}^{r''} + \frac{1}{k \cos\theta_o} \sum_{m=0}^{\infty} U_{mv} \bar{F}_{e_m}$$

$$\bar{E}^{s\perp} = \bar{E}^{r\perp} + \frac{1}{k} \sum_{m=1}^{\infty} X_{mv} \bar{F}_{o_m} \qquad (181)$$

where U_{mv} and X_{mv} are adjusted to satisfy the edge condition.

The summation over m in $\bar{E}^{s\perp}$ begins with m=1 since $\bar{F}_{o_o}$ is well behaved at the edge and does not correct the behavior of $\bar{E}^{r\perp}$. We will successively consider the perpendicular polarization and parallel polarization cases.

a. Perpendicular polarization

Equations (179) and (180) can be rewritten as follows, from Equation (154):

AD-A086 441 OHIO STATE UNIV COLUMBUS ELECTROSCIENCE LAB F/G 20/14
ELECTROMAGNETIC SCATTERING BY A METALLIC DISK.(U)
SEP 79 D P NITHUARD, D B HODGE N00014-78-C-0049
UNCLASSIFIED ESL-718816-8 NL

2 OF 2
AD
A086441

END
DATE FILMED
3-80
DTIC

$$\bar{E}^{i\perp} = \frac{1}{k} \sum_{m=0}^{\infty} \left\{ \sum_{p=m-1}^{\infty} \left[(1+\delta_{1m})(1-\delta_{om}) \gamma_{m-1p}(\theta_o) \, \bar{N}^{+(1)}_{o_{mp}} \right] - \sum_{p=m+1}^{\infty} \gamma_{m+1p}(\theta_o) \, \bar{N}^{-(1)}_{o_{mp}} \right\}$$

$$\bar{E}^{r\perp} = -\frac{1}{k} \sum_{m=0}^{\infty} \left\{ \sum_{p=m-1}^{\infty}{}' \left[(1+\delta_{1m})(1-\delta_{om}) \gamma_{m-1p}(\theta_o) \frac{R^{(1)}_{m-1p}(-ic,io)}{R^{(4)}_{m-1p}(-ic,io)} \bar{N}^{+(4)}_{o_{mp}} \right] - \sum_{p=m+1}^{\infty}{}' \gamma_{m+1p}(\theta_o) \frac{R^{(1)}_{m+1p}(-ic,io)}{R^{(4)}_{m+1p}(-ic,io)} \bar{N}^{-(4)}_{o_{mp}} \right\} \tag{182}$$

We must adjust the coefficient X_{mv} so that the coefficients of the ill-behaved terms in each component disappear at the edge.

Taking advantage of the ϕ-orthogonality, we can write a specific condition for each value of m:

for every $m \geq 0$, at $\eta = \xi = 0$:

$$\left\{ \begin{aligned} &\frac{1}{k} \sum_{p=m-1}^{\infty} (1+\delta_{1m})(1-\delta_{om}) \gamma_{m-1p}(\theta_o) \, \bar{N}^{+(1)}_{o_{mp}} \\ &- \frac{1}{k} \sum_{p=m+1}^{\infty} \gamma_{m+1p}(\theta_o) \, \bar{N}^{-(1)}_{o_{mp}} \\ &- \frac{1}{k} \sum_{p=m-1}^{\infty}{}' \left[(1+\delta_{1m})(1-\delta_{om}) \gamma_{m-1p}(\theta_o) \frac{R^{(1)}_{m-1p}(-ic,io)}{R^{(4)}_{m-1p}(-ic,io)} \bar{N}^{-(4)}_{o_{mp}} \right] \\ &+ \frac{1}{k} \sum_{p=m+1}^{\infty}{}' \left[\gamma_{m+1p}(\theta_o) \frac{R^{(1)}_{m+1p}(-ic,io)}{R^{(4)}_{m+1p}(-ic,io)} \bar{N}^{(4)}_{o_{mp}} \right] \\ &+ \frac{1}{k} X_{mv} \bar{F}_{om} (1-\delta_{om}) \quad \text{must satisfy the edge condition.} \end{aligned} \right. \tag{183}$$

We have seen that the functions of index 1 and $\bar{N}^{(4)}_{o_{op}}$ behave as required by the edge condition. The absence of coefficient X_{o_v} is therefore not a problem. For any other value m, $m \geq 1$, the conditions on X_{m_v} from the three components r, θ, ϕ of Equation (183) are identical since the coefficients of the improper singularities in Equation (168) to (170) are proportional apart from their ϕ-dependence. From Equation (173), we see that this also applies for the ϕ-component of the curl of Equation (183) which corresponds to the m-part of the expansion of the magnetic field.

X_{mv} satisfies, for $m \geq 1$:

$$
\begin{aligned}
&- \sum_{p=m-1}^{\infty}{}' (1+\delta_{1m})(1-\delta_{om}) \gamma_{m-1p}(\theta_o) \frac{i}{c} \frac{S_{m-1p}(-ic,o)}{R^{(4)}_{m-1p}(-ic,io)} \\
&+ \sum_{p=m+1}^{\infty}{}' \gamma_{m+1p}(\theta_o) \frac{i}{c} \frac{S_{m+1p}(-ic,o)}{R^{(4)}_{m+1p}(-ic,io)} \\
&+ X_{mv} \left\{ \sum_{p=m-1}^{\infty}{}' (1+\delta_{1m})(1-\delta_{om}) \gamma_{m-1p}(\pi/2) \frac{i}{c} \frac{S_{m-1p}(-ic,o)}{R^{(4)}_{m-1p}(-ic,io)} \right. \\
&\left. + \sum_{p=m+1}^{\infty}{}' \frac{i}{c} \gamma_{m+1p}(\pi/2) \frac{S_{m+1p}(-ic,o)}{R^{(4)}_{m+1p}(-ic,io)} \right\} = 0
\end{aligned}
\tag{184}
$$

We notice that, from Equation (42), we have, $m \geq 0$:

$$
\begin{aligned}
(1-\delta_{om})(1+\delta_{1m}) \gamma_{m-1p}(\theta_o) &= \frac{4i^p}{N_{m-1p}} S_{m-1p}(-ic, \cos\theta_o)(1-\delta_{om}) \\
\gamma_{m+1p}(\theta_o) &= \frac{4i^p}{N_{m+1p}} S_{m+1p}(-ic, \cos\theta_o)
\end{aligned}
\tag{185}
$$

Introducing the functions W_m and ψ_m as in Meixner's solution, Equations (143) and (144), we have for X_{mv}:

$$
X_{mv} = \frac{W_{m-1} - W_{m+1}}{\psi_{m-1} + \psi_{m+1}} \quad \text{for } m \geq 1 \tag{186}
$$

With those coefficients we can compute the scattered field of the perpendicular polarization case. We obtain from Equations (180), (181) and (186):

$$\bar{E}^{s^{\perp}} = -\frac{1}{k}\sum_{m=0}^{\infty}\sum_{n=m}^{\infty}{}' \gamma_{mn}(\theta_o)\frac{R_{mn}^{(1)}(-ic,io)}{R_{mn}^{(4)}(-ic,io)}\ \bar{N}^{y(4)}_{e_{mn}}$$

$$+\frac{4}{k}\sum_{m=0}^{\infty}\left[X_{m+1v}\sum_{n=m}^{\infty}{}'\frac{i^n}{N_{mn}}S_{mn}(-ic,o)\frac{R_{mn}^{(1)}(-ic,io)}{R_{mn}^{(4)}(-ic,io)}\bar{N}^{(4)}_{o_{m+1n}}\right.$$

$$\left.+(1-\delta_{1m})(1-\delta_{om})X_{m-1v}\sum_{n=m}^{\infty}{}'\frac{i^n}{N_{mn}}S_{mn}(-ic,o)\frac{R_{mn}^{(1)}(-ic,io)}{R_{mn}^{(4)}(-ic,io)}\bar{N}^{(4)}_{m-1n}\right] \tag{187}$$

We can check this solution by comparing it with Equation (156). We compare the coefficients of $\bar{N}^{+(4)}_{o_{m+1n}}$ and $\bar{N}^{-(4)}_{o_{m-1n}}$ in both solutions.

$$\text{for } m \geq 0 \quad \frac{2}{k}\,i^{-m}\,X^{\perp}_{m+1} = \frac{2i^{-m}}{k}\,2i^{+m+1-1}\,\frac{W_m - W_{m+2}}{\psi_m + \psi_{m+2}} = \frac{4}{k}\,X_{m+1v} \tag{188}$$

$$\text{for } m \geq 2 \quad \frac{2}{k}\,i^{-m}\,X^{\perp}_{m-1} = \frac{2i^{-m}}{k}\,2i^{m-1-1}\,\frac{W_{m-2} - W_m}{\psi_{m-2} + \psi_m} = -\frac{4}{k}\,X_{m-1v}$$

The scattered field obtained by this method is identical to the one obtained by Meixner, as expected.

b. Parallel polarization

Equations (179) and (180) can be rewritten as follows, from Equation (154):

$$\bar{E}^{i''} = \frac{1}{k\cos\theta_o}\sum_{m=0}^{\infty}\left\{\sum_{p=m-1}^{\infty}(1+\delta_{1m})(1-\delta_{om})\gamma_{m-1p}(\theta_o)\,\bar{N}^{+(1)}_{e_{mp}}\right.$$

$$\left.+\sum_{p=m+1}^{\infty}\gamma_{m+1p}(\theta_o)\,\bar{N}^{-(1)}_{e_{mp}}\right\} \tag{189}$$

$$\bar{E}^{r''} = -\frac{1}{k\cos\theta_o}\sum_{m=0}^{\infty}\left\{\sum_{p=m-1}^{\infty}{}'(1+\delta_{1m})(1-\delta_{om})\gamma_{m-1p}(\theta_o)\,\bar{N}^{+(4)}_{e_{mp}}\right.$$

$$\left.+\sum_{p=m+1}^{\infty}{}'\gamma_{m+1p}(\theta_o)\,\bar{N}^{-(4)}_{e_{mp}}\right\}$$

We must adjust the coefficients U_{mv} in Equation (181) so that the coefficients of the improper singularities in each component of the fields disappear at the edge.

Taking advantage of the ϕ-orthogonality, we can write a specific condition for each value of m:

for $m \geq 0$ at $\xi = \eta = 0$, the following quantity,

$$\frac{1}{k \cos\theta_o} \sum_{p=m-1}^{\infty} (1+\delta_{1m})(1-\delta_{om})\gamma_{m-1p}(\theta_o)\, \overline{N}^{+(1)}_{e_{mp}}$$
$$+ \frac{1}{k \cos\theta_o} \sum_{p=m+1}^{\infty} \gamma_{m+1p}(\theta_o)\, \overline{N}^{-(1)}_{e_{mp}} \qquad (190)$$
$$- \frac{1}{k \cos\theta_o} \sum_{p=m-1}^{\infty}{}' (1+\delta_{1m})(1-\delta_{om})\gamma_{m-1p}(\theta_o) \frac{R^{(1)}_{m-1p}(-ic,io)}{R^{(4)}_{m-1p}(-ic,io)}\, \overline{N}^{+(4)}_{e_{mp}}$$
$$- \frac{1}{k \cos\theta_o} \sum_{p=m+1}^{\infty} \gamma_{m+1p}(\theta_o) \frac{R^{(1)}_{m+1p}(-ic,io)}{R^{(4)}_{m+1p}(-ic,io)}\, \overline{N}^{-(4)}_{e_{mp}}$$
$$+ \frac{1}{k \cos\theta_o}\, U_{mv}\, \overline{F}_{em}$$

must satisfy the edge condition.

The functions of index 1 behave as required by the edge condition and will, therefore, not contribute to the computation of U_{mv}. For m greater than zero, the conditions on U_{mv} from the three components of Equation (190) and from those of its curl are equivalent since the coefficients of the improper singularities in Equations (168) to (170) are proportional apart from their ϕ-dependence. For m equal to zero, the η- and ξ-components of Equation (190) and the ϕ-component of its curl lead to equivalent conditions on U_{ov}. The ϕ-component of Equation (190), however, contains no improper singularity since the transformation of the coefficient of the singularity of $[\overline{N}^{+(4)}_{e_{m-1,n}}]_\phi$, Equation (170), into that of $[\overline{N}^{-(4)}_{e_{mp}}]_\phi$ leads to a m factor in the latter. It can be seen in $[\overline{F}_{e_{mp}}]_\phi$, Equation (177), for example. For m equal to zero, the ϕ-component of Equation (190) does not impose any condition on U_{ov} in order to satisfy the edge condition. The satisfaction of the three other conditions will then be sufficient at the edge to obtain the scattered field. For any value of m, the condition on U_{mv} is:

$$- \sum_{p=m-1}^{\infty} (1+\delta_{1m})(1-\delta_{om})\gamma_{m-1p}(\theta_o)\frac{i}{c}\frac{S_{m-1p}(-ic,o)}{R^{(4)}_{m-1p}(-ic,io)}$$

$$- \sum_{p=m+1}^{\infty} \gamma_{m+1p}(\theta_o)\frac{i}{c}\frac{S_{m+1p}(-ic,o)}{R^{(4)}_{m+1p}(-ic,io)} \qquad (191)$$

$$+ U_{mv}\left\{ \sum_{p=m-1}^{\infty}{}' (1+\delta_{1m})(1-\delta_{om})\gamma_{m-1p}(\pi/2)\frac{i}{c}\frac{S_{m-1p}(-ic,o)}{R^{(4)}_{m-1p}(-ic,io)}\right.$$

$$\left. + \sum_{p=m+1}^{\infty}{}' \frac{i}{c}\gamma_{m+1p}(\pi/2)\frac{S_{m+1p}(-ic,o)}{R^{(4)}_{m+1p}(-ic,io)}\right\} = 0$$

Introducing the functions W_m and ψ_m as in Meixner's solution, Equation (143) and (144), and using the properties of $\gamma_{mn}(\theta_o)$, Equation (185), we have for U_{mv}:

$$U_{ov} = \frac{W_1}{\psi_1}$$

$$U_{mv} = \frac{W_{m-1} + W_{m+1}}{\psi_{m-1} + \psi_{m+1}} \quad \text{for } m \geq 1 \qquad (192)$$

With those coefficients we can compute the scattered field of the parallel polarization case. We obtain from Equations (180), (181) and (192):

$$\bar{E}^{s''} = -\frac{1}{k\cos\theta_o}\sum_{m=0}^{\infty}\sum_{n=m}^{\infty}{}'\gamma_{mn}(\theta_o)\frac{R^{(1)}_{mn}(-ic,io)}{R^{(4)}_{mn}(-ic,io)}\bar{N}^{x(4)}_{e_{mn}}$$

$$+ \frac{4}{k\cos\theta_o}\sum_{m=0}^{\infty}\sum_{n=m}^{\infty}{}'\frac{i^n}{N_{mn}}S_{mn}(-ic,o)\frac{R^{(1)}_{mn}(-ic,io)}{R^{(4)}_{mn}(-ic,io)} \times \qquad (193)$$

$$\times \left[U_{m+1v}\bar{N}^{(4)}_{e_{m+1n}} + (1-\delta_{om})U_{m-1v}\bar{N}^{(4)}_{e_{m-1n}}\right]$$

We can check this solution by comparing it with Equation (158). We compare the coefficients of $\bar{N}^{+(4)}_{e_{m+1n}}$ and $\bar{N}^{-(4)}_{e_{m-1n}}$ in both solutions.

$$-\frac{2i^{-1}}{k\cos\theta_o}\quad U''_o = \frac{4ii^{-1}}{k\cos\theta_o}\quad \frac{W_1}{\psi_1} = \frac{4}{k\cos\theta_o}\,U_{ov}$$

$$\text{for } m \geq 0\quad \frac{2i^{-m}}{k\cos\theta_o}\,U''_{m+1} = \frac{2i^{-m}i^{m+1-1}2}{k\cos\theta_o}\quad \frac{W_m+W_{m+2}}{\psi_m+\psi_{m+2}} = \frac{4}{k\cos\theta_o}\,U_{m+1v}$$

$$\text{for } m \geq 2\quad \frac{2i^{-m}}{k\cos\theta_o}\,U''_{m-1} = \frac{2i^{-m}2i^{m-1-1}}{k\cos\theta_o}\quad \frac{W_{m-2}+W_m}{\psi_{m-2}+\psi_m} = -\frac{4}{k\cos\theta_o}\,U_{m-1v} \tag{194}$$

We see that the coefficients match exactly. The scattered field obtained by this method is exactly that of Meixner's solution.

We have given a proof of Meixner's solution by dealing with electromagnetic fields only. The scattered field has been determined so that it satisfies the boundary conditions on the surface of the disk and the edge condition. This proof gives more insight in the behavior of the fields in the vicinity of the edge than Meixner's. It, however, requires the calculation of the expansions of the spheroidal vector wave functions in the vicinity of the edge, and its edge condition consists of six conditions whose compatibility must be checked. It is algebraically more complicated than Meixner's, whose edge condition consists in one equation only since Meixner mostly deals with scalar functions. In the next section, we will calculate the scattered field for an incident field equal to a single vector wave function.

3. Scattered field of a single vector wave function

From the solution derived in the previous section, we can easily calculate the scattered field for an incident electric field equal to a single wave function. The purpose of this section is to show that this scattered field contains all the vector wave functions of index 4 which have the same index m in their ϕ-dependences as the incident one. Let us, for example, consider an incident field equal to $\frac{1}{k}\,\overline{N}^{+(1)}_{e_{m+1n}}$. Adjusting Equations (179), (180) and (181) to our case, we have:

$$\overline{E}^i = \frac{1}{k}\;\overline{N}^{+(1)}_{e_{m-1n}}$$

$$\overline{E}^r = -\frac{1}{k}\,\frac{R^{(1)}_{mn}(-ic,io)}{R^{(4)}_{mn}(-ic,io)}\;\overline{N}^{+(4)}_{e_{m+1n}} + \frac{U_{m+1}}{k}\;\overline{F}_{e_{m+1}} \tag{195}$$

Following the same derivation as in the parallel polarization case, we obtain, from Equation (190), the following condition on U_{m+1} due to the edge condition.

$$-\frac{i}{c}\frac{S_{mn}(-ic,o)}{R^{(4)}_{mn}(-ic,io)} + U_{m+1}\frac{i}{c}(\psi_m+\psi_{m+2}) = 0 \qquad (196)$$

Thus,

$$U_{m+1} = \frac{S_{mn}(-ic,o)}{R^{(4)}_{mn}(-ic,io)[\psi_m+\psi_{m+2}]} \quad . \qquad (197)$$

From Equation (195) and the definition of $\overline{F}_{e_{m+1}}$, Equation (166), we see that the obtained scattered field involves all the functions $\overline{N}^{+(4)}_{e_{\delta m+1n}}$ and $\overline{N}^{-(4)}_{e_{\delta m+1n}}$ for the given value of m. If we choose an incident field equal to $\frac{1}{k}\overline{N}^{x(1)}_{e_{mn}}$, instead, the scattered field contains all the functions $\overline{N}^{+(4)}_{e_{m\pm1n}}$ and $\overline{N}^{-(4)}_{e_{m\pm1n}}$ for m given, from Equations (154) and (195). Whatever the vector wave function of vector $\hat{e}_x$ or $\hat{e}_y$, or derived from these, Equation (154), the corresponding scattered field is not equal to the reflected field and contains the other vector wave functions with the same ϕ-dependence.

D. Conclusion

In this part, we have shown that the fields of Meixner's solution can be expressed in terms of spheroidal vector wave functions. We can therefore calculate the fields everywhere directly. In particular, this will allow us to compute the near-fields and the current distribution on the surface of the disk. Meixner's solution is formally as convenient as Flammer's in this region. However, for computational purposes, Meixner's solution should be retained since it only requires the values of the angular and radial spheroidal functions and their derivatives for n-m even. On the surface of the disk, we can see from Equations (23) and (24) that we only need the values of the radial functions at ξ=0, since the derivatives can be expressed from them. We have also shown how the scattered field of a single incident vector wave function involves all the vector wave functions of the same ϕ-dependence. This is a consequence of the fact that the vector wave functions cannot be considered to be modes because of the dependence relationships.

CHAPTER VII
CONCLUSION

Considerable knowledge has been obtained about scattering by a metallic disk in the last three decades. However, most of this work was done in the far-field region.

Meixner's solution can be directly applied in this case because of its vector potential formulation. The purpose of this work was to establish a valid solution everywhere in space.

Flammer's solution was considered first since it leads directly to formulations of the scattered electric and magnetic fields. The validity of this solution, however, still needed to be established. We rederived it for the normal incidence, perpendicular polarization bistatic case and compared numerical results to data obtained from Meixner's solution. The general agreement of both solutions showed that Flammer's solution is acceptable in this case. We, however, encountered problems in the derivation of Flammer's solution in the arbitrary incidence case and its validity is still questionable. Thus, Flammer's solution did not provide us the expressions that we were looking for.

Meixner's approach to the problem leads to a solution that has been, in turn, expanded in spheroidal vector wave functions. Another proof has been given directly using dependence properties of the spheroidal vector wave functions. This formulation of the fields is adequate even for near field computations. For example, the computation of the surface currents on the disk should be made with Meixner's solution.

In parallel to the solution of the scattering by a disk, we have shown some dependence properties of the spheroidal functions. The derivatives of the spheroidal angular functions are not independent as the original functions are. Some dependence relations of the spheroidal vector wave functions of index 1 have been derived, and it is therefore impossible to consider a single vector wave function as a mode in these cases.

Some questions remain after this work. The formal agreement of the scattered far-field of Flammer's and Meixner's solution in the normal incidence, perpendicular polarization bistatic case should

be numerically checked as explained in Section VIB. The validity of Flammer's arbitrary incidence solution should be tested as explained in Section VB. If the validity of Flammer's solution can be established, it should be interesting to compute the surface current distribution on the disk from Flammer's and Meixner's solution. This could be a good test since the general formal solutions are too complicated to be matched term by term.

REFERENCES

1. G. Mie, Ann. Physik, 25, 377 (1908).

2. Lord Rayleigh, Phil. Mag. 44, 28 (1897).

3. J. Meixner and W. Andrejewski, Ann. Physik 7, 157 (1950).

4. J. Meixner, Ann. Physik (6), 6, 2 (1949).

5. C. J. Bouwkamp, Philips Research Rep. 5, 401 (1950).

6. D. B. Hodge, "Eigenvalues and Eigenfunctions of the Spheroidal Wave Equation," J. Mathematical Physics, Vol. 11, p. 2308 (1970).

7. C. Flammer, "The Vector Wave Function Solution of the Diffraction of Electromagnetic Waves by Circular Disks and Apertures," J. Appl. Phys., Vol. 24, pp. 1218-1231 (1953).

8. D. B. Hodge, "Spectral and Transient Response of a Circular Disk to Plane Electromagnetic Waves," IEEE Trans. Vol. AP-19, p. 558 (1971).

9. D. B. Hodge, "The Calculation of Far Field Scattering by a Circular Metallic Disk," Report 710816-2, February 1979, The Ohio State University ElectroScience Laboratory, Department of Electrical Engineering; prepared under Contract N00014-78-C-0049, Department of the Navy, Office of Naval Research, Arlington, Virginia.

10. C. Flammer, Spheroidal Wave Functions, Stanford University Press (1957).

11. J. A. Stratton, Electromagnetic Theory, McGraw-Hill Book Company, Inc., New York, pp. 38-51 (1941).

12. C. Flammer, "The Vector Wave Solution of the Diffraction of Electromagnetic Waves by Circular Disks and Apertures," Report No. 27, SRI Project No. 591, September 1952, Stanford Research Institute; prepared under Contract No. AF19(604)-266, Air Force.

APPENDIX A
THE OBLATE SPHEROIDAL COORDINATE SYSTEM

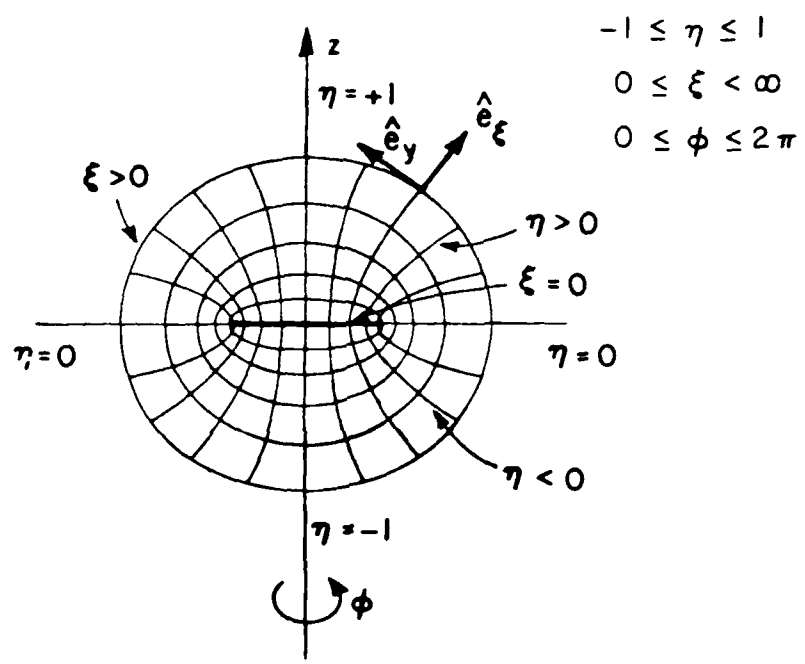

Figure A-1. The oblate coordinate system.

The oblate spheroidal coordinate system has the components (η, ξ, ϕ) whose characteristics are:

- the ξ-constant surfaces are ellipsoids of revolution (around the z axis, in our case). The intersection of those surfaces with a plane containing the z-axis are ellipses whose foci are the edge points of the circular disk in this plane.

- the ξ-constant surfaces are hyperboloids of revolution around the z axis. In the same way, the foci of the intersections with a radial plane are the edge points of the circular disk.

- ϕ is the usual azimuthal coordinate as in the cylindrical case.

$\xi=0$ represents the surface of the disk of radius d/2, $c=\frac{1}{2}$ kd.

ξ varies from 0 to infinity whereas η varies from -1 to 1.

The following formulas have been rederived from the general orthogonal coordinates systems transformations as explained, for example, by Stratton[11].

We first establish the relations between the usual coordinates systems and the spheroidal coordinate system.. We then consider the limiting cases of large radial argument, $c\xi$, of the surface of the disk, $\xi=0$, and of the neighborhood of the edge, $\xi=0$ and $\eta=0$.

1. Coordinate Transformations

a. Components

from Cartesian:

$$\begin{cases} x = \frac{d}{2}\,[(1-\eta^2)(1+\xi^2)]^{\frac{1}{2}}\cos\phi \\ y = \frac{d}{2}\,[(1-\eta^2)(1+\xi^2)]^{\frac{1}{2}}\sin\phi \\ z = \frac{d}{2}\,\eta\xi \end{cases} \qquad (A1)$$

from cylindrical:

$$\rho = \frac{d}{2}\,[(1-\eta^2)(1+\xi^2)]^{\frac{1}{2}} \qquad (A2)$$

from spherical:

$$\begin{cases} r = \sqrt{\rho^2+z^2} = \frac{d}{2}\,\sqrt{1-\eta^2+\xi^2} \\ \cos\theta = \eta\,\frac{\xi}{\sqrt{1-\eta^2+\xi^2}} \\ \sin\theta = \left[\frac{(1-\eta^2)(1+\xi^2)}{1-\eta^2+\xi^2}\right]^{\frac{1}{2}} \end{cases} \qquad (A3)$$

The metric-coefficients are computed from the following formula:

$$h_i = \sqrt{\left(\frac{\partial x}{\partial v^i}\right)^2 + \left(\frac{\partial y}{\partial v^i}\right)^2 + \left(\frac{\partial z}{\partial v^i}\right)^2} \quad \text{where } v^i = \eta, \xi, \phi \tag{A4}$$

From Equation (A1), we obtain

$$\begin{cases} h_\eta = \frac{d}{2}\left[\frac{\eta^2+\xi^2}{1-\eta^2}\right]^{\frac{1}{2}} & h_\xi = \frac{d}{2}\left[\frac{\eta^2+\xi^2}{1+\xi^2}\right]^{\frac{1}{2}} \\ h_\phi = \frac{d}{2}\left[(1-\eta^2)(1+\xi^2)\right]^{\frac{1}{2}} \end{cases} \tag{A5}$$

b. Unit basis vectors

We give in Table A6 the dot products between the basis vectors of the spheroidal coordinate system and those of the common coordinate systems. The different formulas can be obtained using the general relationship in a basis $(\vec{e}_i)$:

$$\vec{a} = \sum_i (\vec{a}.\vec{e}_i)\vec{e}_i \tag{A7}$$

The dot products are computed using the relation

$$\hat{e}_\alpha \cdot \hat{e}_\beta = \left(\frac{\partial \alpha}{\partial \beta}\right) \frac{1}{h_\beta} \tag{A8}$$

where α and β can be x, y, z; ρ, r, θ, η, ξ, ϕ.

2. Large c Approximations

a. Components

Since ξ is always positive Equations (A1) to (A3) reduce to:

$$\begin{cases} x = \frac{d}{2}\,\xi\sqrt{1-\eta^2}\,\cos\phi \\ y = \frac{d}{2}\,\xi\sqrt{1-\eta^2}\,\sin\phi \\ \rho = \frac{d}{2}\,\xi\sqrt{1-\eta^2} \\ r = \frac{d}{2}\,\xi \\ \eta = \cos\theta \\ \sin\theta = \sqrt{1-\eta^2} \qquad \text{for } c\xi \gg 1 \end{cases} \tag{A9}$$

Table A6

	$\hat{e}_\eta$	$\hat{e}_\xi$	$\hat{e}_\phi$
$\hat{e}_x$	$-\eta\left[\frac{1+\xi^2}{\eta^2+\xi^2}\right]^{\frac{1}{2}}\cos\phi$	$\xi\left[\frac{1-\eta^2}{\eta^2+\xi^2}\right]^{\frac{1}{2}}\cos\phi$	$-\sin\phi$
$\hat{e}_y$	$-\eta\left[\frac{1+\xi^2}{\eta^2+\xi^2}\right]^{\frac{1}{2}}\sin\phi$	$\xi\left[\frac{1-\eta^2}{\eta^2+\xi^2}\right]^{\frac{1}{2}}\sin\phi$	$\cos\phi$
$\hat{e}_z$	$\xi\left[\frac{1-\eta^2}{\eta^2+\xi^2}\right]^{\frac{1}{2}}$	$\eta\left[\frac{1+\xi^2}{\eta^2+\xi^2}\right]^{\frac{1}{2}}$	0
$\hat{e}_\rho$	$-\eta\left[\frac{1+\xi^2}{\eta^2+\xi^2}\right]^{\frac{1}{2}}$	$\xi\left[\frac{1-\eta^2}{\eta^2+\xi^2}\right]^{\frac{1}{2}}$	0
$\hat{e}_r$	$-\frac{\eta}{(1-\eta^2+\xi^2)^{\frac{1}{2}}}\left[\frac{1-\eta^2}{\eta^2+\xi^2}\right]^{\frac{1}{2}}$	$\frac{\xi}{(1-\eta^2+\xi^2)^{\frac{1}{2}}}\left[\frac{1+\xi^2}{\eta^2+\xi^2}\right]^{\frac{1}{2}}$	0
$\hat{e}_\theta$	$-\frac{\xi}{(1-\eta^2+\xi^2)^{\frac{1}{2}}}\left[\frac{1+\xi^2}{\eta^2+\xi^2}\right]^{\frac{1}{2}}$	$-\frac{\eta}{(1-\eta^2+\xi^2)^{\frac{1}{2}}}\left[\frac{1-\eta^2}{\eta^2+\xi^2}\right]^{\frac{1}{2}}$	0

This leads us back to the spherical coordinate system. The two main relationships are:

$$\eta = \cos\theta \text{ and } \xi = \frac{2r}{d} \tag{A10}$$

b. Basis vectors

For $c\xi >> 1$

$$\begin{cases} \hat{e}_\eta \to -\eta\hat{e}_\rho + (1-\eta^2)\hat{e}_z \to -\hat{e}_\theta \\ \hat{e}_\xi \to \hat{e}_r. \end{cases} \tag{A11}$$

3 On the Surface of the Disk

The disk is represented by $\xi = 0$. We have the relationships:

$$\begin{cases} \rho = r = \frac{d}{2}\sqrt{1-\eta^2} \\ \hat{e}_\eta \to -\frac{\eta}{|\eta|}\hat{e}_\rho \\ \hat{e}_\xi \to \frac{\eta}{|\eta|}\hat{e}_z \end{cases} \tag{A12}$$

4. Edge Coordinate System

To determine how a component of the field behaves in the vicinity of the edge of the disk, the significant quantity of interest is the distance from the edge to the observation point. Let us call this quantity s in the coordinate system shown in Figure A-2.

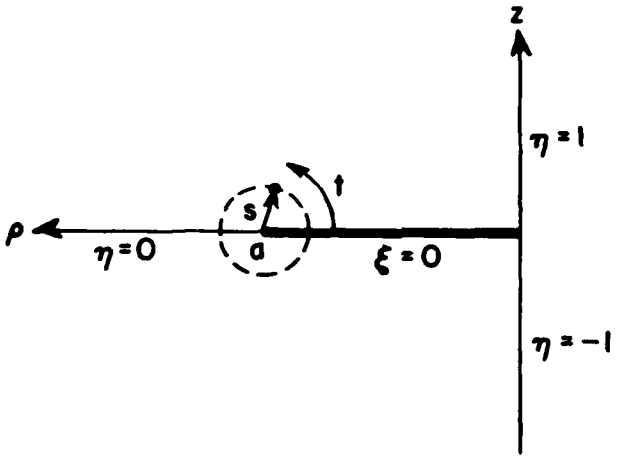

Figure A-2. (s,t,ϕ) coordinate system.

We will use the following notation:

s distance from the edge to the observation point.

t angle between the positive side ($\eta>0$) of the disk to the observation point.

We restrict our domain to small distances from the edge: $s \ll d$. We notice that, in this system, with $s \ll d$:

$t = 0$ is the disk itself

$t = \pi$ is the plane of the disk outside the disk.

We will derive the relations between the spheroidal coordinate of small argument and this edge system.

In the following, we have $\xi \ll 1, |\eta| \ll 1.$

By definition, we have

$$s^2 = \left(\rho - \frac{d}{2}\right)^2 + z^2 \tag{A13}$$

In spheroidal coordinates, this equation can be written

$$s^2 = \frac{d^2}{4}\left\{\left[(1-\eta^2)^{\frac{1}{2}}(1+\xi^2)^{\frac{1}{2}} - 1\right]^2 + \eta^2\xi^2\right\} \tag{A14}$$

For η and ξ small, we may write:

$$\left[(1-\eta^2)(1+\xi^2)\right]^{\frac{1}{2}} = 1 - \frac{\eta^2}{2} + \frac{\xi^2}{2} + O(\eta^4, \xi^4, \eta^2, \xi^2) \tag{A15}$$

which leads to

$$s^2 = \frac{d^2}{4}\left\{\frac{1}{4}\ (\xi^2-\eta^2)^2 + \eta^2\xi^2\right\} = \frac{d^2}{16}\ (\eta^2+\xi^2)^2$$

Finally

$$s = \frac{d}{4}\ (\eta^2+\xi^2) \tag{A16}$$

In order to compute η and ξ as functions of s and t, we use

$$\begin{cases} \rho - a = -s\cos t = \frac{d}{4}(\xi^2 - \eta^2) \\ z = s \sin t = \frac{d}{2}\eta\xi \end{cases} \tag{A17}$$

$$\begin{cases} \cos t = \frac{\eta^2 - \xi^2}{\eta^2 + \xi^2} \\ \sin t = \frac{2\eta\xi}{\eta^2 + \xi^2} \end{cases} \tag{A18}$$

Since $\cos t = \cos^2 t/2 - \sin^2 t/2$
$\sin t = 2 \cos t/2 \sin t/2$

$$\begin{cases} \eta = \sqrt{\eta^2 + \xi^2}\cos t/2 = 2\sqrt{\frac{s}{d}}\cos t/2 \\ \xi = 2\sqrt{\frac{s}{d}}\sin t/2 \end{cases} \tag{A19}$$

The equations (A16), (A18) and (A19) summarize the transformation between the edge coordinate system and the spheroidal coordinate system.

APPENDIX B
DIFFERENTIAL OPERATORS IN THE OBLATE SPHEROIDAL COORDINATE SYSTEM

Gradient

$$\nabla\Phi = \frac{2}{d}\left[\frac{1-\eta^2}{\xi^2+\eta^2}\right]^{\frac{1}{2}}\frac{\partial\Phi}{\partial\eta}\ \hat{e}_\eta + \frac{2}{d}\left[\frac{1+\xi^2}{\xi^2+\eta^2}\right]^{\frac{1}{2}}\frac{\partial\Phi}{\partial\xi}\ \hat{e}_\xi + \frac{2}{d}\ \frac{1}{[(1-\eta^2)(1+\xi^2)]^{\frac{1}{2}}}\ \frac{\partial\Phi}{\partial\phi}\ \hat{e}_\phi$$

Divergence

$$\nabla\cdot\bar{F} = \frac{2}{d}\ \frac{1}{\xi^2+\eta^2}\left[\frac{\partial}{\partial\eta}\left([(1-\eta^2)(\eta^2+\xi^2)]^{\frac{1}{2}}F_\eta\right) + \frac{\partial}{\partial\xi}\left([(1+\xi^2)(\eta^2+\xi^2)]^{\frac{1}{2}}F_\xi\right) + \frac{\xi^2+\eta^2}{\sqrt{1-\eta^2}\sqrt{1+\xi^2}}\ \frac{\partial F_\phi}{\partial\phi}\right] \tag{B2}$$

Curl

$$\nabla\times\bar{F} = \frac{2}{d}\left\{\left[\frac{1}{\sqrt{\eta^2+\xi^2}}\ \frac{\partial}{\partial\xi}\left(\sqrt{\xi^2+1}F_\phi\right) - \frac{1}{\sqrt{(1-\eta^2)(1+\xi^2)}}\ \frac{\partial}{\partial\phi}\left(F_\xi\right)\right]\hat{e}_\eta + \left[\frac{1}{\sqrt{(1+\xi^2)(1-\eta^2)}}\ \frac{\partial}{\partial\phi}\left(F_\eta\right) - \frac{1}{\sqrt{\eta^2+\xi^2}}\ -\left(\sqrt{1-\eta^2}F_\phi\right)\right]\hat{e}_\xi + \frac{1}{\xi^2+\eta^2}\left[\sqrt{1-\eta^2}\ \frac{\partial}{\partial\eta}\left(\sqrt{\eta^2+\xi^2}F_\xi\right) - \sqrt{1+\xi^2}\ \frac{\partial}{\partial\xi}\left(\sqrt{\eta^2+\xi^2}\ F_\eta\right)\right]\hat{e}_\phi\right\} \tag{B3}$$

Laplacian of a scalar function

$$\nabla^2\Phi = \frac{4}{d^2}\left[\frac{\partial}{\partial\eta}\left((1-\eta^2)\ \frac{\partial\Phi}{\partial\eta}\right)+\ \frac{\partial}{\partial\xi}\left((1+\xi^2)\ \frac{\partial\Phi}{\partial\xi}\right)\right.$$

$$\left.+\ \frac{\xi^2+\eta^2}{(1-\eta^2)(1+\xi^2)}\quad\frac{\partial^2\Phi}{\partial\phi^2}\right]\frac{1}{\eta^2+\xi^2} \qquad \text{(B4)}$$

APPENDIX C
ERRATA IN FLAMMER'S WORKS

The errata contained in this appendix have been collected by Dr. Hodge, Dr. Garbacz of the ElectroScience Laboratory and myself. The following corrections should be made.

A. Errata in Flammer's Book [10]

Page 42 - Equation (4-6-14) should be replaced by the following, for n-m odd:

$$R_{mn}^{(1)'}(-ic,io) = \frac{i^{n-m-1}\, 2^m m!\, c^{m+1}\, d_1^{mn}(-ic)}{(2m+3)\sum_{r=1}^{\infty}{}' d_r^{mn}(-ic)\,\frac{(2m+r)!}{r!}}, \qquad (C1)$$

and Equation (4-6.15b) by, for n-m odd:

$$R_{mn}^{(2)}(-ic,io) = \frac{1}{cR_{mn}^{(1)}(-ic,io)} = \frac{i^{n-m+1}(2m+3)\sum_{r=1}^{\infty}{}' d_r^{mn}(-ic)\,\frac{(2m+r)!}{r!}}{2^m\, m!\, c^{m+2}\, d_1^{mn}(-ic)} \qquad (C2)$$

Page 43 - $\left(\frac{n-m+1}{2}\right)!$ should be replaced by

$\left(\frac{n-m-1}{2}\right)!$ in $R_{mn}^{(2)'}(-ic,io)$ for n-m odd, Equation (4.6.16b)

Page 47 - The ϕ-dependence term $\cos m(\phi - \phi')$ should be introduced in the expansions of the Green's functions in Equation (5-2-11) and (5-2-12).

B. Errata in Flammer's Paper [7]

Part I

Page 1219 - Read i^{r+m-n} instead of $(-1)^{r+m-n}$ in the definition of $R_{mn}^{(i)}(-ic,i\xi)$, Equation (14).

Page 1221 - In the definition of a_{on}, Equation (36), the right-hand side of the equation should be:

$$2i^m N_{on}^{-1} \sum_{r=0,1}^{\infty}{}' f_r^{on} \tag{C3}$$

Part II

Page 1225 - The last inner bracket of Equation (11) should involve the derivation of the radial function and be written as follows:

$$\left[R_{1n}^{(1)'}(-ic,i\xi) - \frac{R_{in}^{(1)}(-ic,io)}{R_{1n}^{(3)}(-ic,io)} R_{1n}^{(3)}(-ic,i\xi)\right] \tag{C4}$$

Page 1226 - $R_{on}^{(1)'}(-ic,io)$ should be replaced by $S_{on}^{(1)'}(-ic,o)$ as noted by Flammer in the errata to his original report of this work.

C. Errata in Flammer's Original Report [12]

Page 12 - Replace $\sin\varsigma$ by $\cos\varsigma$ in Equations (49).

APPENDIX D
COMPUTER PROGRAM

This appendix presents the Fortran program used in Section VC of this work. This program has been written to compare Flammer's and Meixner's scattered bistatic far-field in the normal incidence perpendicular polarization case. It is based on Hodge's program[9] for Meixner's solution, which provides the structure and most of the subroutines used. The reader is referred to reference [9] for more complete details concerning the input and output, and for structural questions. First, the use of the program will be described. Some remarks will then be made on the programming, and a listing of the program will be provided.

1. Use of the Program

The program uses the same input procedures as Hodge's program except that the two following data, angle of incidence and polarization, have been suppressed since only the normal incidence perpendicular polarization case is considered. The inputs are made free-format on a teletype as follows:

1. KA = c, electrical circumference of the disk.
2. THETA SCATTERED = θ_s [degrees].
3. PHI SCATTERED - ϕ_s [degrees].

As in Hodge's program, any of these variables can be incremented. The corresponding inputs and the output formats are identical to Hodge's. The command "ESC" has been maintained. It interrupts the current calculation and requests a new set of data. No negative size of the disk should be entered and a disk of size 0 will terminate the program.

Unlike the general case treated by Hodge, this expresison of the far-scattered field in the normal incidence case is here a double infinite summation over n and r, the index m taking only the values 0 or 1. The summations are truncated in the same way as in Hodge's work. The function involved in each term of the summation are compared to a limit fixed in the program, 10^{30} in this case, near the overflow level, i.e., 10^{38} for the computer of the ElectroScience Laboratory. To prevent any overflow, the summation is truncated when one of the tested functions passes this limit. This procedure allows a full use of the capacity of the computer and suppresses the need for a manual search for the optimum truncation. Flammer's solution involves

the spheroidal functions for n-m even and odd and their derivatives. The subroutines computing the eigenvalue of the spheroidal scalar wave equation $\lambda_{mn}(-ic)$ and the expansion coefficients $d_r^{mn}(-ic)$ have been extended to the n-m odd case from a previous work of Dr. Hodge. The subroutines computing the functions for n odd have been added.

2. Remarks

The following remarks refer to the program listed in Section 3 of this Appendix. As in Hodge's work we will refer to a line of the program by LN. First, the different parts of the program are outlined. The structure is similar to that of Hodge's program.

LN 10-53 Input

LN 54-75 Computations of the needed functions

LN 76-101 Computations of the components of the E-field:
- cross-section
- phase

LN 102-104 Output

LN 105-108 Incrementation of the chosen variable.

The needed subroutines are listed in LN 113-564. The notations of the spheroidal functions for n-m even as defined in Hodge's program [9] have been preserved. The derivatives of the functions are characterized by a letter "P" at the end of the name of the function while a suffix OD refers to the function for n-m odd. The following notations must be introduced:

A and B are the two summations involved in the computation of $\beta_x^{\perp}$ and $\beta_z^{\perp}$.

ALPHA and BETA in the main program are equal to $\beta_x^{\perp}$ and $\beta_z^{\perp}$, respectively. Those names come from Flammer's definition [7].

EØ and El are the summations in Equation (112) apart from the ϕ-dependence and some trigonometric functions of θ. The coefficients necessary for the computation of EØ, and El, are computed in the $R_{op}^{(i)'}$ and $R_{ln}^{(i)}(-ic,io)$ subroutines, respectively, under the name COF.

3. Listing

In this section is given the listing of the program described above.

```
      OPTIONS 32K
C     FAR FIELD SCATTERING BY A CIRCULAR METALLIC DISK
C           NORMAL INCIDENCE
C           PERPENDICULAR POLARISATION
      INCLUDE 'ESSD.SYS9'
      DIMENSION LABEL(8),VAR(3)
      COMPLEX F4,F4P,F0,I,IX,A,B,COF,ETHF,EPHI,ALPHA,BETA
      COMMON E1G(200),E(100,50),UNEG(50),F4(50),F4P(50),COF(50)
     1,S0(50),S0P(50),P(50),P0(50),SETA(50),SETA0D(50)
      DATA LABEL/24H   KA THE S PHI S       /
      IX=(0.,1.)
      WRITE(8,26)
26    FORMAT(1X,///,'(TYPE "ESC" TO RESTART PROGRAM)',/,
     1'(TYPE KA=0 TO STOP PROGRAM)')
      CALL ESC(342)
4     NOC=1
      ILL1=11
      INDEX=1
      WRITE(8,27)
27    FORMAT(1X,///,1X,'1.  KA',14X,'= ')
      READ(8,*) VAR(1)
      IF(VAR(1).LE.0.)GO TO 5
      WRITE(8,28)
28    FORMAT(1X,'2.  THETA SCATTERED = ')
      READ(8,*) VAR(2)
      WRITE(8,29)
29    FORMAT(1X,'3.  PHI SCATTERED   = ')
      READ(8,*) VAR(3)
      WRITE(8,30)
30    FORMAT(1),//,1X,'WHICH VARIABLE IS TO BE INCREMENTED?')
      READ(8,*)NVAR
      IF((NVAR.LE.0).OR.(NVAR.GT.6))GO TO 23
      WRITE(8,31)
31    FORMAT(1X,'TYPE NUMBER OF CASES:')
      READ(8,*) NOC
      WRITE(8,32)
32    FORMAT(1X,'WHAT IS THE INCREMENT?')
      READ(8,*)VINCRE
      NNVAR=NVAR
      ILL1=2*NNVAR-1
23    ILL2=ILL1+1
      WRITE(8,24)LABEL(ILL1),LABEL(ILL2)
24    FORMAT(1X,//,2X,'ANGLE',4X,'CROSS SECTION',21X,'F NORM',/,
     110X,'SIGMA/(PI*A**2)',11X,'THETA',15X,'PHI',/,13X,
     1'THETA',7X,'PHI',8X,'MAG',5X,'PHASE',6X,'MAG',6X,
     1'PHASE',/)
6     C=VAR(1)
      MMMAX=45
      NNMAX=45
      IRMAX=45
      THES=VAR(2)*3.14159/180
      ETA=COS(THES)
      PHIS=VAR(3)*3.14159/180
      DO 10 MM=1,2
      M=MM-1
```

```
      IQ=0
      CALL OPEIGN(C,M,NMMAX)
      CALL OPCOPN(C,M,MMMAX,NNMAX,IRRMAX)
      IF(M) 55,55,56
   55 CALL SMNUP(M,NNMAX)
      CALL OPRADF(C,M,A,IJ,MMMAX,NNMAX,IRRMAX)
      CALL POLYN(ETA,M,IRRMAX)
      CALL OPANG(IJMAX,IRRMAX)
      CALL FIELDO(NNMAX,E0)
      GO TO 57
   56 CALL SMNO(M,NNMAX)
      CALL OPEGN(C,M,NNMAX)
      CALL OPRAD(C,M,3.16,MMMAX,NNMAX,IRRMAX)
      CALL POLYN(ETA,M,IRRMAX)
      CALL OPANG(INMAX,IRRMAX)
      CALL FIELD1(NNMAX,E1)
   57 CONTINUE
   10 CONTINUE
      ALPHA=R/(B-A)
      BETA=-A/(B-A)
      ETHE=ALPHA*E0*SIN(PHIS)
      EPHI=ALPHA*E0*ETA*COS(PHIS)-BETA*E1*SIN(THES)*COS(PHIS)
    8 EMAGT=CABS(ETHE)
      EMAGP=CABS(EPHI)
      SIGTHE=(EMAGT*2/C)**2
      SIGPHI=(EMAGP*2/C)**2
      ER=REAL(ETHE)
      EI=AIMAG(ETHE)
      IF(ER.EQ.0.) GO TO 16
      ARG=EI/ER
      EPHAT=180/3.14159*ATAN(ARG)
      IF((ER.LT.0.).AND.(EI.GT.0.))EPHAT=EPHAT+180
      IF((ER.LT.0.).AND.(EI.LT.0.))EPHAT=EPHAT-180
   16 EPHAT=90
      IF(EI.LT.0.)EPHAT=-90
   17 ER=REAL(EPHI)
      EI=AIMAG(EPHI)
      IF(ER.EQ.0.) GO TO 18
      ARG=EI/ER
      EPHAP=180/3.14159*ATAN(ARG)
      IF((ER.LT.0.).AND.(EI.GT.0.))EPHAP=EPHAP+180
      IF((ER.LT.0.).AND.(EI.LT.0.))EPHAP=EPHAP-180
      GO TO 19
   18 EPHAP=90
      IF(EI.LT.0.)EPHAP=-90
   19 IF(NVAR.EQ.0)NNVAR=1
      WRITE(3,25)VAR(NNVAR),SIGTHE,SIGPHI,EMAGT,EPHAT,
     1EMAGP,EPHAP
   25 FORMAT(1X,F7.2,2(1X,E10.3),2(1X,E10.3,1X,F7.2))
   37 IF(INDEX.EQ.NOC)GO TO 4
      INDEX=INDEX+1
      VAR(NNVAR)=VAR(NNVAR)+VINCRE
      GO TO 6
    5 CALL EXIT
   42 CONTINUE
```

```
      GO TO 4
      END
C
C     OBLATE SPHEROIDAL ANGULAR FUNCTION, S, OF ARGUMENT 0;
C     ORDER M,N; WITH N-M EVEN; OF TYPE ORDER M=M+2*NNMAX-2,
C     (EQUAL TO M=M(0))
C
      SUBROUTINE SMN0(M,NNMAX)
      COMPLEX F4,F4P,COF
      COMMON EIG(100),D(100,50),UNEG(50),F4(50),F4P(50),COF(50)
     1,S0(50)
      S0(1)=1
      IF(M.EQ.0)GO TO 1
      DO 2 MM=1,M
    2 S0(1)=(2*MM-1)*S0(1)
    1 DO 3 NN=1,NNMAX
      N=2*(NN-1)+M
      S0(NN+1)=-(N+M+1)*S0(NN)/(N-M+2)
    3 CONTINUE
      RETURN
      END
C
C     DERIVATIVE OF OBLATE SPHEROIDAL ANGULAR
C     FUNCTION S OF ARGUMENT 0; ORDER M,N,
C     WITH N-M ODD;
C
      SUBROUTINE SMNOP(M,NNMAX)
      COMMON EIG(100),D(100,50),UNEG(50),F4(50),F4P(50),COF(50)
     1,S0(50),S0P(50)
      COMPLEX F4,F4P,COF
      S0P(1)=1
      MD=M+1
      DO 2 MM=1,MD
      S0P(1)=(2*MM-1)*S0P(1)
    2 CONTINUE
      DO 3 NN=1,NNMAX
      N=2*NN+M-1
      S0P(NN+1)=-(N+M+2)*S0P(NN)/(N-M+1)
    3 CONTINUE
      RETURN
      END
C
C     OBLATE SPHEROIDAL EIGENVALUES OF ARGUMENT C, ORDER M,N
C
      SUBROUTINE OBEIGN(C,M,NNMAX)
      COMMON EIG(100)
      DIMENSION IP(50),P(50),ALPHA(50),BETA(50)
    4 CONTINUE
      M2=2*M
      C2=C*C
      ACC=1.0E-05
      NN2=NNMAX+2
      N1=NN2+1
      P(1)=1
      IP(1)=1
```

```
      IS=0
    1 CONTINUE
      DO 2 IQQ=1,NN2
      IV=2*IQQ+IS-1
      IW=NN2+2*IQQ+IS
      IX=NN2+4+IQQ+2*IS-1
      ALPHA(IQQ)=(C2*(M2*(2*IV-1)+2*IV*(IV-1)-1))/(IX*(IX-4))
     1-(M+IV-1)*(IV+M)
    2 BETA(IQQ+1)=C2/IX*SQRT(IV*(IV+1)*IW*(IW-1)/(IX*IX-4.0))
      BETA(NN2+1)=0.
      B0=ABS(ALPHA(1))+ABS(BETA(2))
      DO 3 IQQ=2,NN2
      A0=ABS(BETA(IQQ))+ABS(ALPHA(IQQ))+ABS(BETA(IQQ+1))
      BETA(IQQ)=BETA(IQQ)*BETA(IQQ)
      IF(A0.GT.B0) B0=A0
    3 CONTINUE
      A0=-B0
      B0=B0
   13 CONTINUE
      P0=B0
      DO 20 IQQ=1,NNMAX
      L=2*IQQ-1+IS
      N=L+M-1
      A=A0
      B=P0
      IERR=-1
   21 IIS=0
      C0=(A+B)/2
      IF(C0)50,22,50
   50 ERR=(B-A)/ABS(C0)
      IERR=IERR+1
      IF(IERR-60)40,41,41
   41 WRITE(6,42)M
   42 FORMAT(1X,'ITERATIONS EXCEEDED FOR EIGENVALUE ',I3)
      GO TO 700
   40 IF(ERR-ACC)24,24,22
   22 P(2)=ALPHA(1)-C0
      DO 5 I=3,NI
      P(I)=(ALPHA(I-1)-C0-BETA(I-1)*(P(I-2)/P(I-1)))*P(I-1)
      PMAG=ABS(P(I))
      IF(PMAG.GT.1.0E+35)GO TO 7
    5 CONTINUE
   12 CONTINUE
      DO 6 I=2,NI
      IF(P(I))4,6,9
    6 IF(P(I-1))9,9,14
   14 IP(I)=-1
      GO TO 10
    9 IP(I)=1
   10 IF(IP(I)-IP(I-1))6,11,6
   11 IIS=IIS+1
    6 CONTINUE
      IF(IIS-IQQ)16,15,15
   15 A=C0
      GO TO 21
```

```
      16    P=C0
            GO TO 21
      24    PU=C0
      700   EIG(L)=-C0
      20    CONTINUE
            IF(TS) 800,900,801
      800   IS=1
            GO TO 1
      801   CONTINUE
            RETURN
      7     MNMAX=L+4
            NNMAX=NNMAX+3
            GO TO 4
            END
C
C     OBLATE SPHEROIDAL EIGENFUNCTION EXPANSION COEFFICIENTS
C     OF ARGUMENT C: ORDER M,N,R.
C
            SUBROUTINE OBCOEF(C,M,MMMAX,NNMAX,IRRMAX)
            COMMON EIG(100),D(100,50)
            DIMENSION DP(100)
            C2=C*C
            MM=M+1
            NNMAX2=2*NNMAX
            DO 1 NN=1,NNMAX2
            N=M+NN-1
            IS=(-1)**NN
            IF(TS.LE.0) IS=0
            S=IS
      4     DP(IRRMAX+3)=0
            DP(IRRMAX+2)=1.0E-30
            D(NN,1)=0
            D(NN,2)=1
            JJ=(NN-IS)/2+1
            DO 107 LL=1,IRRMAX
            L=LL-1
            IF(LL.GE.JJ) L=IRRMAX+JJ-LL
            IR=2*L+IS
            IRM=M+IR
            AR=(M+IRM+2)*(M+IRM+1)*C2/((2*IRM+3)*(2*IRM+5))
            BR=(2*IRM*(IRM+1)-2*(M*M-1)+C2/((2*IRM-1)*
           1  (2*IRM+3))-IRM*(IRM+1)
            CR=IR*(IR-1)*C2/((2*IRM-3)*(2*IRM-1))
            IF(LL-JJ)106,106,106
      105   D(NN,L+3)=-(CR*D(NN,L+1)+(BR+EIG(NN))*D(NN,L+2))/AR
            DMAG=ABS(D(NN,L+3))
            IF(DMAG,GT,1.0E+30)GO TO 3
            GO TO 107
      106   DP(L+1)=-(AR*DP(L+3)+(BR+EIG(NN))*DP(L+2))/CR
            DMAG=ABS(DP(L+1))
            IF(DMAG.GT.1.0E+30)GO TO 3
      107   CONTINUE
            DL=ABS(D(NN,JJ+1))
            DL=ALOG10(DL)
            DLP=ABS(DP(JJ+1))
```

```
      DLP=ALOG10(DLP)
      DL=ABS(DL)
      DLP=ABS(DLP)
      DL=DL+DLP
      IF(DL.GT.30.)GO TO 5
      COR=D(NN,JJ+1)/DP(JJ+1)
      ACOR=ABS(COR)
      IF(ACOR.GE.1.0E+32)GO TO 2
      DO 110 J=JJ,IRRMAX
  110 D(NN,J+2)=COR*DP(J+2)
      F=1
      ISM=IS+M
      IF(ISM)198,198,199
  199 F=2.0**(-IS)
      DO 110 I=1,ISM
  110 F=F*(ISM+1)
  198 SUM=0
      MMX=IRRMAX+1
      DO 113 I=1,MMX
      IR=2*I+IS
      SUM=SUM+F*D(NN,I+1)
      IF(I-JJ) 113,197,113
  197 ENM=F
  113 F=(-F*(IR+2*M+IS-1))/(IR-IS)
      ALE=ENM/SUM
      DO 114 I=1,MMX
      D(NN,I)=ALE*D(NN,I+1)
  114 CONTINUE
    1 CONTINUE
      RETURN
    3 IRRMAX=LL-1
      GO TO 4
    2 IRRMAX=IRRMAX-1
      GO TO 4
    5 NNMAX=(NN-1)/2
      RETURN
      END
C
C     NEGATIVE D COEFFICIENT SUBROUTINE
C             N-M EVEN.
C
      SUBROUTINE DNEGN(C,M,NNMAX)
      COMMON EIG(100),D(100,50),DNEG(50)
      DO 4 NN=1,NNMAX
      C2=C*C
      NK=2*NN-1
      IF (M.GE.1) GO TO 2
      DO 5 NN=1,NNMAX
      NK=2*NN-1
    5 DNEG(NN)=D(NK,1)
      GO TO 3
    2 PA=1.0
      P2=0.0
      FI=EIG(NK)
      DO 1 IRR=1,M
```

```
      IR=2*IRR-2*M-2
      AR=(2*M+IR+2)*(2*M+IR+1)*(2/((2*M+2*IR+3)
     1*(2*M+2*IR+5))
      BR=(M+IR)*(M+IR+1)-R1*(2*(M+IR)*(M+IR+1)-2*M*M-1)
     1*C2/((2*M+2*IR-1)*(2*M+2*IR+3))
      CR=(IR)*(IR-1)*C2/((2*M+2*IR-3)*(2*M+2*IR-1))
      B3=B2
      B2=B1
    1 B1=(BR*B2-CR*B3)/AR
      A=D(NK,1)/B1
      DNEG(NN)=A
      DUM=ABS(DNEG(NN))
      IF(DUM.LT.1.E-35)GO TO 6
    4 CONTINUE
    5 RETURN
    6 NMAX=NN-1
      RETURN
      END
C
C     OBLATE SPHEROIDAL RADIAL FUNCTION R(4) OF ARGUMENT C;
C     ORDER M+N; WITH N-M EVEN; UP TO ORDER N=M+2*NRMAX-2.
C     ALSO NORMALIZATION FUNCTION, N.
C     ALSO COEFFICIENT COF FOR COMPUTATION OF E1
C
      SUBROUTINE OBRAD(C,M,B,IC,NMMAX,NRMAX,IRRMAX)
      COMMON EIG(100),D(100,50),DNEG(50),E4(50),E4P(50),COF(50)
     1,S0(50),SOP(50)
      COMPLEX IX,R4,E4,B,COF,E4P
      IX=(0.0,1.0)
      EFAC=1
      FAC=1
      FAC2=1
      GR0=1
      IF(M.EQ.0) GO TO 20
      MAXM=M+1
      DO 19 MM=2,MAXM
      IM=MM-1
      GR0=(2*IM-1)*(2*IM)*GR0
      EFAC=(2*IM-1)*EFAC
      FAC2=(2*IM-1)*(2*IM)*FAC2
   19 FAC=IM*FAC
      IF(EFAC.GE.1.0E+17)GO TO 4
      IF(FAC2.GE.1.0E+30)GO TO 4
   20 R=(0.0,0.0)
      DO 17 NN=1,NRMAX
      NK=2*NN-1
      N=2*(NN-1)+M
      SUM=0
      GR=GR0
      ENORM=0.
      DO 15 IR=1,IRRMAX
      IR=2*(IR-1)
      SUMP=GR*D(IR,NR)
      SUM=SUM+SUMP
      EMAG=ABS(D(NK,NK))
```

```
      IF(DMAG.LT.1.0E-30)GO TO 1
      ENORMP=2*GR*(D(NK,IR))**2/(2*IR+2*M+1)
    2 ENORM=ENORM+ENORMP
      GRMAG=ABS(GR)
      IF(GRMAG.GT.1.0E+30) GO TO 5
      GK=(IR+2*M+1.)/(IR+1.)*(IR+2*M+2.)/(IR+2.)*GR
   18 CONTINUE
      R1=(-1)**(M-1)*2**M*FAC*C**M*D(NK,1)/((2*M+1)*SUM)
      R2=(-1)**(M-1)*(2**M-1)*FAC*C**(M-1)/(2*FAC2)*3.14159
     1*(FFAC**2/SUM)*2**M/GNEG(NN)
      AR2=ABS(R2)
      IF(AR2.GE.1.0E+30)GO TO 4
      FFAC=(M+M+1)*FFAC/(M-M+2)
      IF(FFAC.GE.1.0E+17)NNMAX=NN
      R4=R1-IX*R2
      A5=ABS(ENORM)
      A1=ALOG10(A5)
      A4=ABS(R2)
      A2=ALOG10(A4)
      A3=A1+A2
      IF(A3.GT.30.)GO TO 3
      A5=ABS(R1)
      A1=ALOG10(A5)
      A3=ABS(A1)+ABS(A2)
      IF(A3.GT.30.)GO TO 3
      F4(NN)=1/(ENORM*R4)
   16 CONTINUE
      F=F+2*(-1)**NN*F4(NN)*S0(NN)*SUM
      COF(NN)=2*I*R1*F4(NN)*SUM
   17 CONTINUE
      RETURN
    1 ENORMP=0
      GO TO 2
    4 F4(NN)=(0.,0.)
      GO TO 16
    5 GR=0
      GO TO 18
    3 MMMAX=M
      IG=1
      RETURN
      END
C
C     DERIVATIVES OF THE RADIAL FUNCTIONS R1 AND R4
C     OF ORDER M=0,N, A CODE OF ARGUMENT 0.
C     ALSO NORMALIZATION FUNCTION, N.
C     ALSO COEFFICIENT COF FOR COMPUTATION OF E0.
C
      SUBROUTINE CBRADP (C,M,A,IQ,MMMAX,NNMAX,IRRMAX)
      COMMON FIO(100),D(100,50),ENEG(50),F4(50),F4P(50),COF(50)
     1,S0(50),SUF(50)
      COMPLEX IX,R4,F4,R4P,F4P,A,COF
      IX=(0.0,1.0)
      FFAC=1
   21 A=(0.0,0.0)
      DO 17 NN=1,NNMAX
```

```
      NK=2*NN
      N=2*NN-1
      SUM=0
      ENORM=0.
      DO 18 NR=1,IRRMAX
      IK=2*NR-1
      SUM =SUM+D(IK,NR)
      EMAG=ABS(D(IK,NR))
      IF(EMAG.LT.1.0E-30)GO TO 1
      ENORM=2*(D(IK,NR))**2/(2*IR+1)
    2 ENORM=ENORM+ENORM
   18 CONTINUE
      FAC=(-1)**(IM-1)*C*D(IK,1)/(3*SUM)
      P2P=(-1)**(IM-1)*3*3.14159/(C*C*D(NK,1)*SUM*2)*FFAC
      ER2=ABS(R2P)
      IF(ER2.GE.1.0E+30)GO TO 4
      FF/C=(M+2)*FFAC/(N+1)
      IF(FFAC.GE.1.0E+17)NNMAX=NN
      F4P=R1P*1X*R2P
      AS=ABS(ENORM)
      A1=ALOG10(AS)
      A4=ABS(P2P)
      A2=ALOG10(A4)
      A3=A1+A2
      IF(A4.GT.30.)GO TO 5
      AS=ABS(R1P)
      A1=ALOG10(AS)
      A3=ABS(A1)+ABS(A2)
      IF(A3.GT.30.)GO TO 3
      F4P(NN)=1/(ENORM*R4P)
   14 CONTINUE
      A=2.+2*(-1)**(MM-1)*F4P(NN)*S0P(NN)*SUM
      COF(MM)=2*(-1)*IX*P1P*F4P(NN)*SUM
   17 CONTINUE
      RETURN
    1 ENORMP=0
      GO TO 2
    3 F4P(NN)=(0.,0.)
      GO TO 16
    4 MMMAX=M
      IG=1
      RETURN
      END
C
C     ASSOCIATED LEGENDRE POLYNOMIALS OF ARGUMENT ETA0:
C     ORDER M=MI WITH N=2 EVEN: P, UP TO ORDER N=M+2*NNMAX-2:
C     WITH N=M ODD: P0, UP TO ORDER N=M+2*NNMAX-1.
C
      SUBROUTINE POLYN(ETA0,M,NNMAX)
      DIMENSION PP(3)
      COMMON EIG(100),D(100,50),LNFG(50),F4(50),F4D(50),COF(50)
     1,S0(50),S0P(50),P(50),P0(50)
      COMPLEX F4,F4P,COF
      S0=SQRT(1-ETA0*ETA0)
      PP(1)=0
```

```
      PP(2)=1
      IF(M.EQ.0)GO TO 1
      DO 2 L=1,M
    2 PP(2)=(2*L-1)*SQ*PP(2)
    1 P(1)=PP(2)
      NNMAX1=NNMAX+1
      DO 5 NN=2,NNMAX1
      N=M+2*NN-3
      DO 4 L=1,2
      PP(3)=((2*N-1)*ETA0*PP(2)-(N+M-1)*PP(1))/(N-M)
      IF(NN.EQ.NNMAX1) GO TO 5
      N=N+1
      PP(1)=PP(2)
    4 PP(2)=PP(3)
      P(NN)=PP(3)
    5 CONTINUE
      NL=NN-1
    3 PO(NL)=PP(1)
      RETURN
      END
C
C     OBLATE SPHEROIDAL ANGULAR FUNCTIONS, S. OF ARGUMENTS
C     C AND ETA0; ORDER M+N; WITH N=M EVEN; SETA, UP TO ORDER
C     N=M+2*NNMAX-2; WITH N=M ODD; SETAOD, UP TO ORDER
C     M=M+2*NNMAX-1.
C
      SUBROUTINE OBANG(NNMAX,IRRMAX)
      COMMON EIG(100),D(100,50),UNFG(50),F4(50),F4P(50),COF(50)
     1,SO(50),SOP(50),P(50),PO(50),SETA(50),SETAOD(50)
      COMPLEX F4,F4P,COF
      N=0
      DO 1 NN=1,NNMAX
      NK=2*NN-1
      SETA(NN)=0
      NKO=2*NN
      SETAOD(NN)=0
      DO 2 IRR=1,IRRMAX
      SETAOD(NN)=SETAOD(NN)+D(NKO,IRR)*PO(IRR)
      SETA(NN)=SETA(NN)+D(NK,IRR)*P(IRR)
    2 CONTINUE
    1 CONTINUE
      RETURN
      END
C
C     SUBROUTINE FIELD0
C
      SUBROUTINE FIELD0(NNMAX,F0)
      COMMON EIG(100),D(100,50),UNFG(50),F4(50),F4P(50),COF(50)
     1,SO(50),SOP(50),P(50),PO(50),SETA(50),SETAOD(50)
      COMPLEX COF,E0,F4,F4P
      E0=(0.0,0.0)
      DO 1 NN=1,NUMAX
      E0=E0+COF(NN)*SETAOD(NN)
    1 CONTINUE
      RETURN
```

```
      END
C
C     SUBROUTINE FIELD1
C
      SUBROUTINE FIELD1(NMAX,F1)
      COMMON E1R(100),E1I(100,50),DIFG(50),F4(50),F4P(50),COF(50)
     1,SI(50),SGI(50),P(50),PC(50),SETA(50),SETAOD(50)
      COMPLEX COF,F1,F4,F4P
      F1=(0.0,0.0)
      DO 1 N1=1,NMAX
      F1=F1+COF(N1)*SETA(N1)
    1 CONTINUE
      RETURN
      END
```